

# Chiral Cu(II), Co(II) and Ni(II) complexes based on 2,2'-bipyridine modified peptoids

Maria Baskin and Galia Maayan

Schulich Faculty of Chemistry, Technion- Israel Institute of Technology, Haifa, Israel, 32000

## Supporting Information

**Table S1.** Peptoid oligomer sequences and their molecular weights.

Ns1npe = (S)-N-(1-naphthylethyl)glycine, Nbp-(2,2'-bipyridine-3'-yloxy) ethylamine, Ns1tbe -

Peptoid oligomers	Molecular weight
	Calc: Found (gr/mol)
<b>6P1</b> (Ns1tbe-Nbp -Ns1tbe- Ns1tbe-Nbp-Ns1tbe)	1092.42 : 1092.77
<b>6P1Ac</b> (Ns1tbe-Nbp -Ns1tbe- Ns1tbe-Nbp-Ns1tbe-Ac)	1134.45 : 1135.47
<b>4P1</b> (Nbp -Ns1tbe- Ns1tbe-Nbp)	810.00 : 810.58
<b>4P1Ac</b> (Nbp -Ns1tbe- Ns1tbe-Nbp-Ac)	852.03 : 852.66
<b>6P2</b> (Ns1npe-Nbp-Ns1npe-Ns1npe-Nbp- Ns1npe)	1372.61: 1372.55
<b>6P2Ac</b> (Ns1npe-Nbp-Ns1npe-Ns1npe-Nbp-Ns1npe-Ac)	1414.65 : 1414.78
<b>4P2</b> (Nbp-Ns1npe-Ns1npe-Nbp )	950.09 : 950.10
<b>4P2Ac</b> (Nbp-Ns1npe-Ns1npe-Nbp-Ac)	992.13 : 992.08

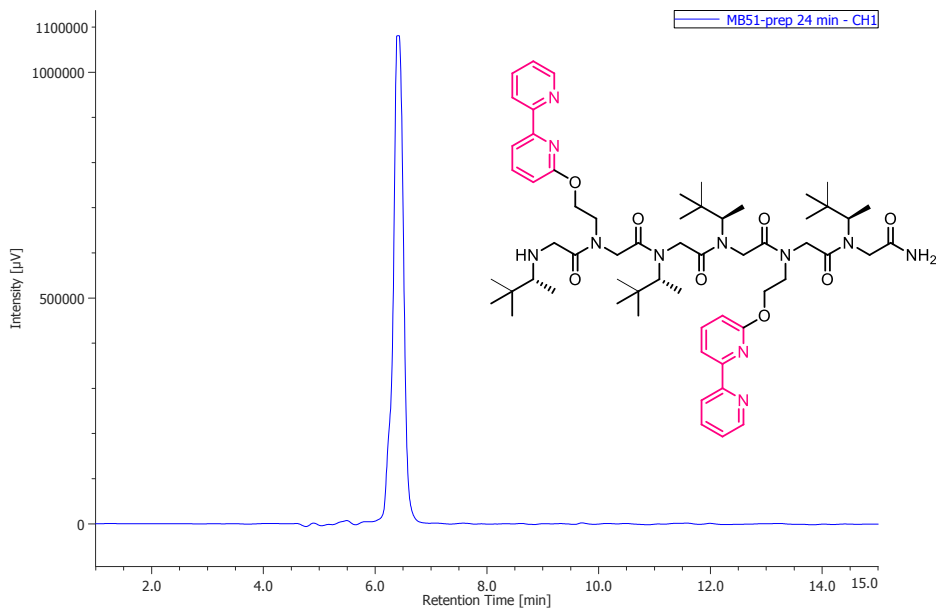
(S)-N-(1-tert-butylethyl)glycine, Ac= acetylated.

**Table S2.** Molecular weights of the Peptoid metal complexes.

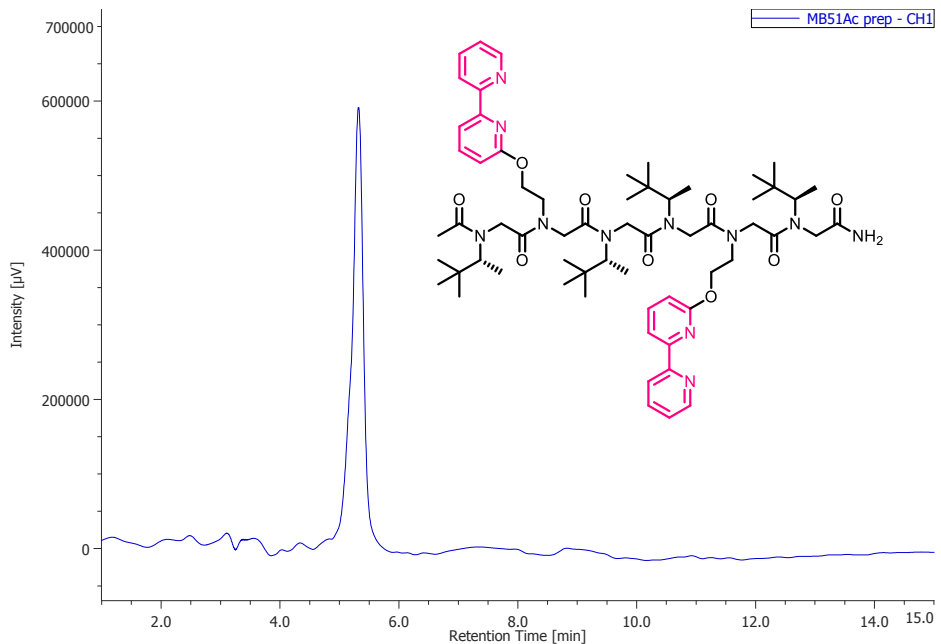
Peptoid -Metal complex	Molecular weight
	Calc.: Found (gr/mol)
(L2B)Cu	1234.49 : 1234.49
(L2B)Co	1230.50 : 1230.49
(L2B)Ni	1229.50: 1228.49
(R-L2B)Cu	1234.49 : 1234.49
(R-L2B)Co	1344.33 (m/z+TFA) : 1344.46
(R-L2B)Ni	1229.50 : 1228.48
(C3B)Cu	1425.56 : 1425.56
(C3B)Co	1534.55 (m/z+TFA): 1534.55
(C3B)Ni	1420.57 : 1419.56
(R-C3B)Cu	1425.56 : 1425.55
(R-C3B)Co	1534.55 (m/z+TFA): 1535.55
(R-C3B)Ni	1420.57 : 1420.55
(6P1)Cu	1154.45 : 1154.62
(6P1)Co	1149.45 : 1150.62
(6P1)Ni	1149.62 : 1149.45
(6P1Ac)Cu	1196.63 : 1196.46
(6P1Ac)Co	1192.63 : 1192.53
(6P1Ac)Ni	119.64 : 1191.47
(6P2)Cu	1434.56 : 1434.44
(6P2)Co	1430.56 : 1429.43
(6P2)Ni	1542.54 (m/z+TFA) : 1542.43
(6P2Ac)Cu	1476.57 : 1476.48

(6P2Ac)Co	1472.57 : 1471.45
(6P2Ac)Ni	1471.57 : 1470.47
(4P1)Cu	872.39 : 871.29
(4P1)Co	868.39 : 867.32
(4P1)Ni	867.39 : 866.31
(4P1Ac)Cu	914.40 : 914.32
(4P1Ac)Co	910.40 : 909.33
(4P1Ac)Ni	909.40 : 908.32
(4P2)Cu	1012.36 : 1011.30
(4P2)Co	1008.36 : 1008.32
(4P2)Ni	1120.35(m/z+TFA) : 1120.31
(4P2Ac)Cu	1054.37 : 1054.32
(4P2Ac)Co	1050.37 : 1049.29
(4P2Ac)Ni	1049.37 : 1048.33

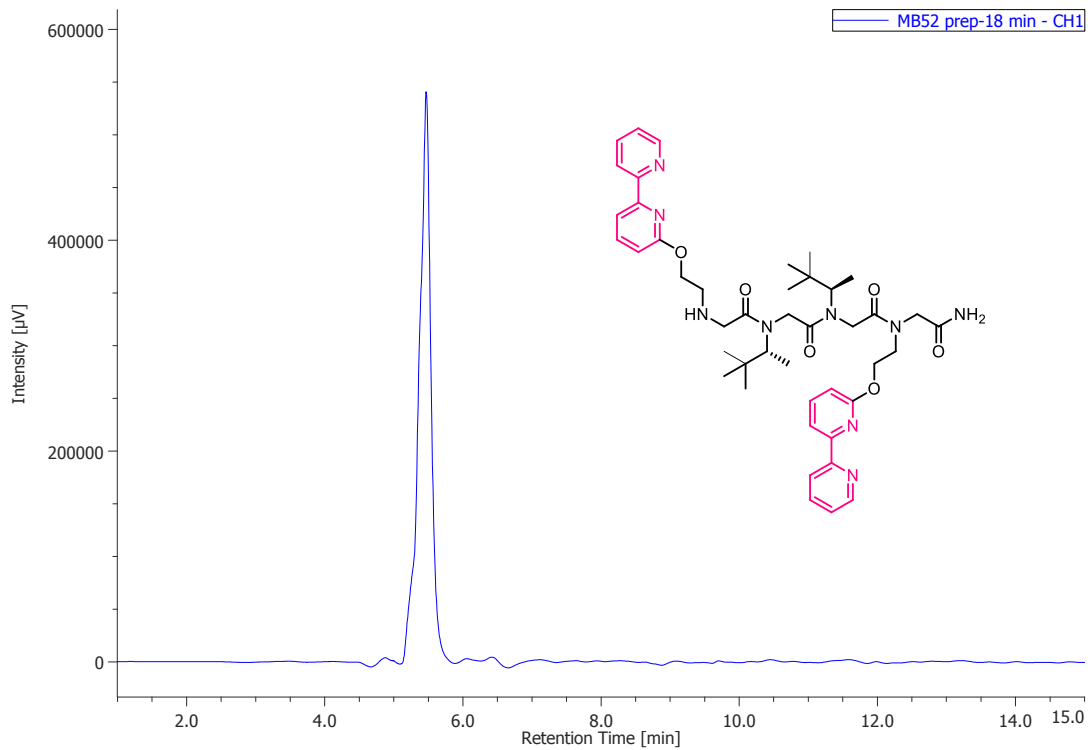
## HPLC of peptoid oligomers



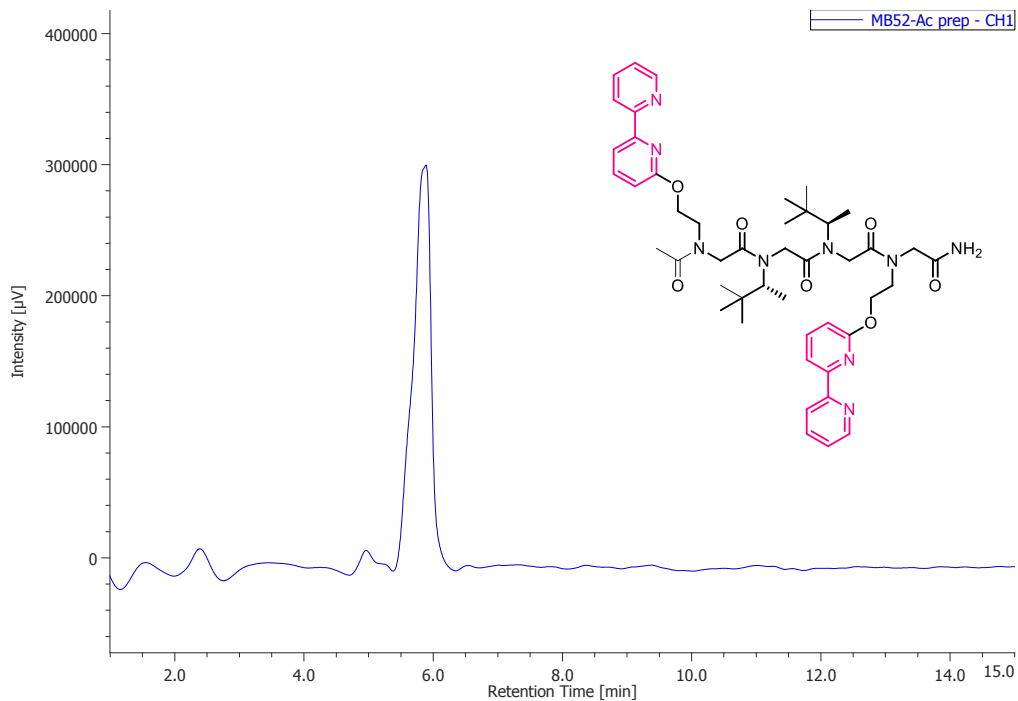
**Figure S1.** HPLC traces of purified peptoid oligomer **6P1** at 214nm.



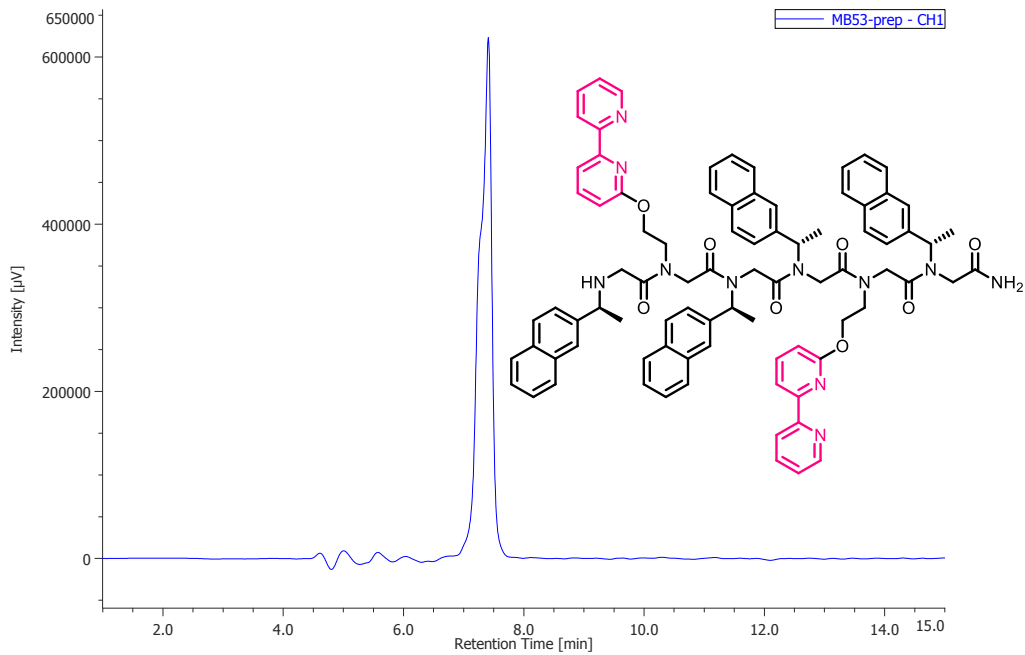
**Figure S2.** HPLC traces of purified peptoid oligomer **6P1Ac** at 214nm.



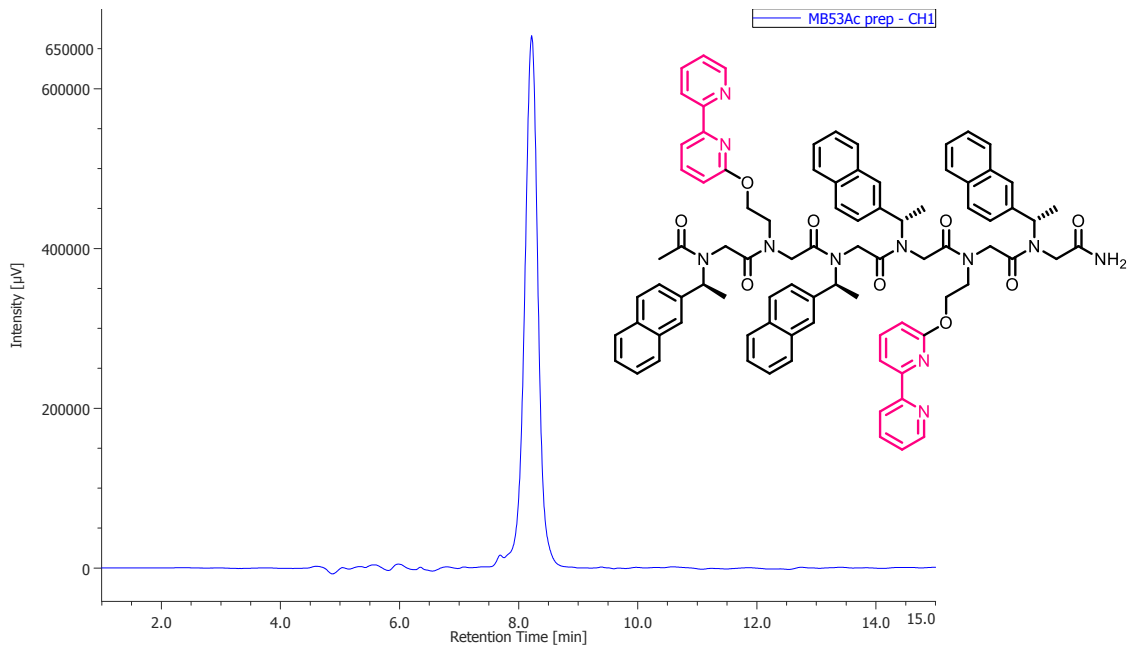
**Figure S3.** HPLC traces of purified peptoid oligomer **4P1** at 214nm.



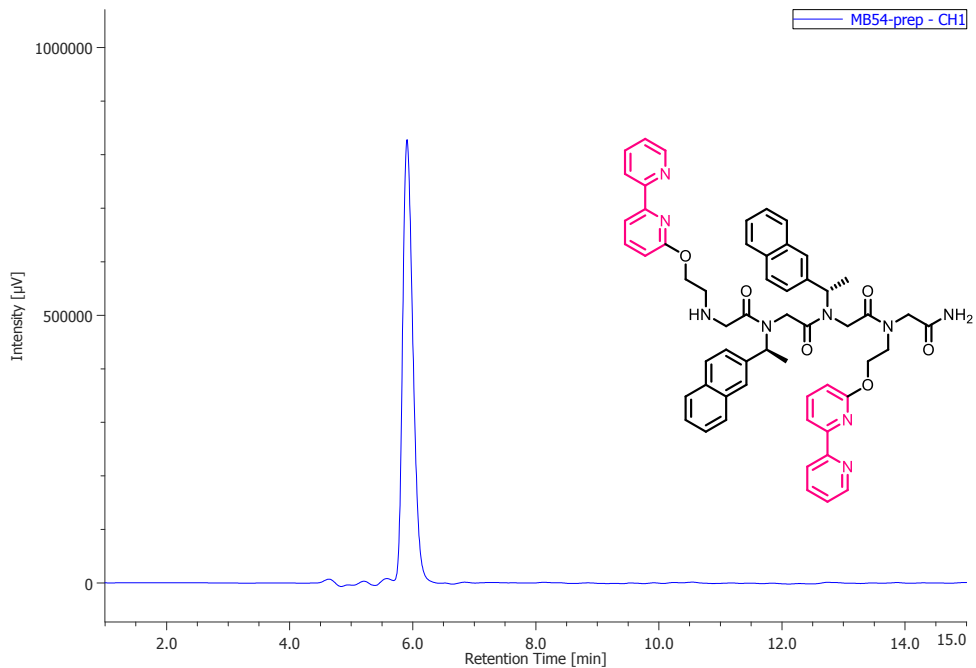
**Figure S4.** HPLC traces of purified peptoid oligomer **4P1Ac** at 214nm.



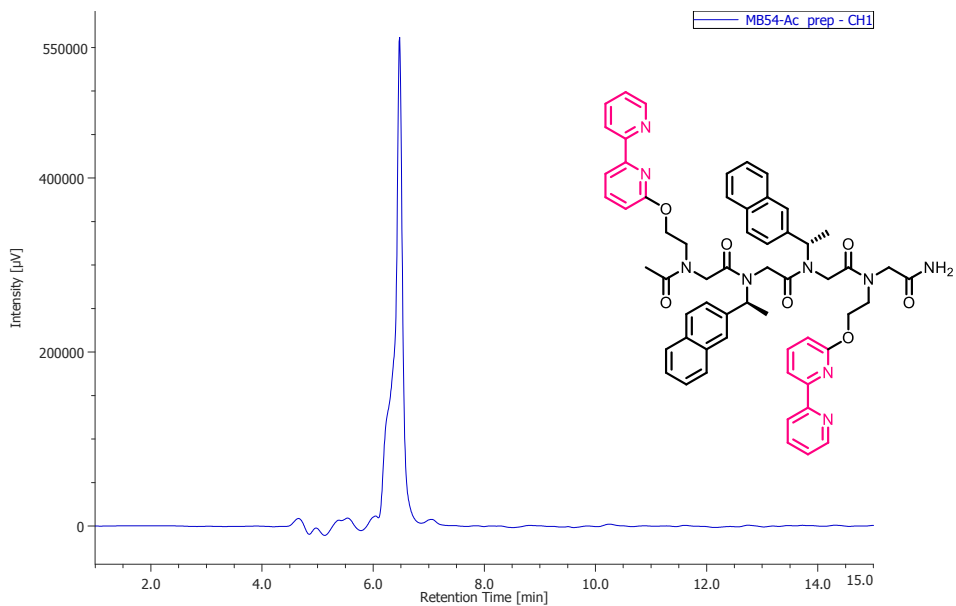
**Figure S5.** HPLC traces of purified peptoid oligomer **6P2** at 214nm.



**Figure S6.** HPLC traces of purified peptoid oligomer **6P2Ac** at 214nm.

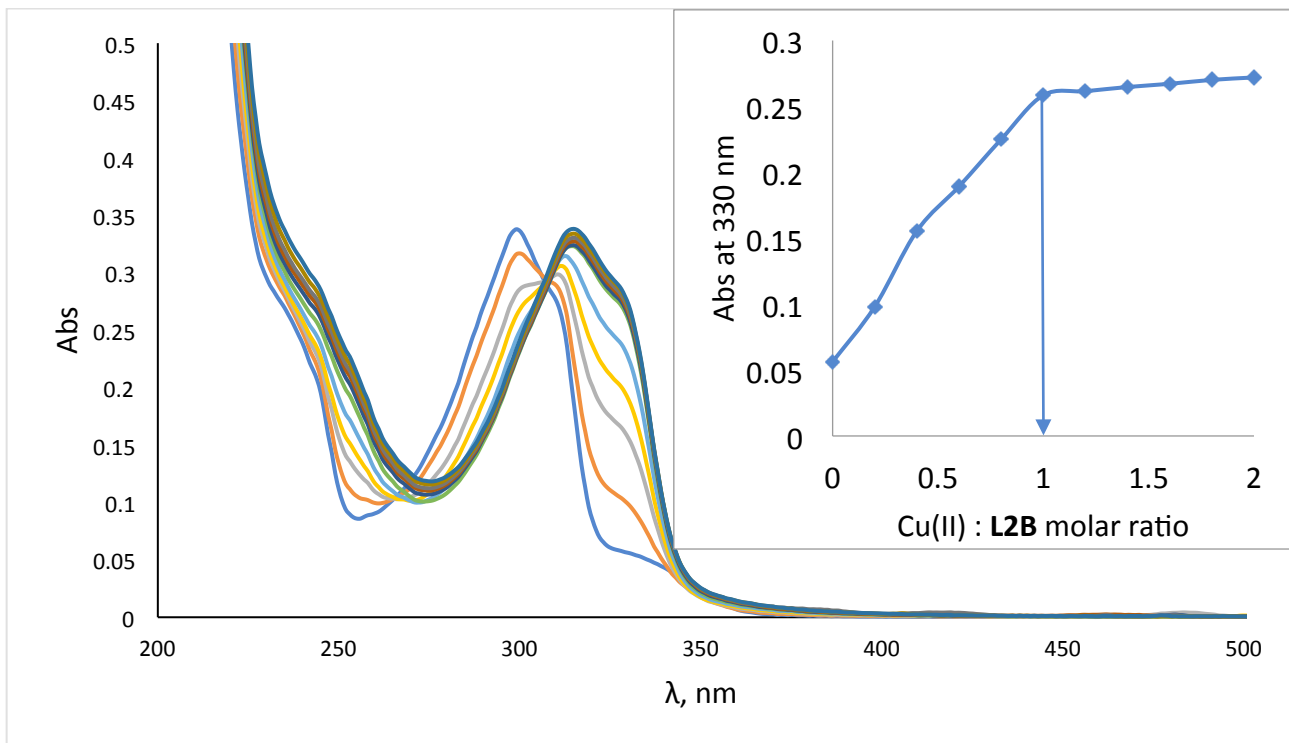


**Figure S7.** HPLC traces of purified peptoid oligomer **4P2** at 214nm.

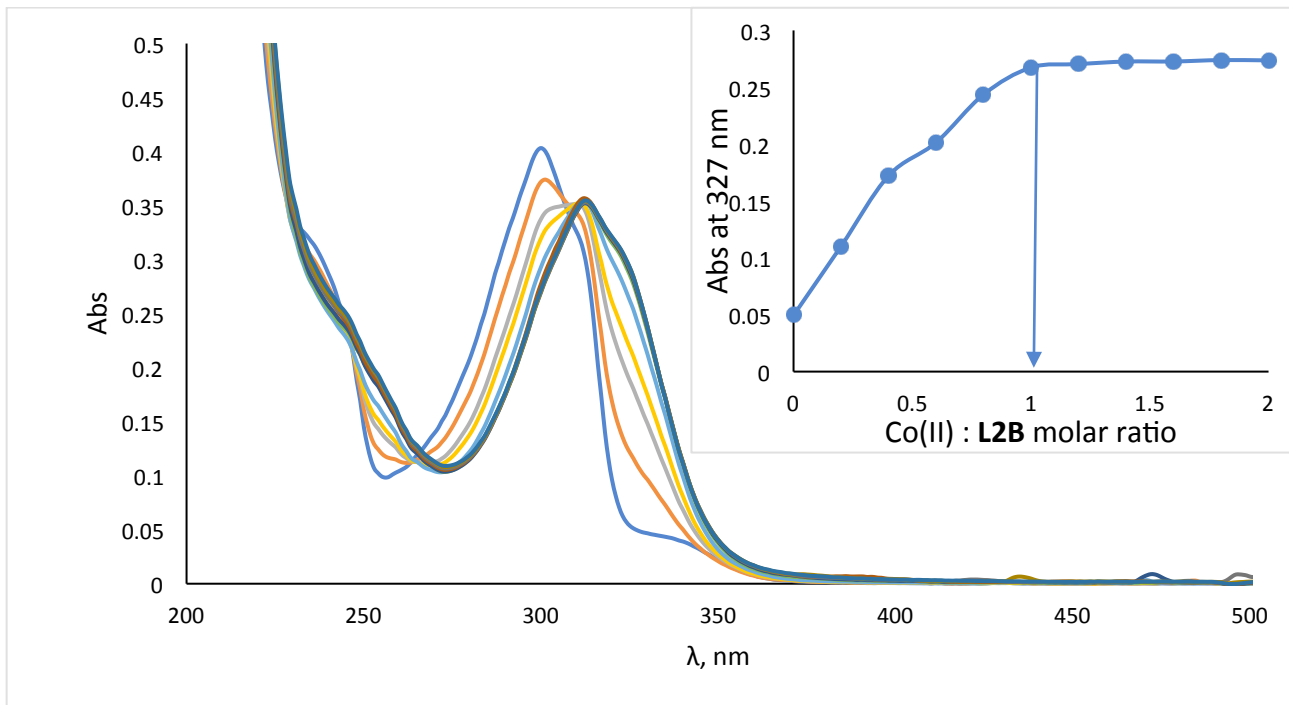


**Figure S8.** HPLC traces of purified peptoid oligomer **4P2Ac** at 214nm.

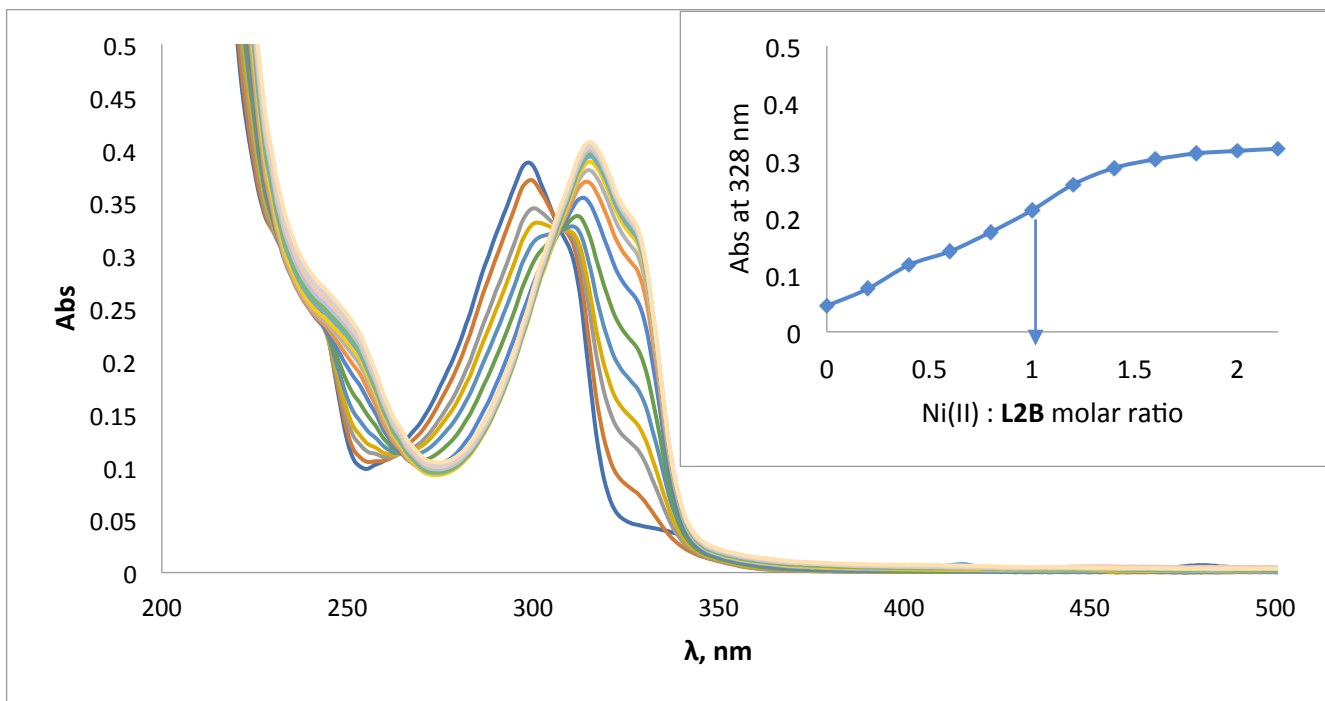
## UV-VIS Spectroscopy



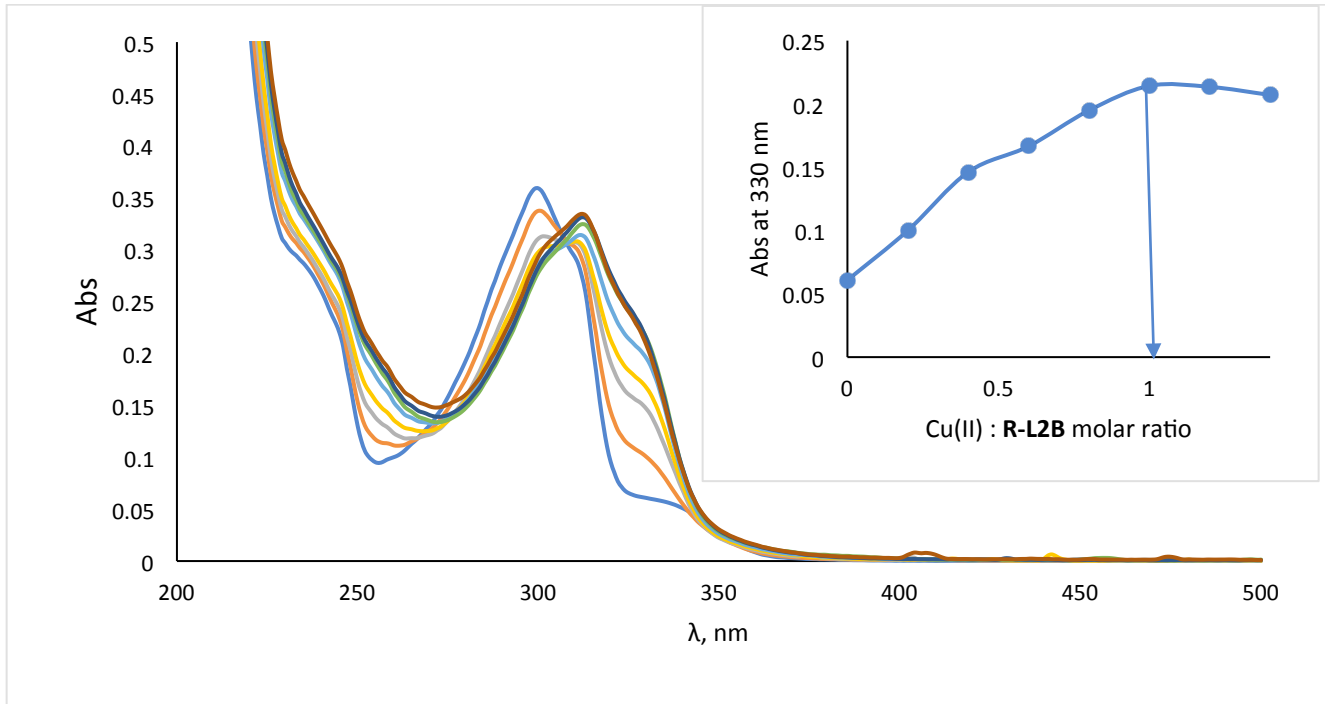
**Figure S9.** UV-Vis titration of **L2B** (17  $\mu\text{M}$ ) with  $\text{Cu}^{2+}$  acetate in ACN.

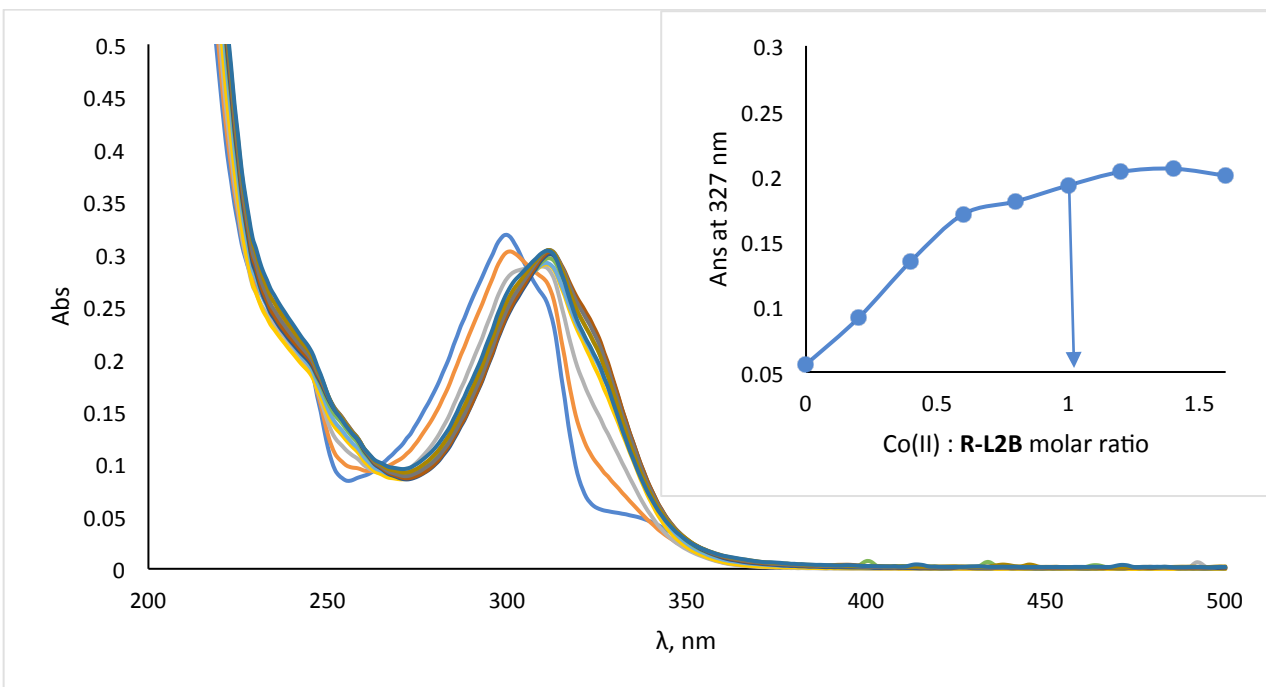


**Figure S10.** UV-Vis titration of **L2B** (17  $\mu\text{M}$ ) with  $\text{Co}^{2+}$  acetate in ACN.

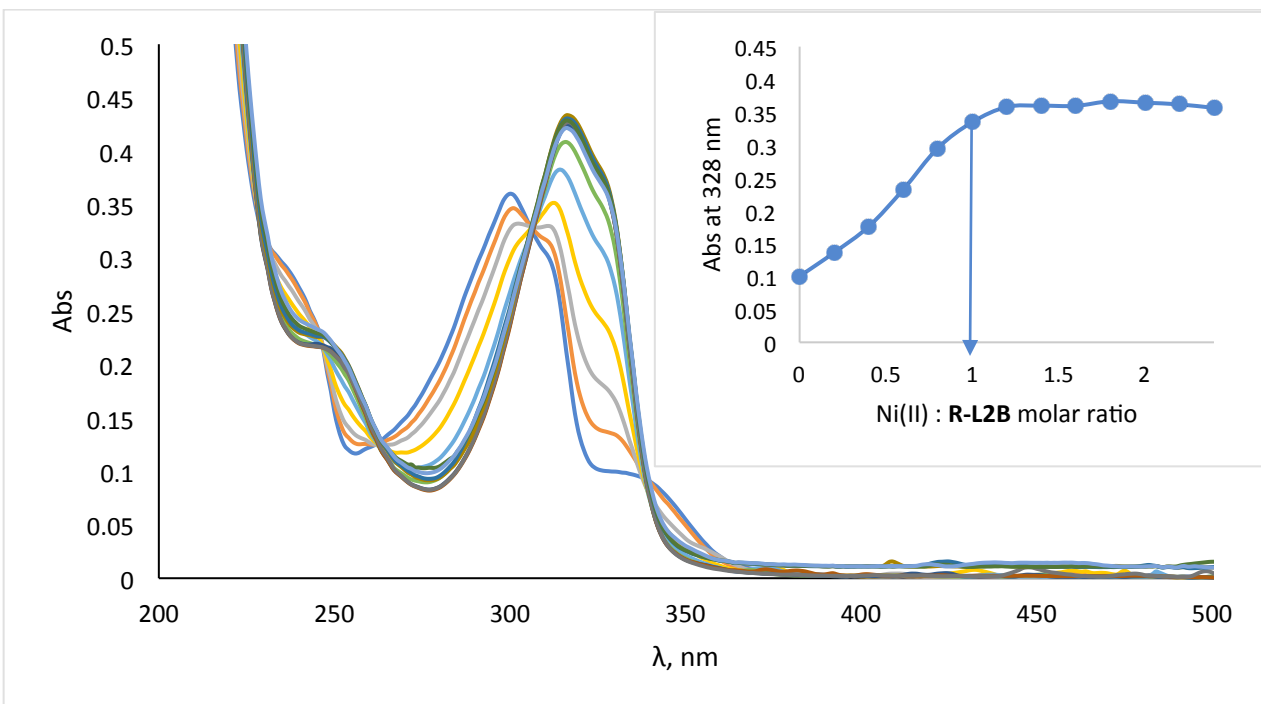


**Figure S11.** UV-Vis titration of **L2B** (17  $\mu\text{M}$ ) with  $\text{Ni}^{2+}$  acetate in ACN.

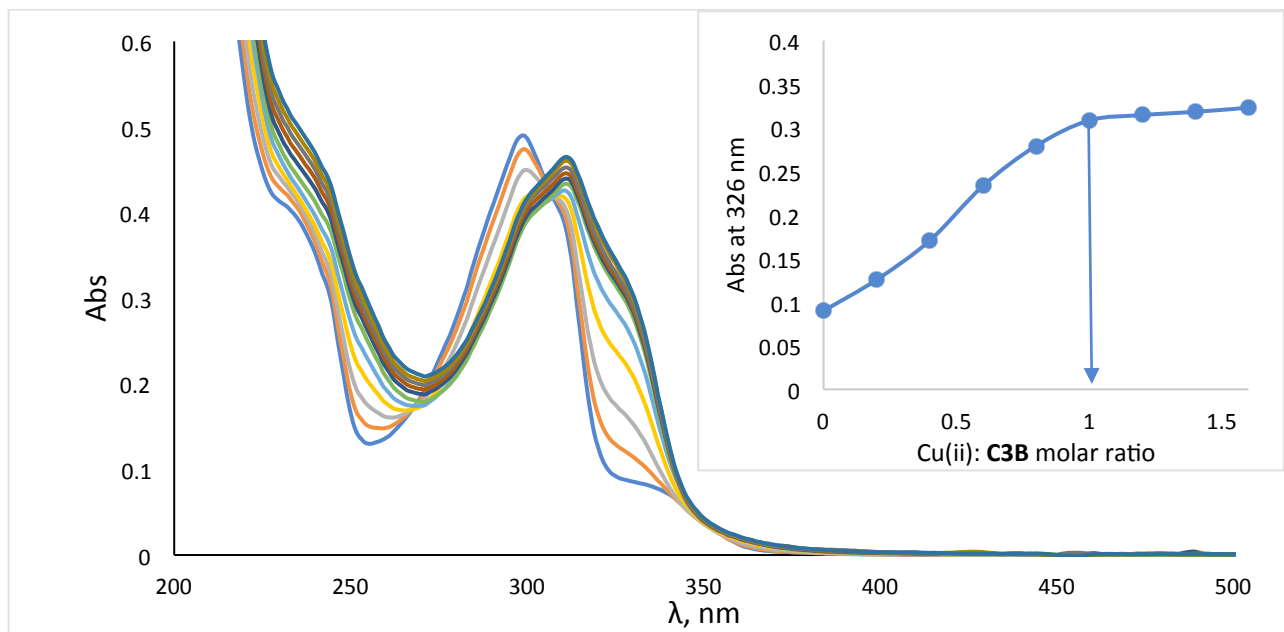




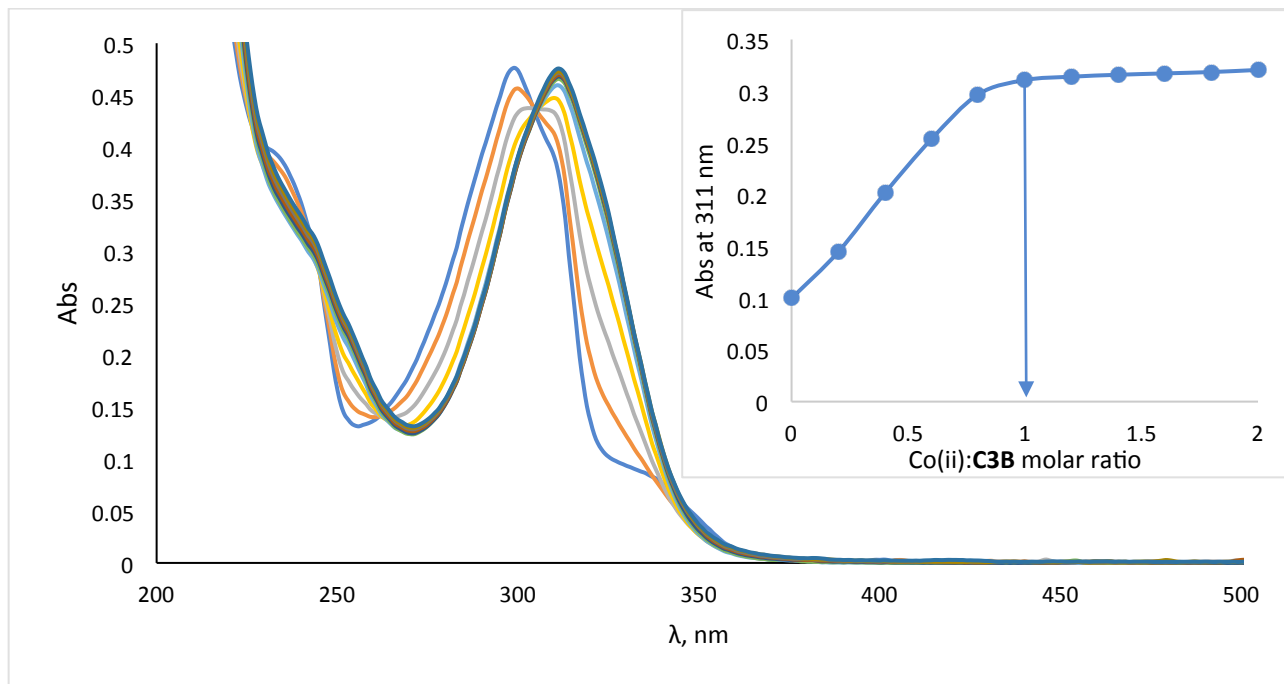
**Figure S13.** UV-Vis titration of **R-L2B** (17  $\mu\text{M}$ ) with  $\text{Co}^{2+}$  acetate in ACN.



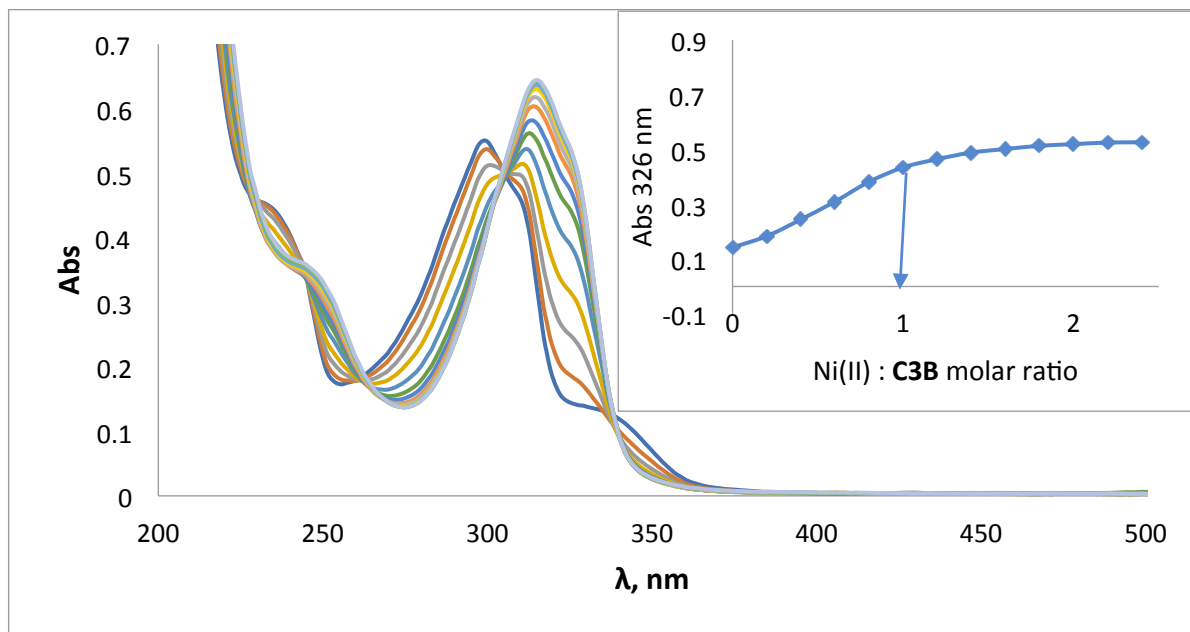
**Figure S14.** UV-Vis titration of **R-L2B** (17  $\mu\text{M}$ ) with  $\text{Ni}^{2+}$  acetate in ACN.



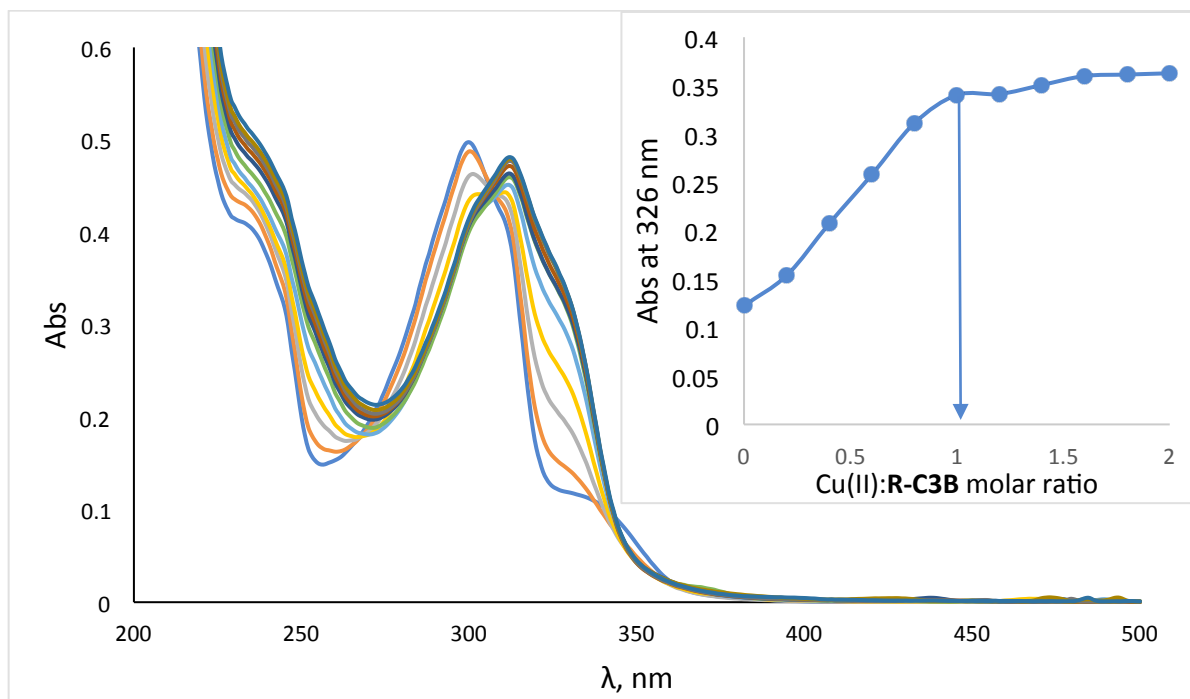
**Figure S15.** UV-Vis titration of **C3B** (17  $\mu\text{M}$ ) with  $\text{Cu}^{2+}$  acetate in ACN.



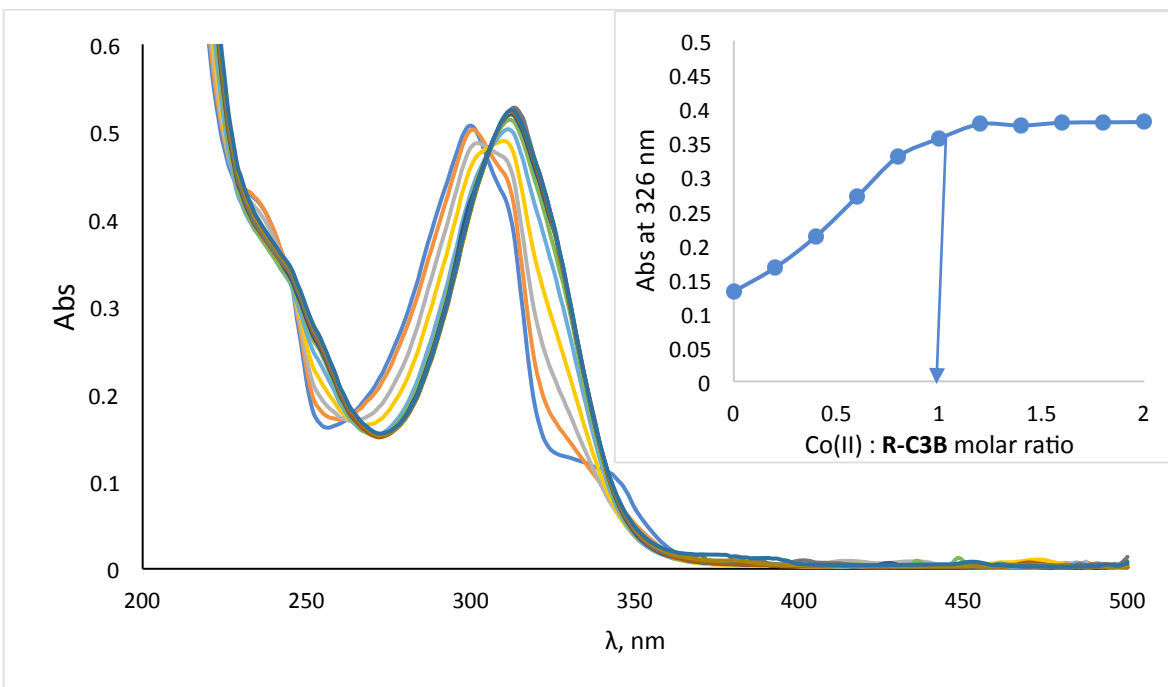
**Figure S16.** UV-Vis titration of **C3B** (17  $\mu\text{M}$ ) with  $\text{Co}^{2+}$  acetate in ACN.



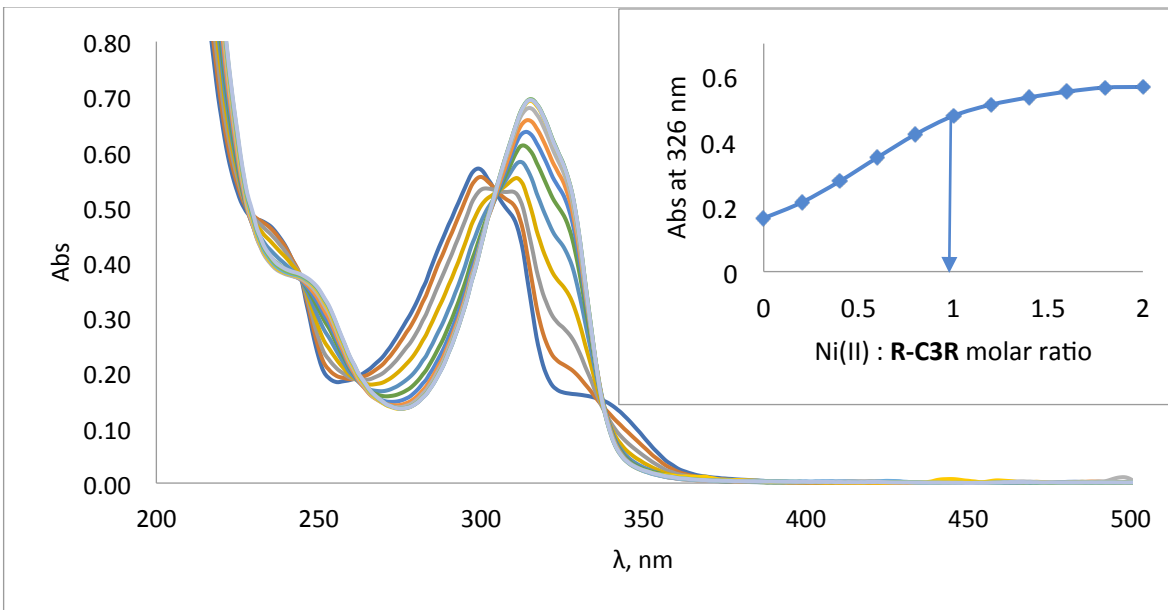
**Figure S17.** UV-Vis titration of **C3B** (17  $\mu\text{M}$ ) with  $\text{Ni}^{2+}$  acetate in ACN.



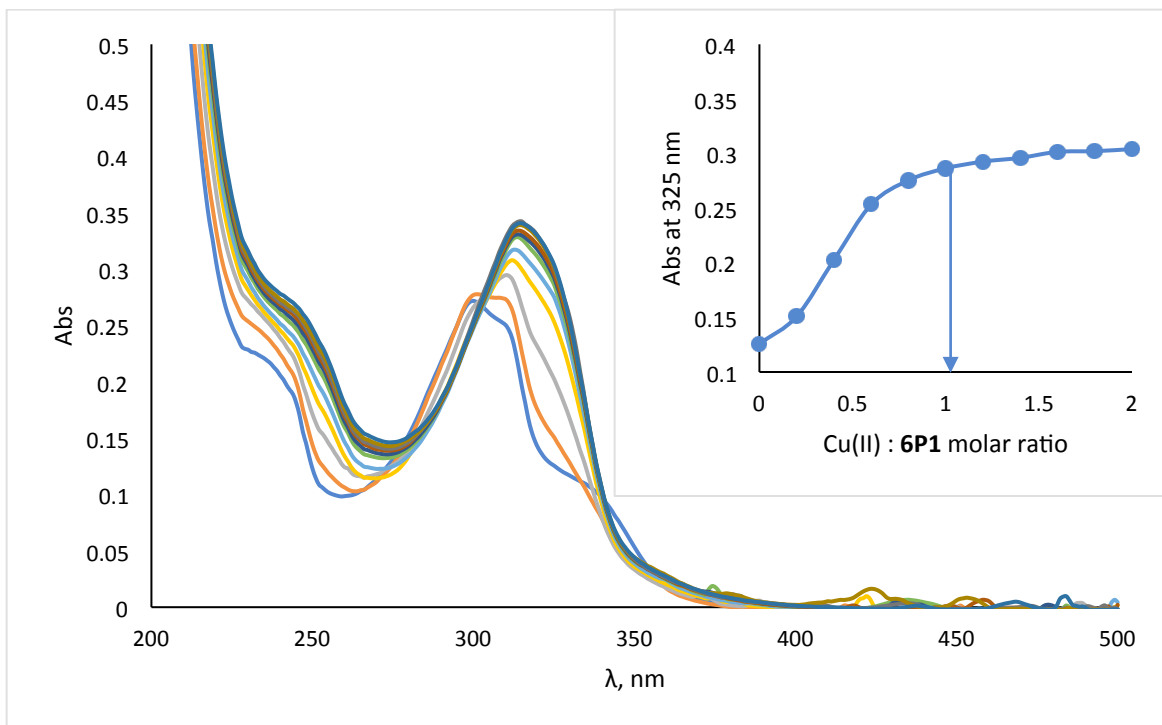
**Figure S18.** UV-Vis titration of **R-C3B** (17  $\mu\text{M}$ ) with  $\text{Cu}^{2+}$  acetate in ACN.



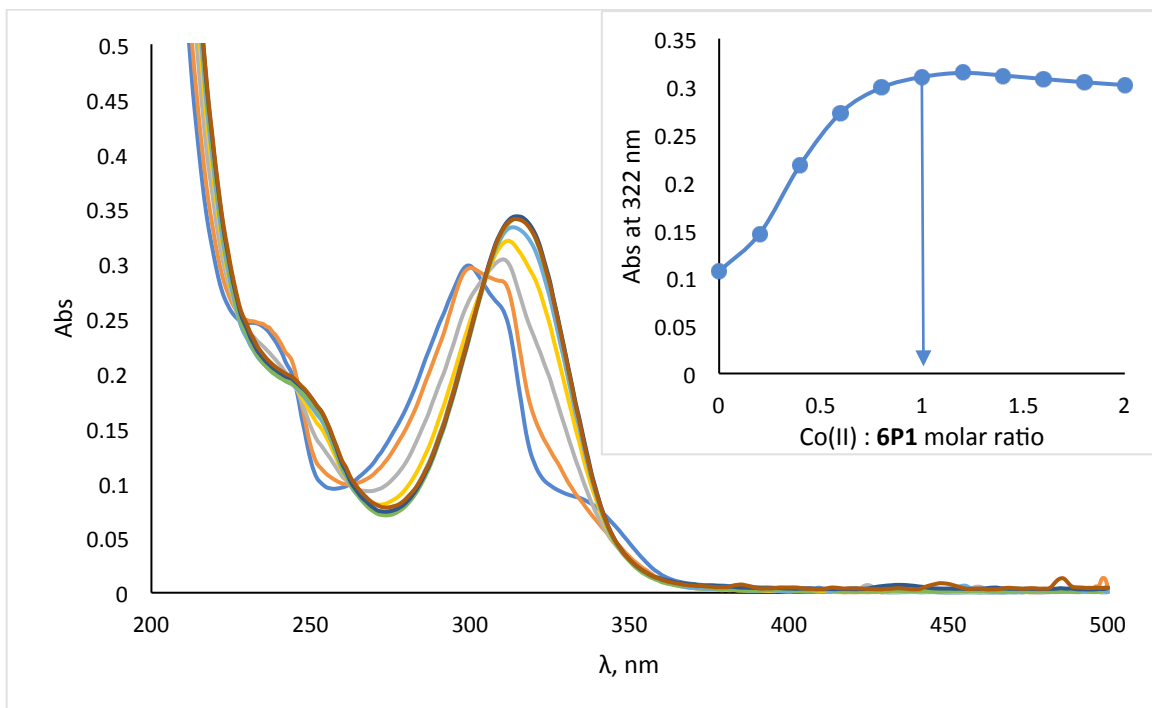
**Figure S19.** UV-Vis titration of **R-C3B** ( $17 \mu\text{M}$ ) with  $\text{Co}^{2+}$  acetate in ACN.



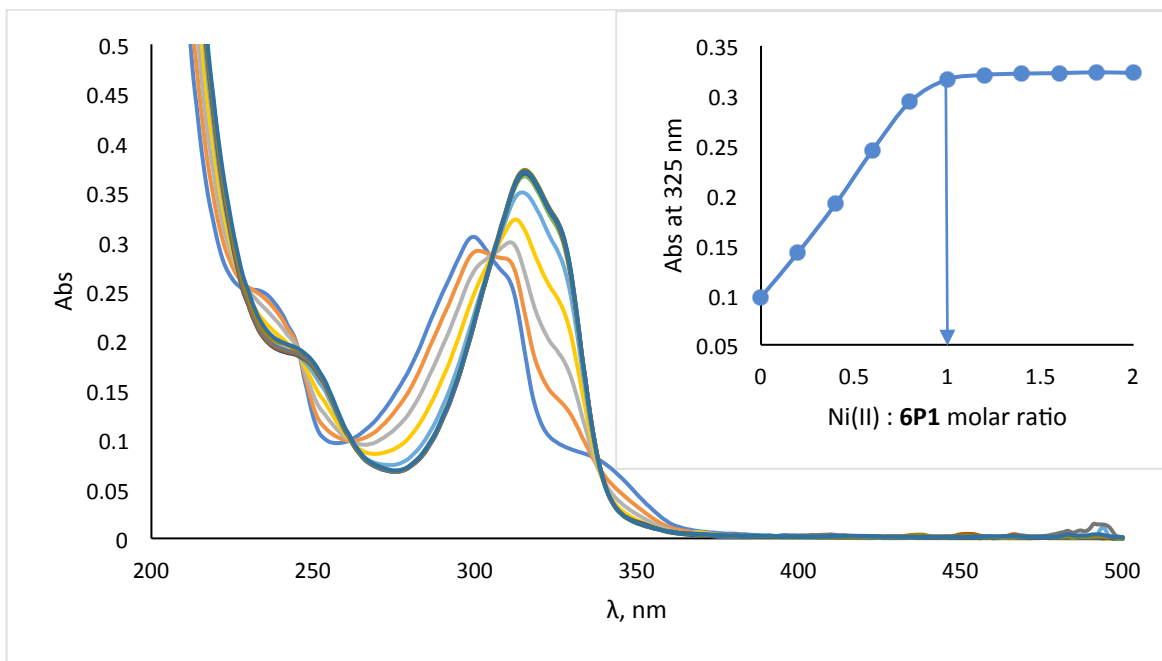
**Figure S20.** UV-Vis titration of **R-C3B** ( $17 \mu\text{M}$ ) with  $\text{Ni}^{2+}$  acetate in ACN.



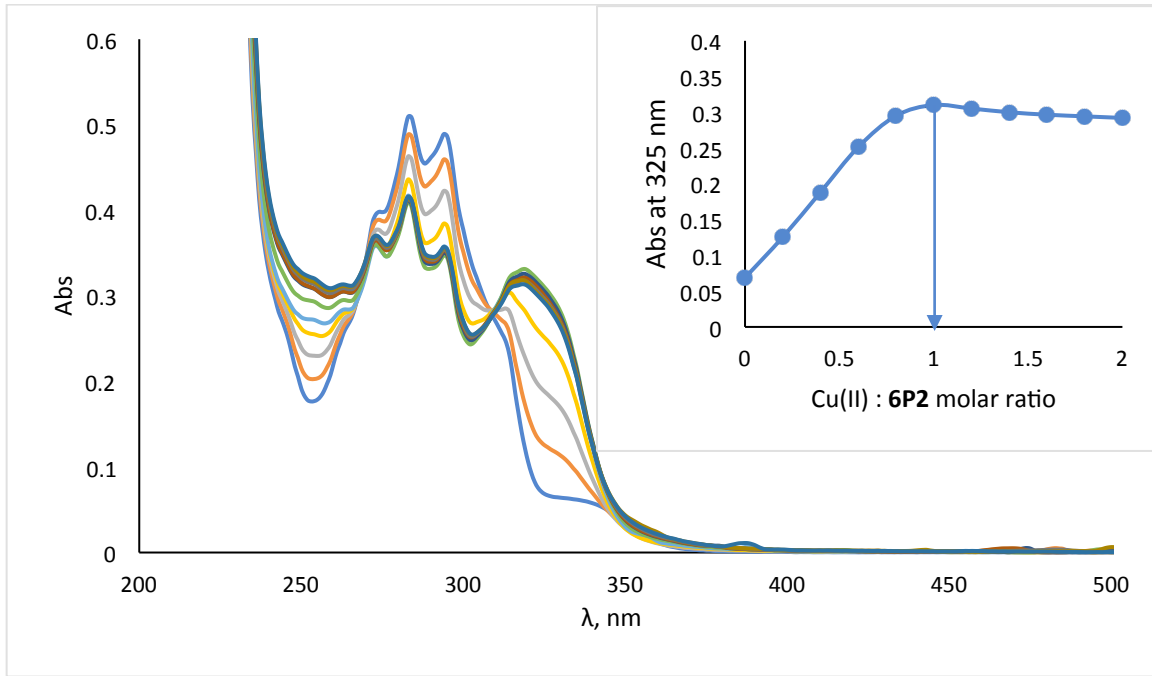
**Figure S21.** UV-Vis titration of **6P1** (17  $\mu\text{M}$ ) with  $\text{Cu}^{2+}$  acetate in ACN.



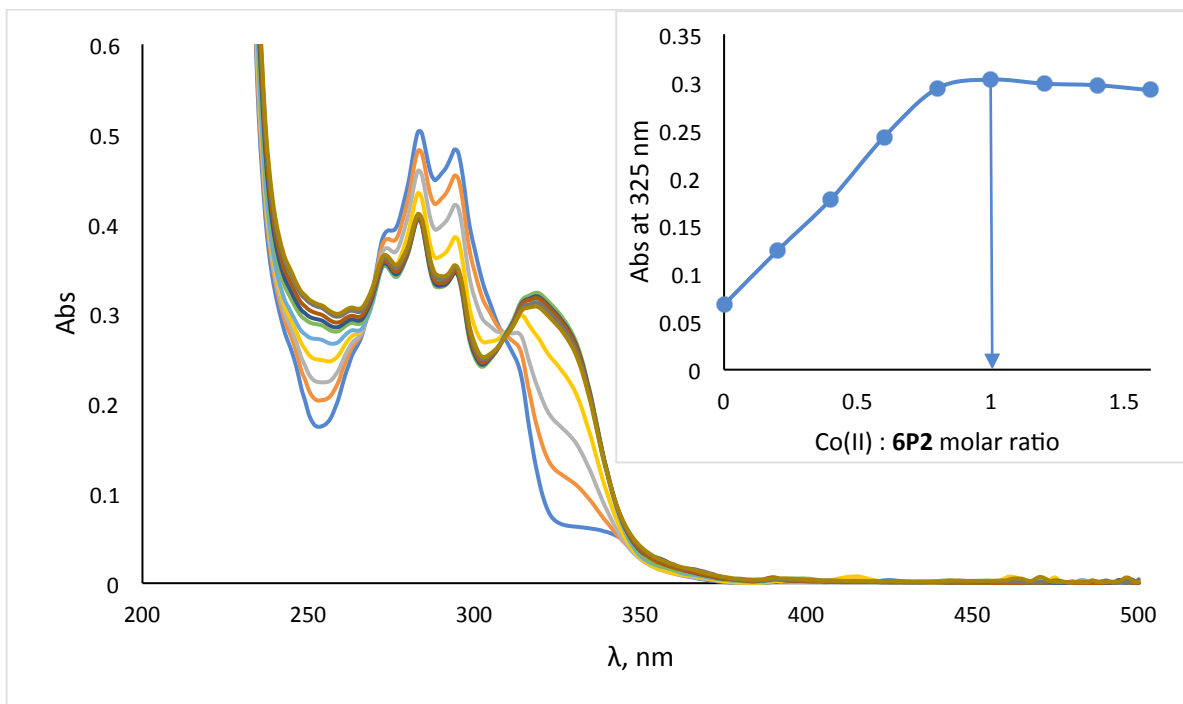
**Figure S22.** UV-Vis titration of **6P1** (17  $\mu\text{M}$ ) with  $\text{Co}^{2+}$  acetate in ACN.



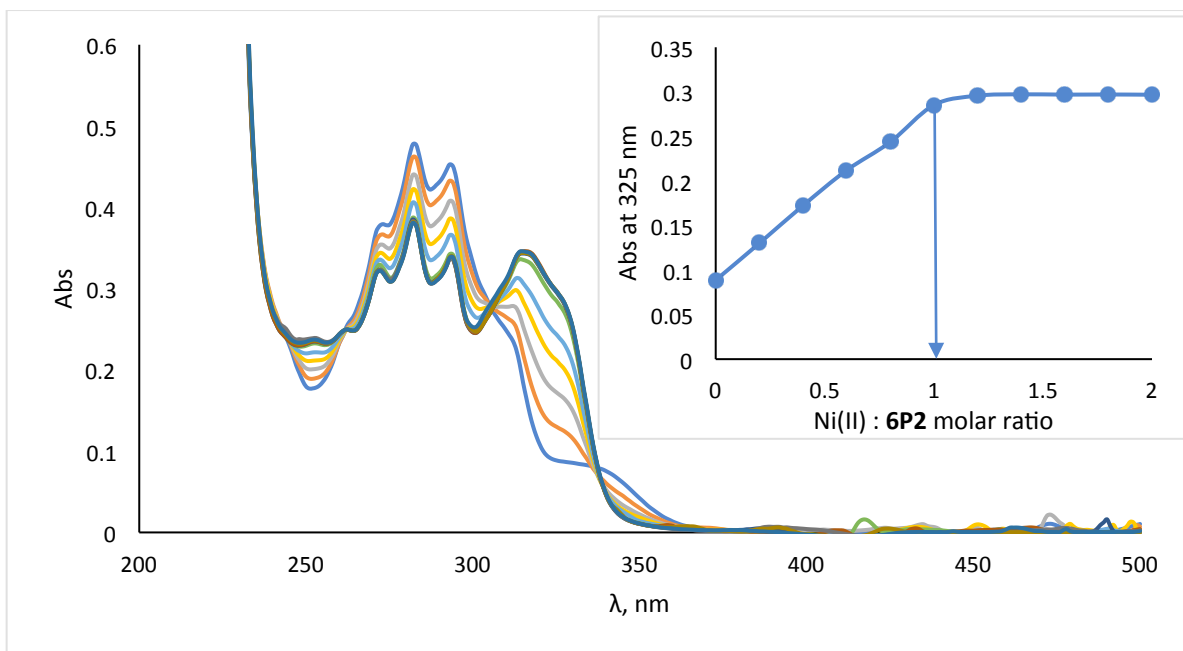
**Figure S23.** UV-Vis titration of **6P1** (17  $\mu\text{M}$ ) with  $\text{Ni}^{2+}$  acetate in ACN.



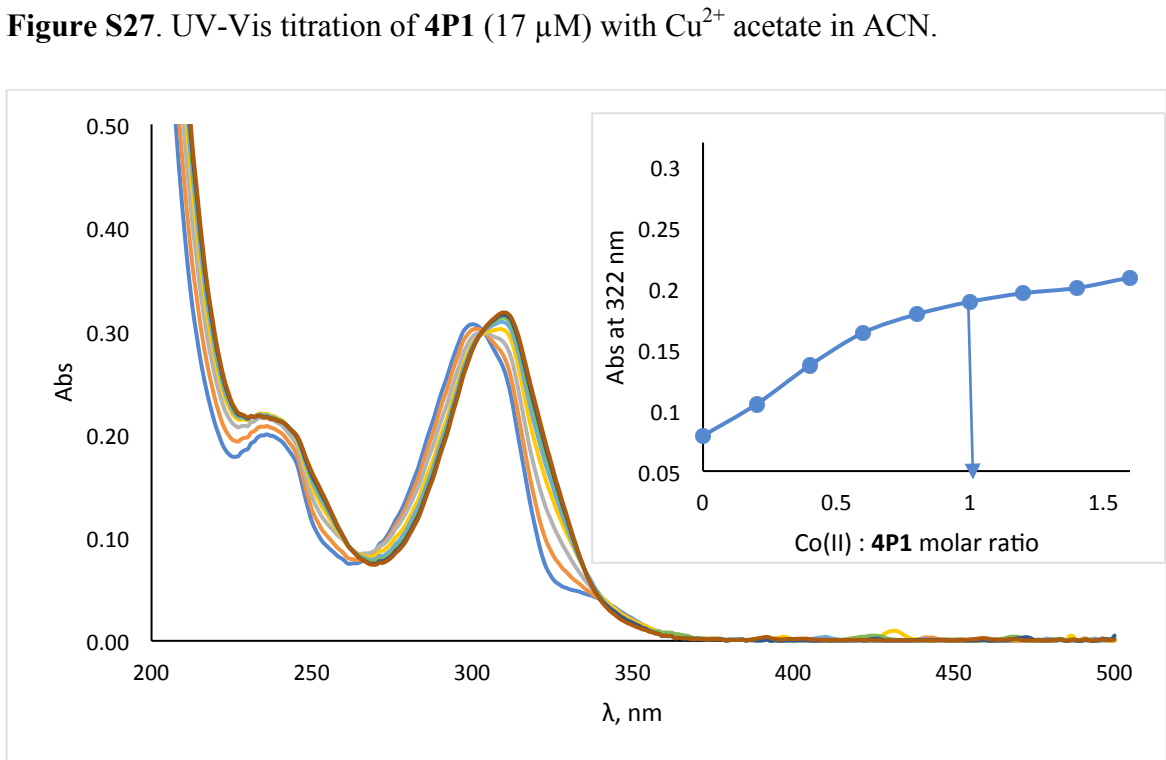
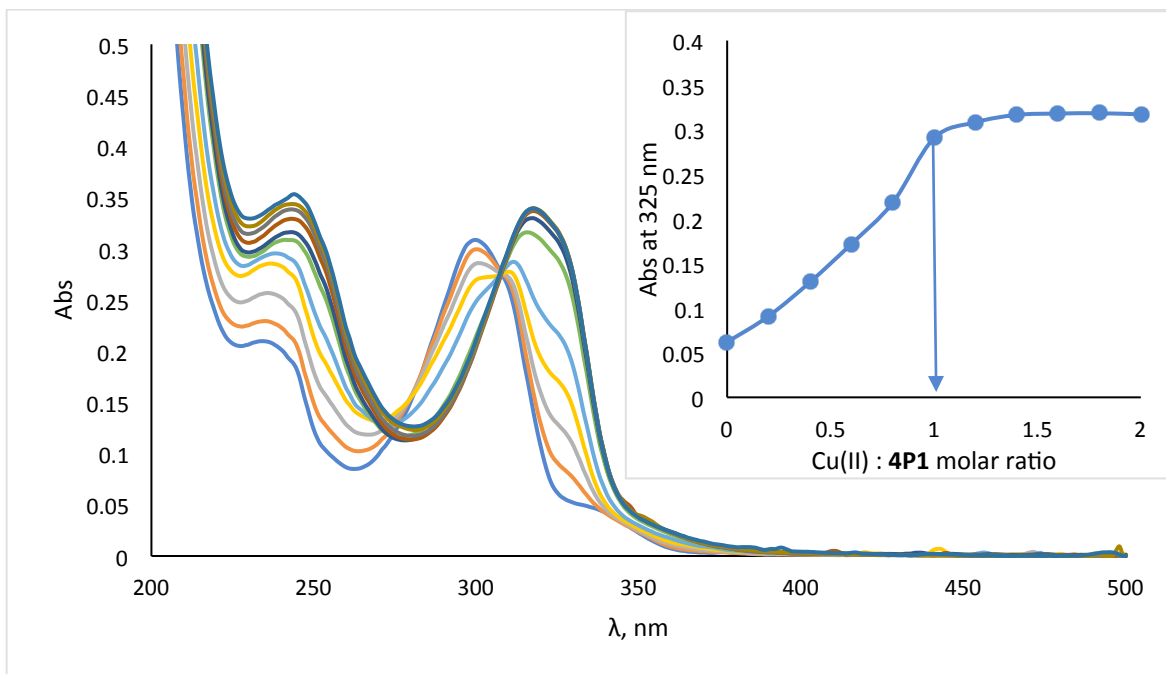
**Figure S24.** UV-Vis titration of **6P2** (17  $\mu\text{M}$ ) with  $\text{Cu}^{2+}$  acetate in ACN.



**Figure S25.** UV-Vis titration of **6P2** (17  $\mu\text{M}$ ) with  $\text{Co}^{2+}$  acetate in ACN.



**Figure S26.** UV-Vis titration of **6P2** (17  $\mu\text{M}$ ) with  $\text{Ni}^{2+}$  acetate in ACN.



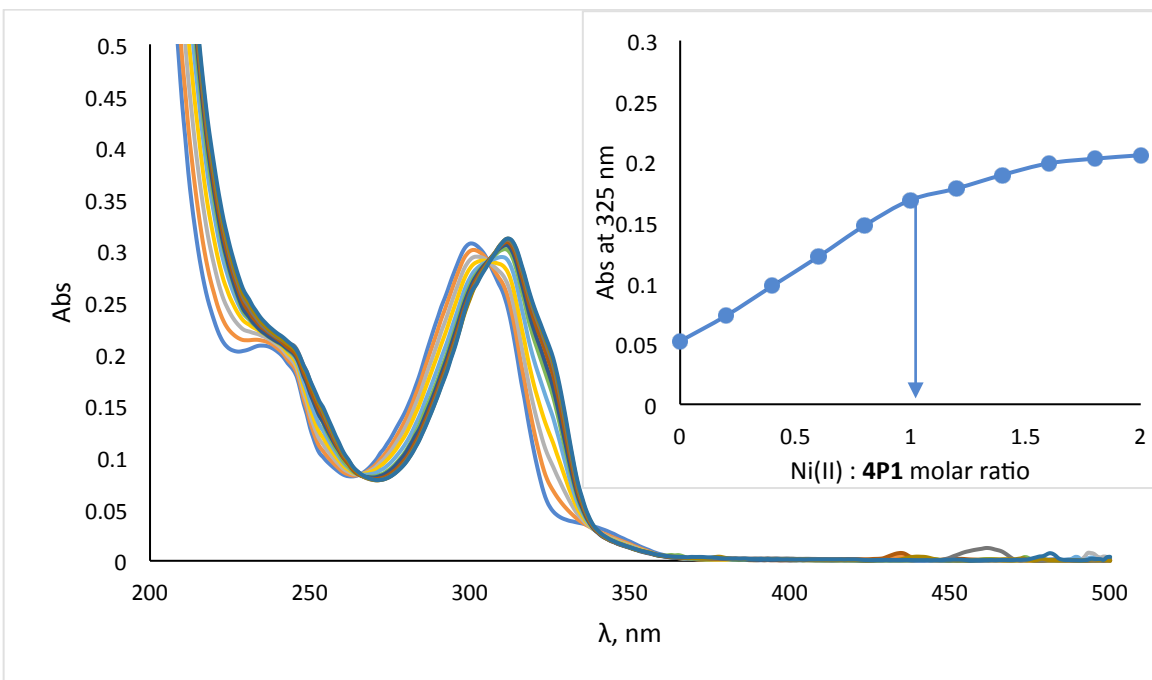


**Figure S29.** UV-Vis titration of **4P1** (17  $\mu\text{M}$ ) with  $\text{Ni}^{2+}$  acetate in ACN.

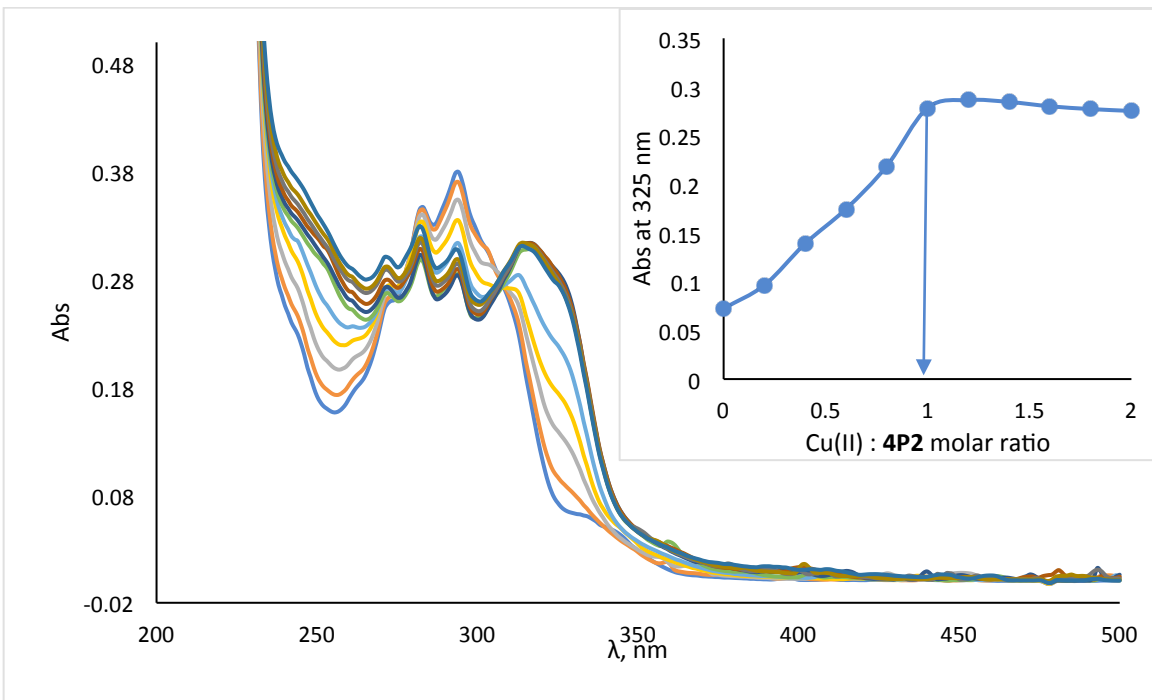


**Figure S30.** UV-Vis titration of **4P2** (17  $\mu\text{M}$ ) with  $\text{Cu}^{2+}$  acetate in ACN.

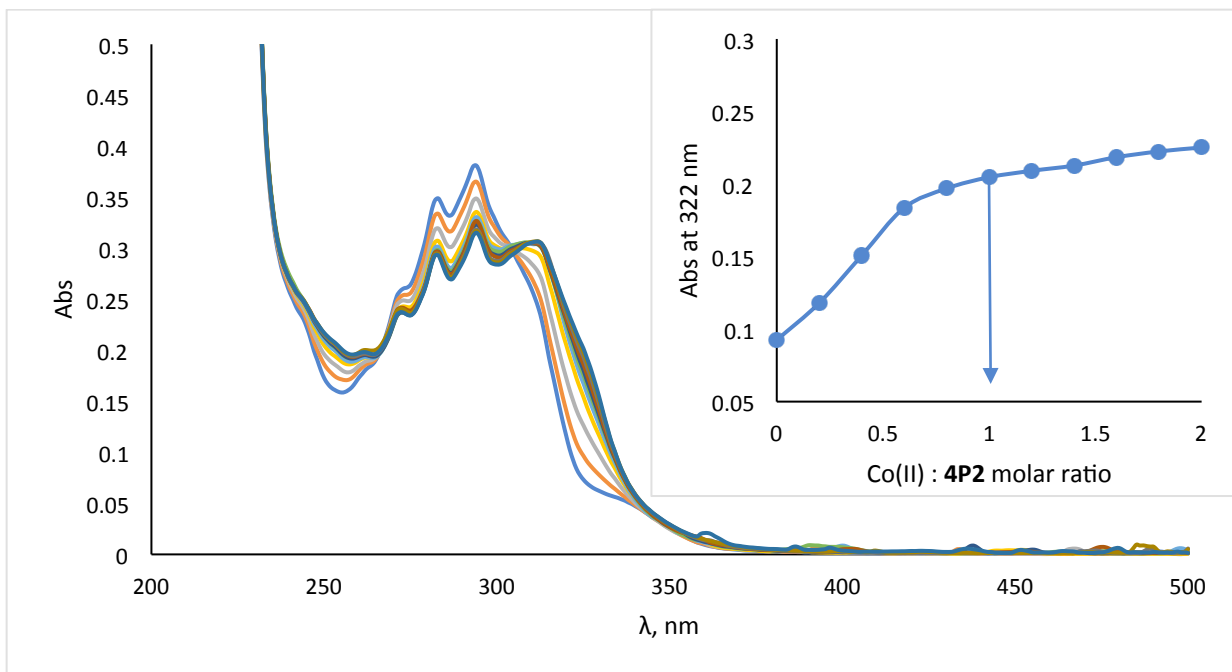


**Figure S31.** UV-Vis titration of **4P2** (17  $\mu\text{M}$ ) with  $\text{Co}^{2+}$  acetate in ACN.

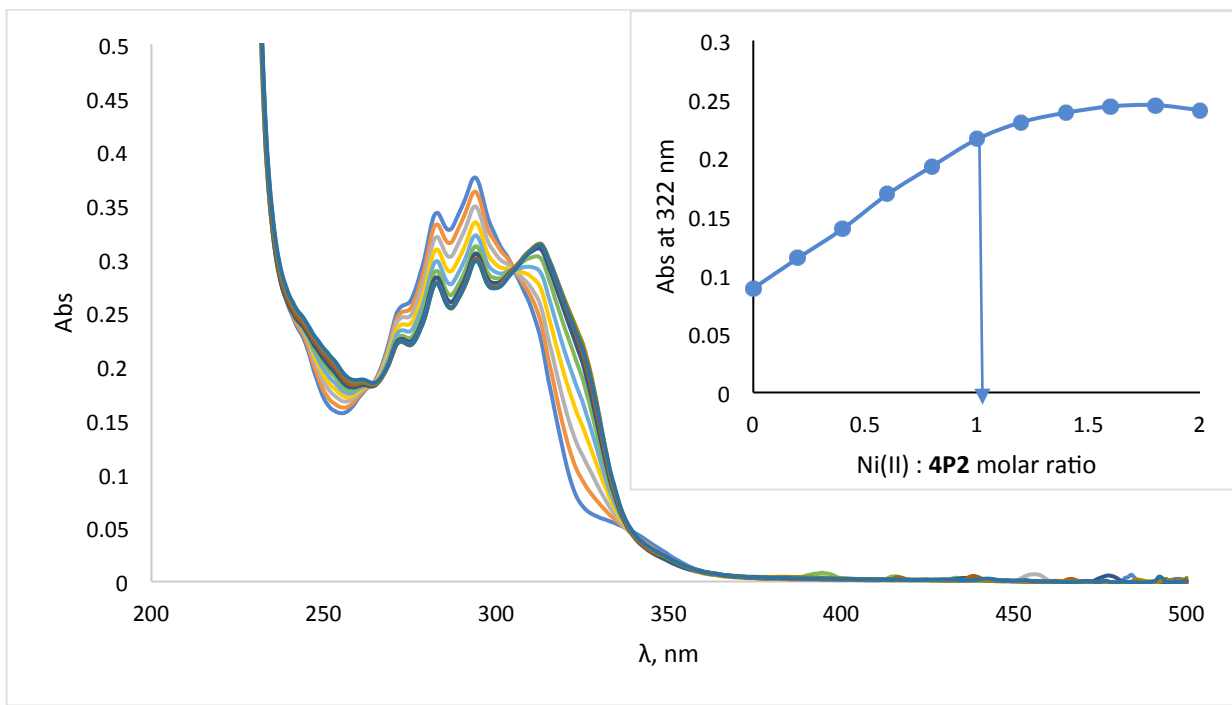


**Figure S32.** UV-Vis titration of **4P2** (17  $\mu\text{M}$ ) with  $\text{Ni}^{2+}$  acetate in ACN.

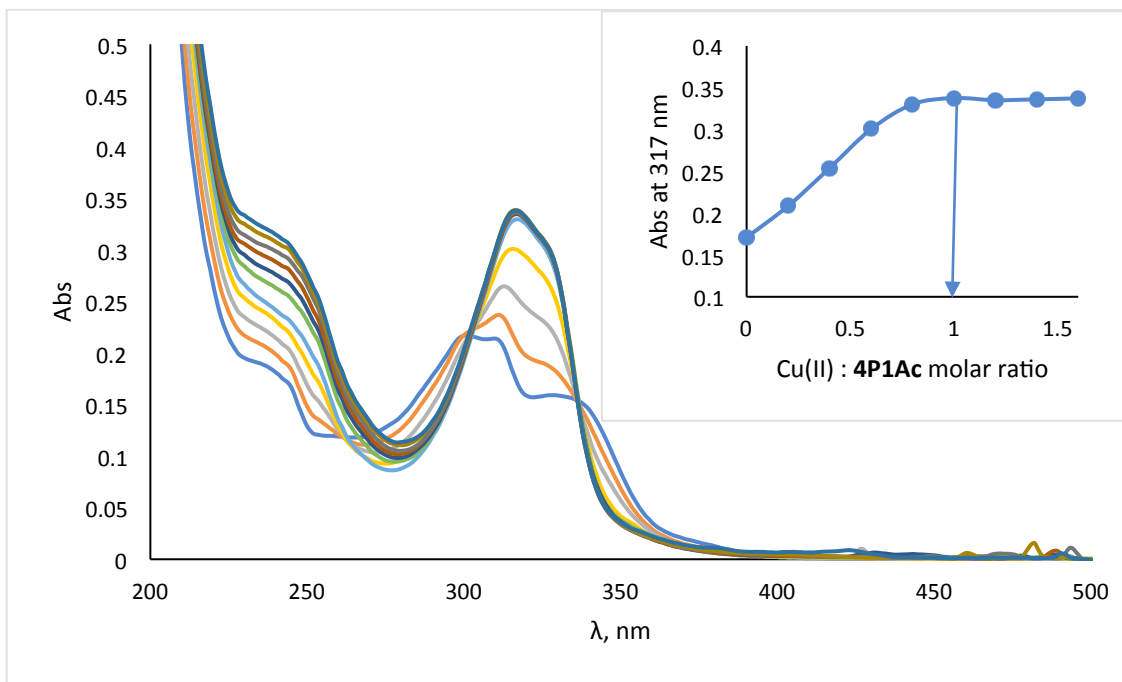


**Figure S33.** UV-Vis titration of **4P1Ac** (17  $\mu\text{M}$ ) with  $\text{Cu}^{2+}$  acetate in ACN.

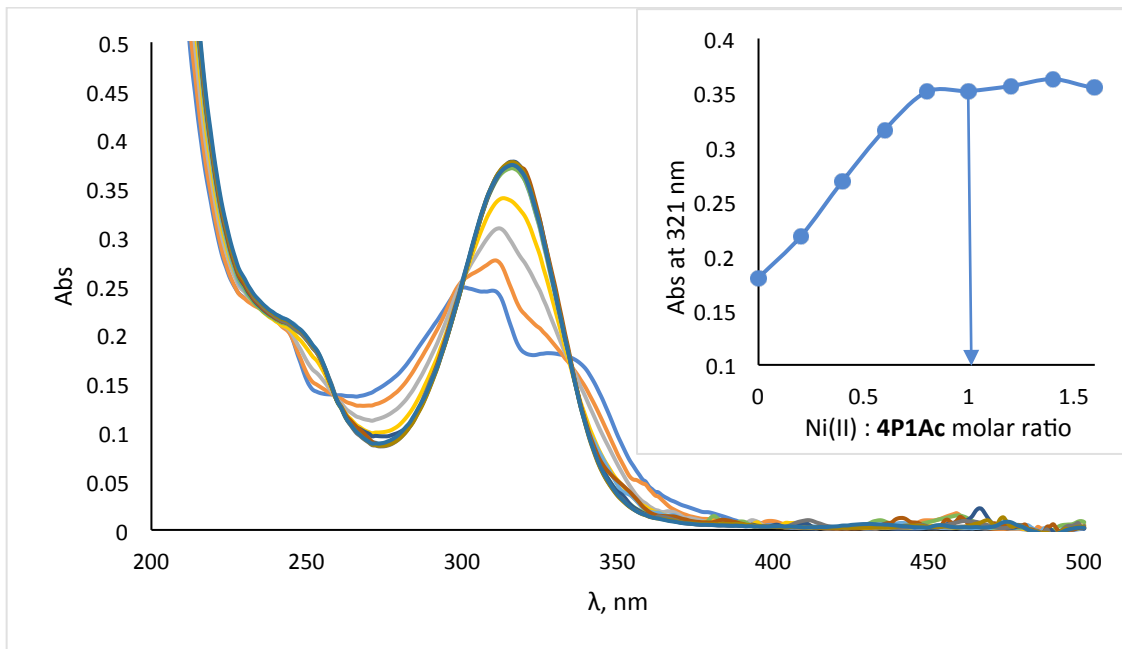


**Figure S34.** UV-Vis titration of **4P1Ac** (17  $\mu\text{M}$ ) with  $\text{Co}^{2+}$  acetate in ACN.

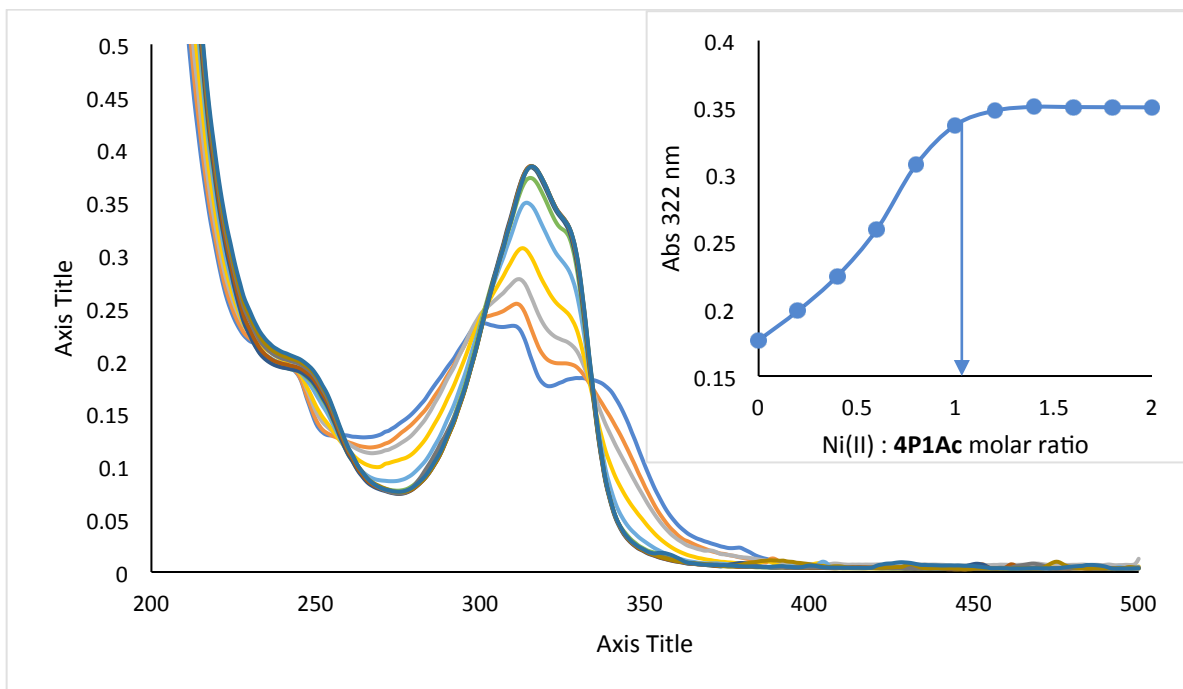


**Figure S35.** UV-Vis titration of **4P1Ac** (17  $\mu\text{M}$ ) with  $\text{Ni}^{2+}$  acetate in ACN.

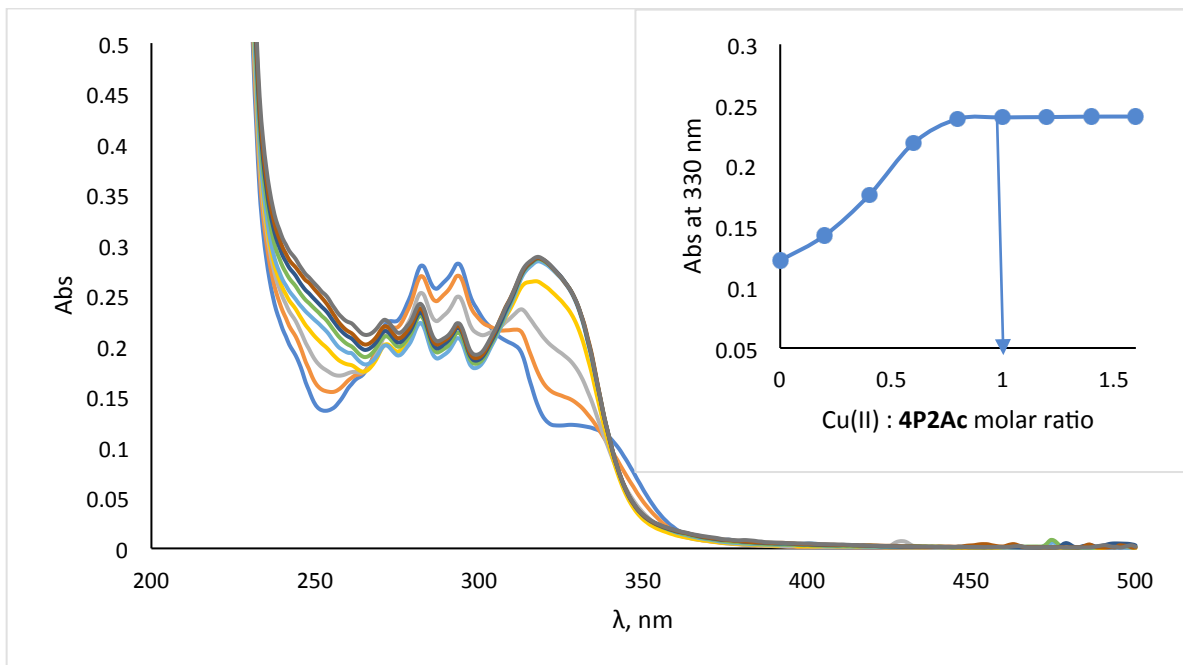


**Figure S36.** UV-Vis titration of **4P2Ac** (17  $\mu\text{M}$ ) with  $\text{Cu}^{2+}$  acetate in ACN.

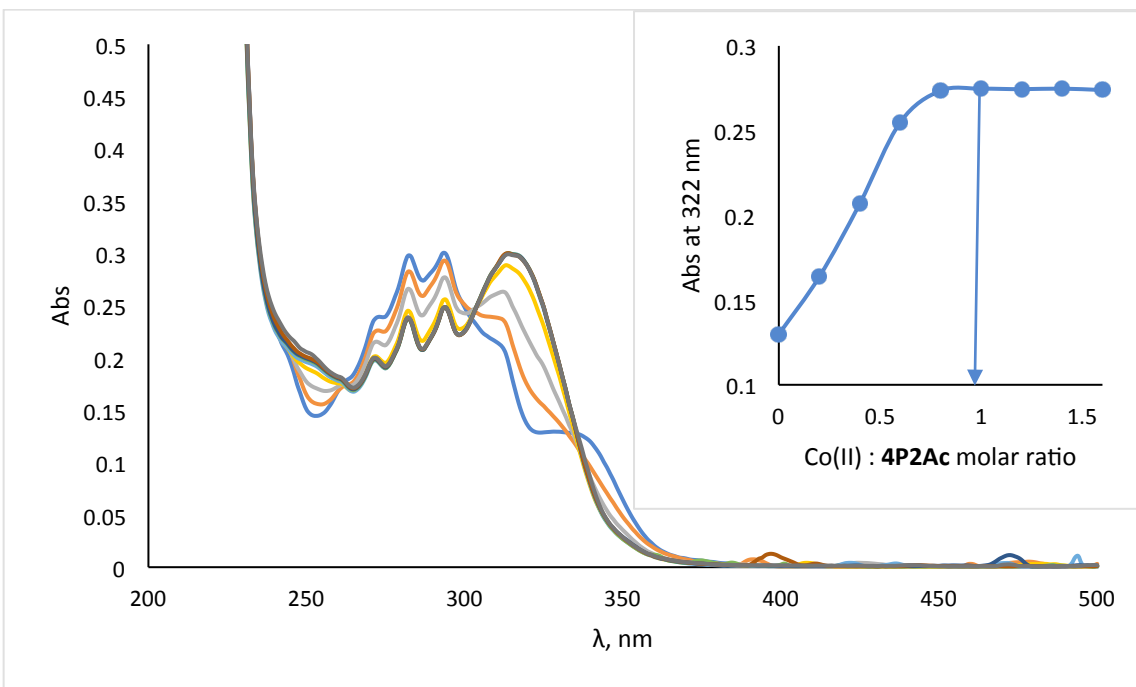


**Figure S37.** UV-Vis titration of **4P2Ac** (17  $\mu$ M) with  $\text{Co}^{2+}$  acetate in ACN.

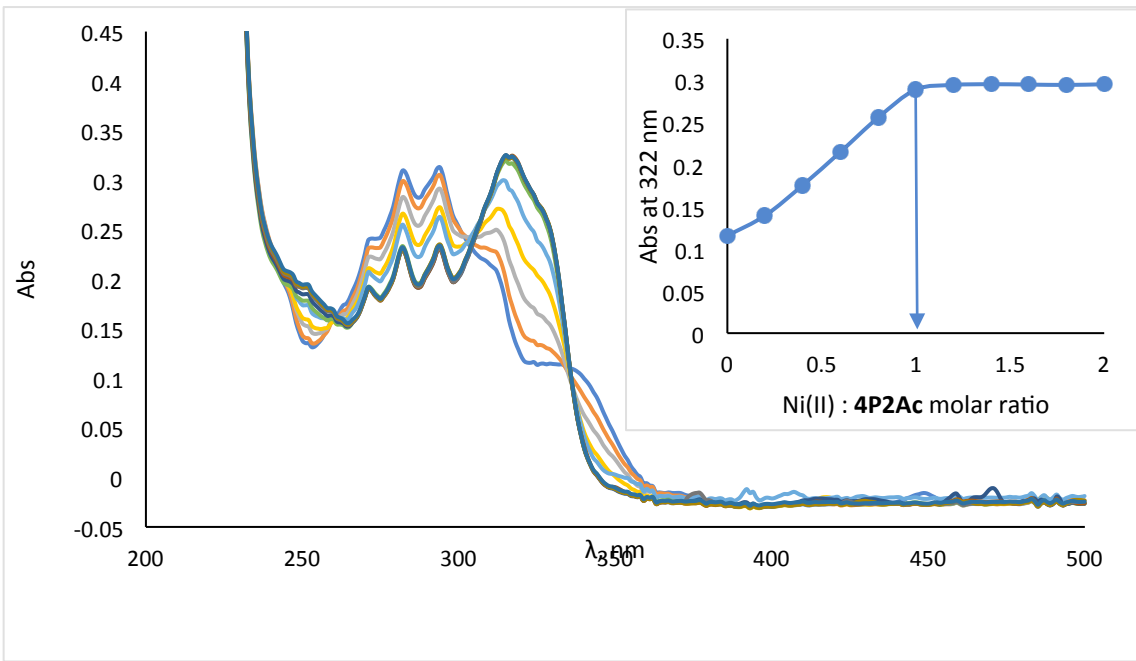


**Figure S38.** UV-Vis titration of **4P2Ac** (17  $\mu$ M) with  $\text{Ni}^{2+}$  acetate in ACN.

### Job plot data

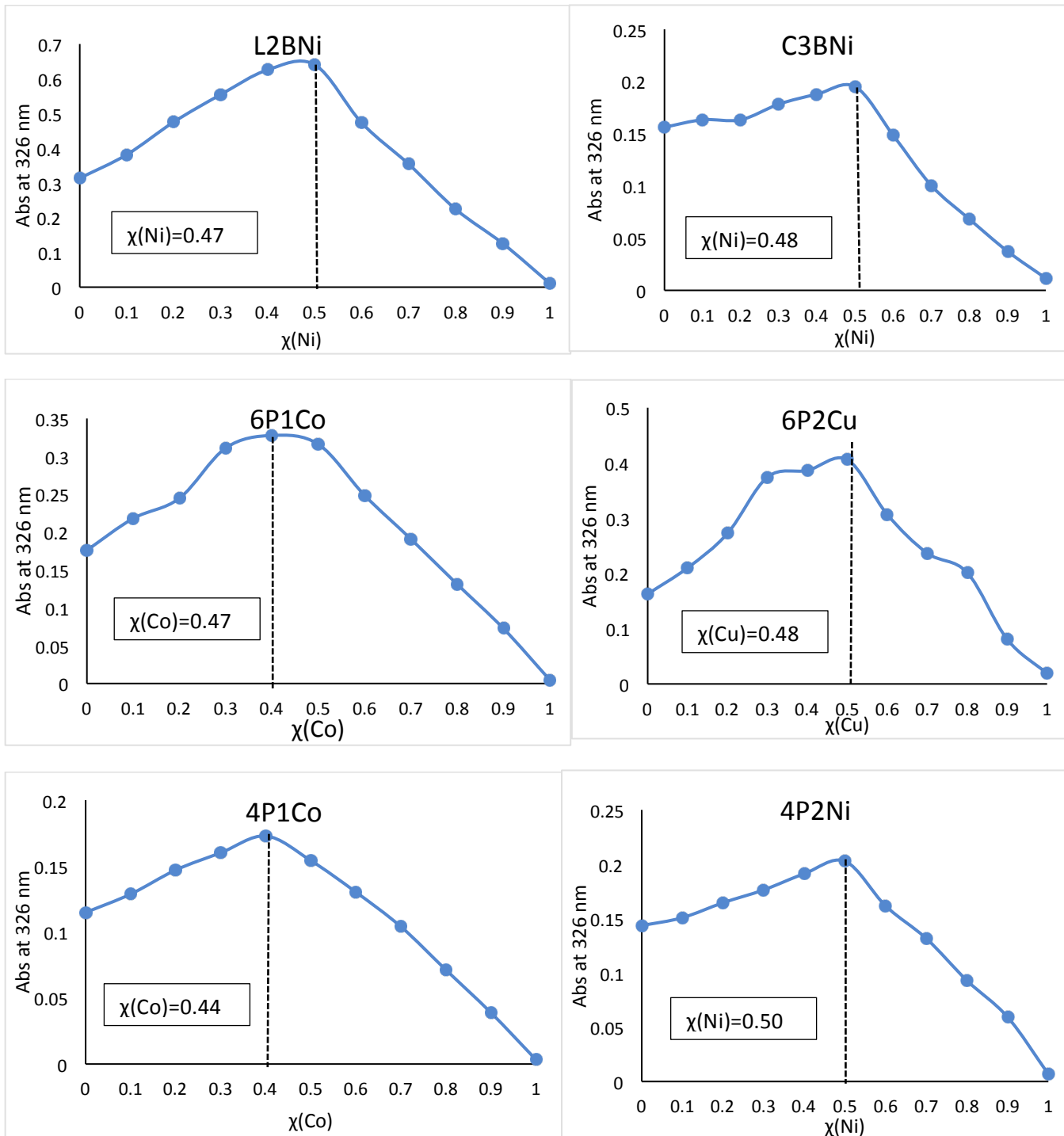


**Figure S39.** Job-plot of peptoid oligomers with metal ions measured in acetonitrile (22-66  $\mu\text{M}$  total concentration).

## CD data

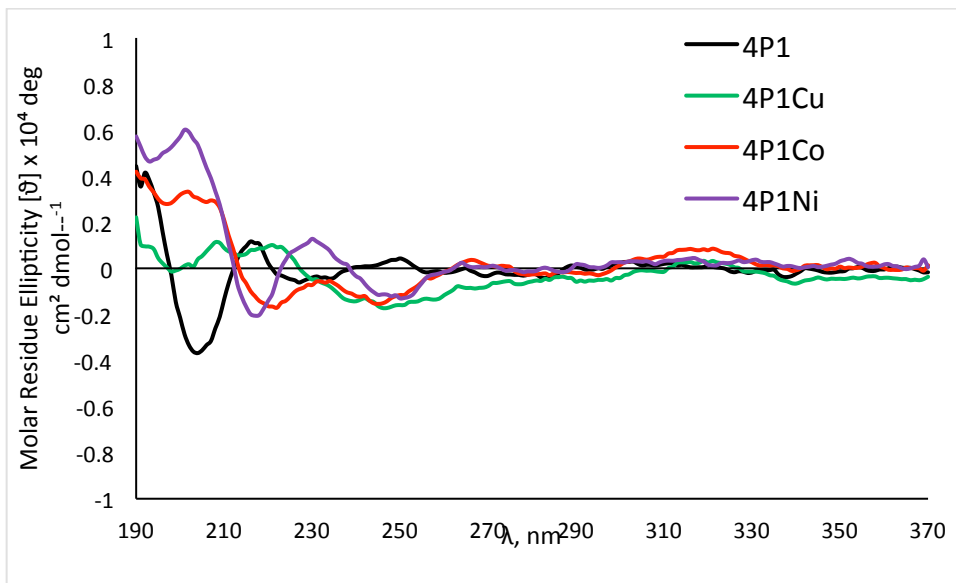


**Figure S40.** CD spectra of the peptoid oligomer **4P1** and its metal complexes measured at the concentration of 100 μM in ACN solution.

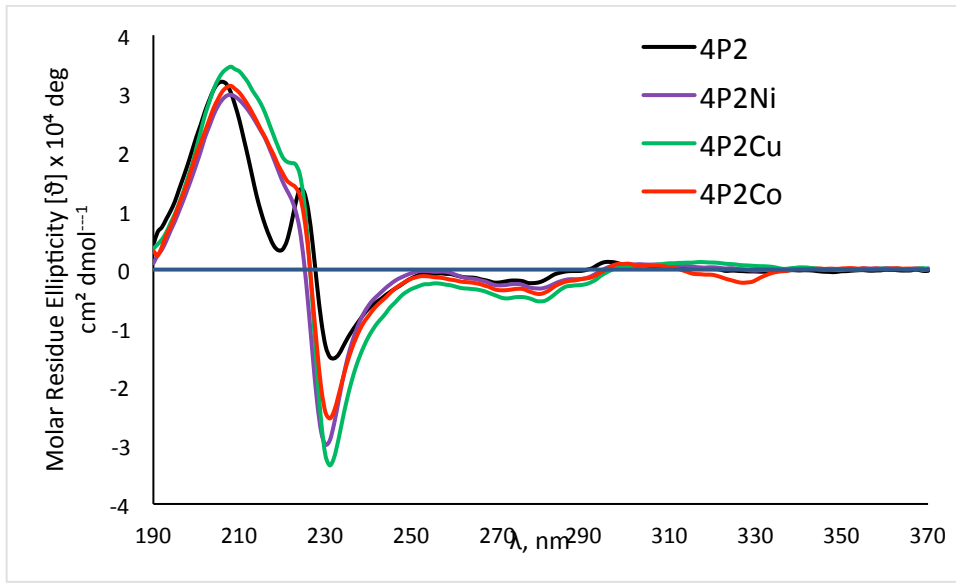


**Figure S41.** CD spectra of the peptoid oligomer **4P2** and its metal complexes measured at the concentration of 100 μM in ACN solution.

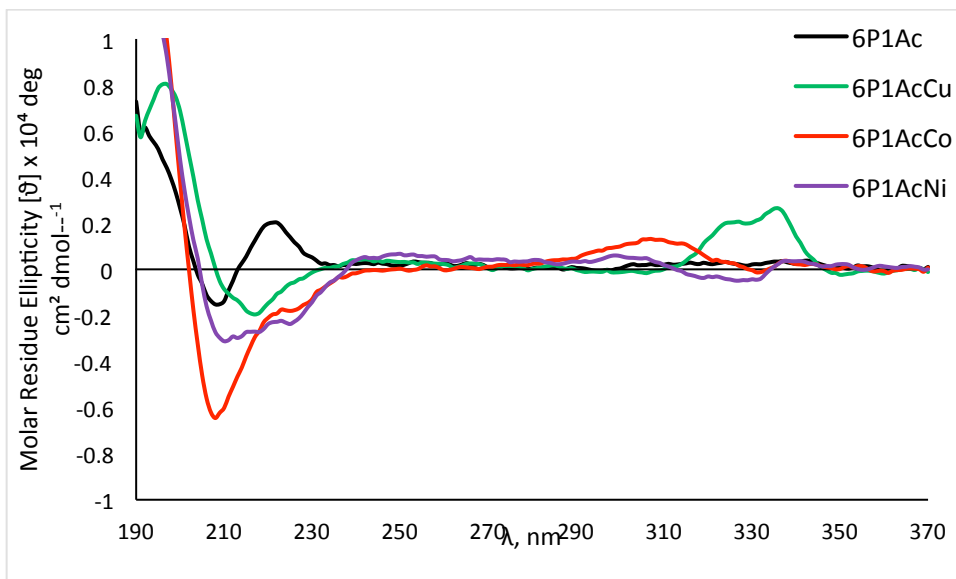


**Figure S42.** CD spectra of the peptoid oligomer **6P1Ac** and its metal complexes measured at the concentration of 100 μM in ACN solution.

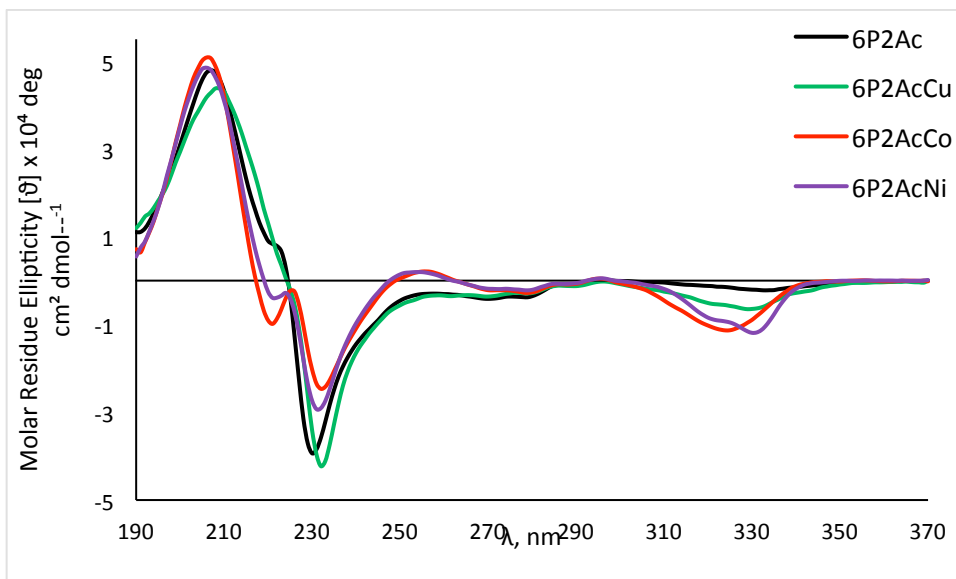


**Figure S43.** CD spectra of the peptoid oligomer **6P2Ac** and its metal complexes measured at the concentration of 100 μM in ACN solution.

### FTIR data

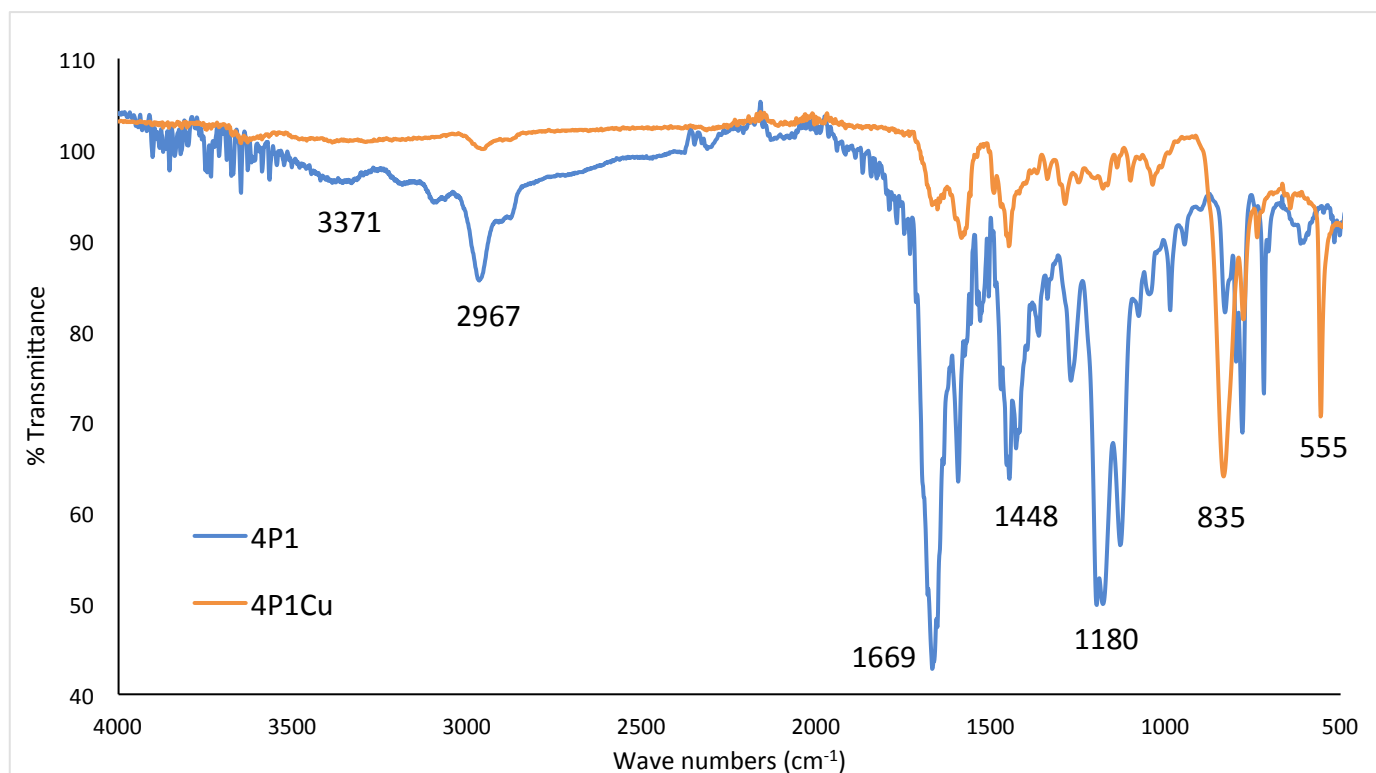


**Figure S44.** ATR-FTIR spectra of the peptoid oligomer **4P1** and its  $\text{Cu}^{2+}$  complex.

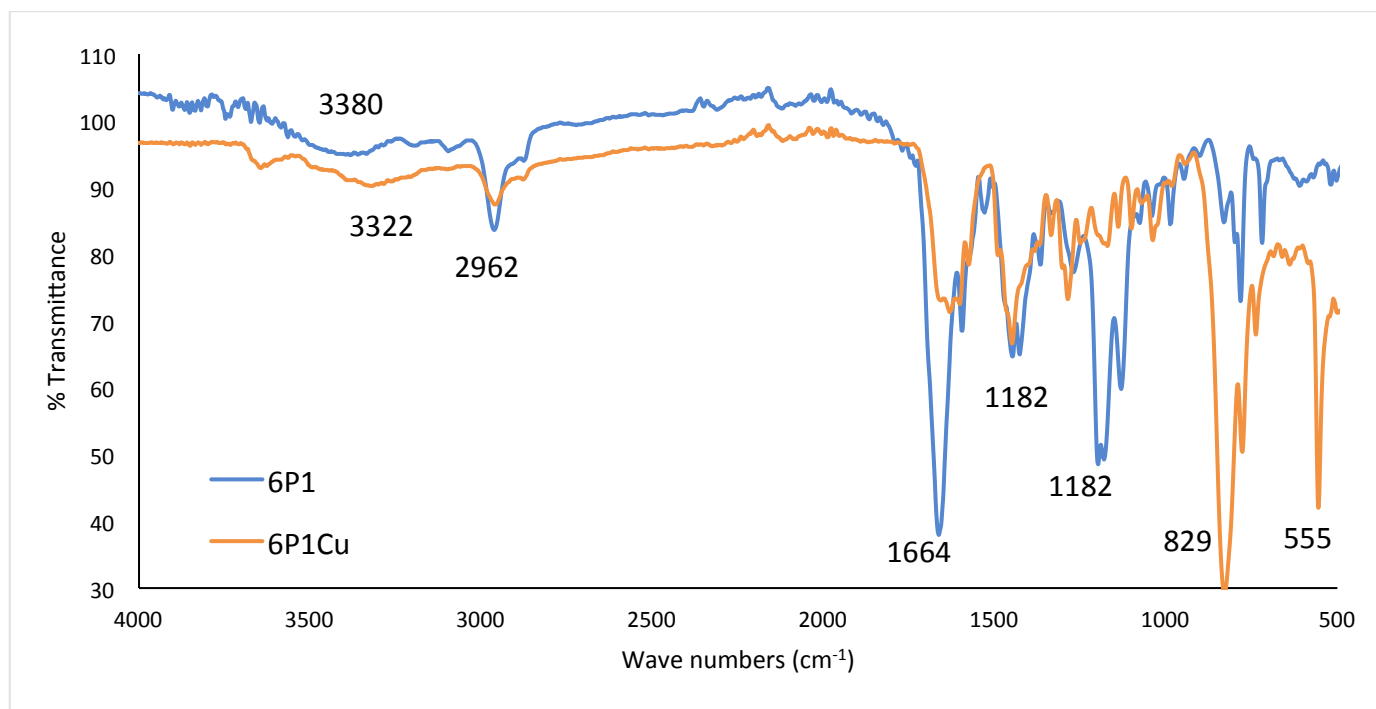


**Figure S45.** ATR-FTIR spectra of the peptoid oligomer **6P1** and its  $\text{Cu}^{2+}$  complex.

### ESI-MS of the peptoid oligomers:

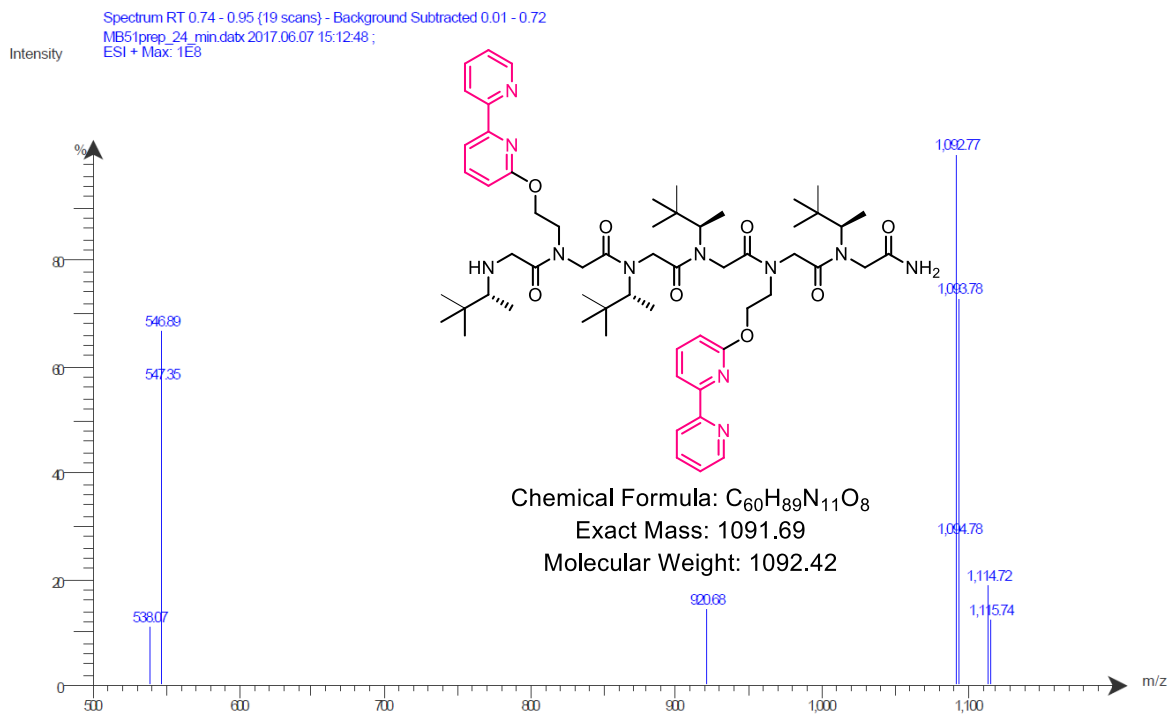


**Figure S46.** ESI-MS traces of peptoid oligomer **6P1**

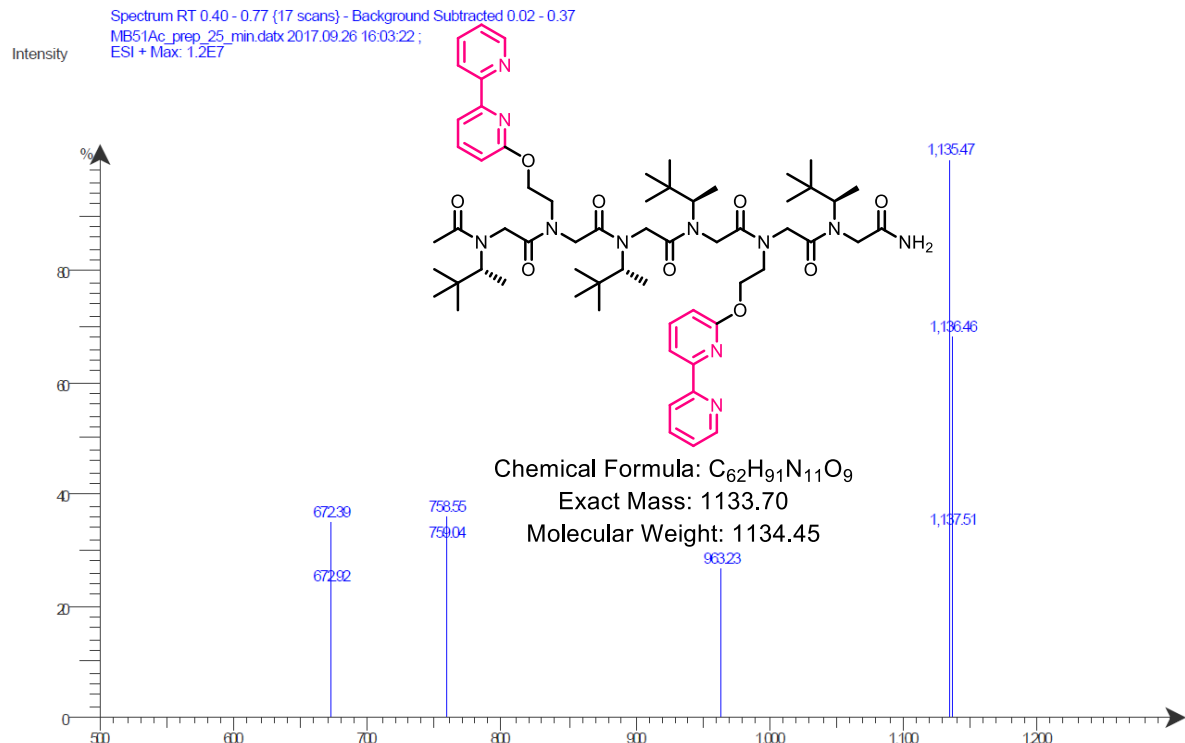


**Figure S47.** ESI-MS traces of peptoid oligomer **6P1Ac**

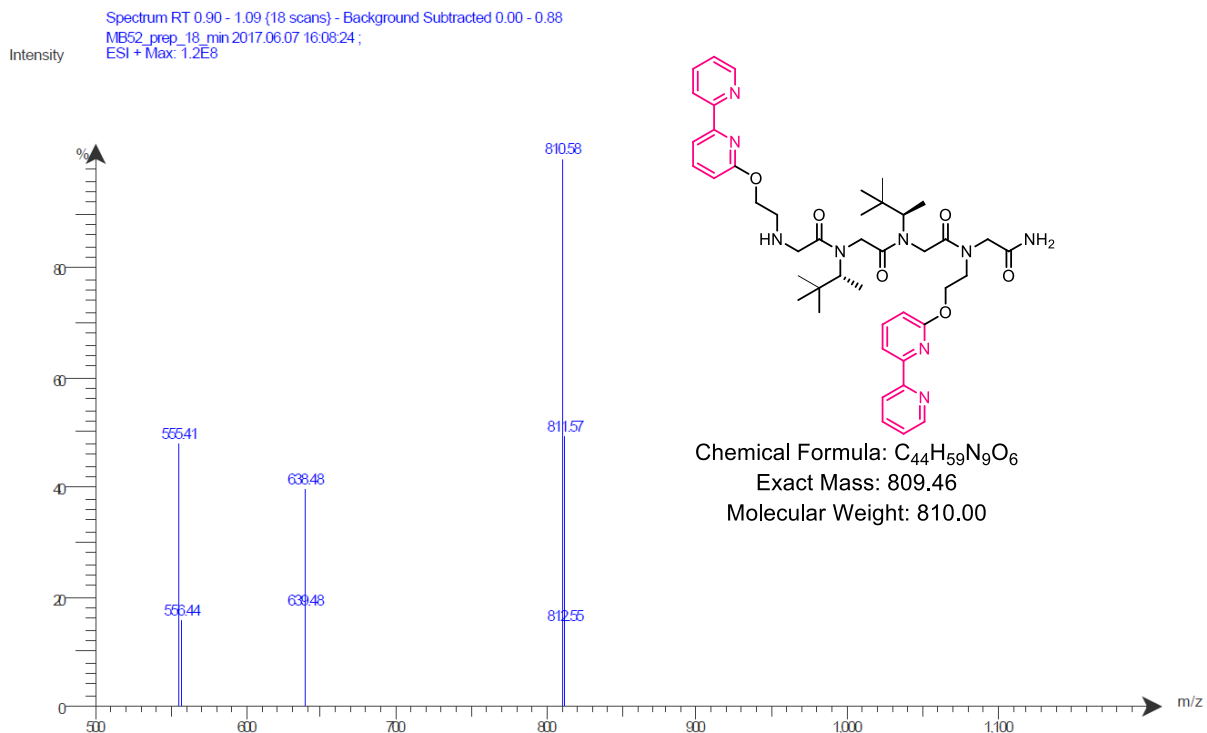


**Figure S48.** ESI-MS traces of peptoid oligomer **4P1**

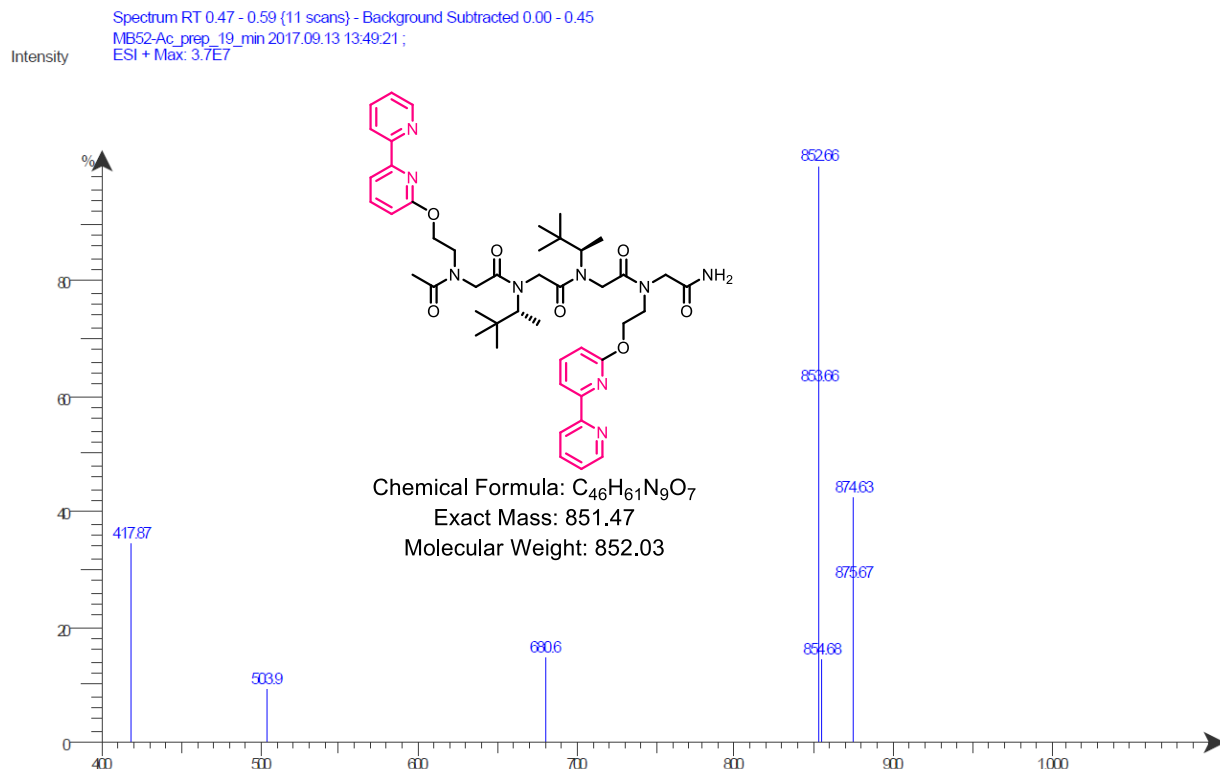


**Figure S49.** ESI-MS traces of peptoid oligomer **4P1Ac**

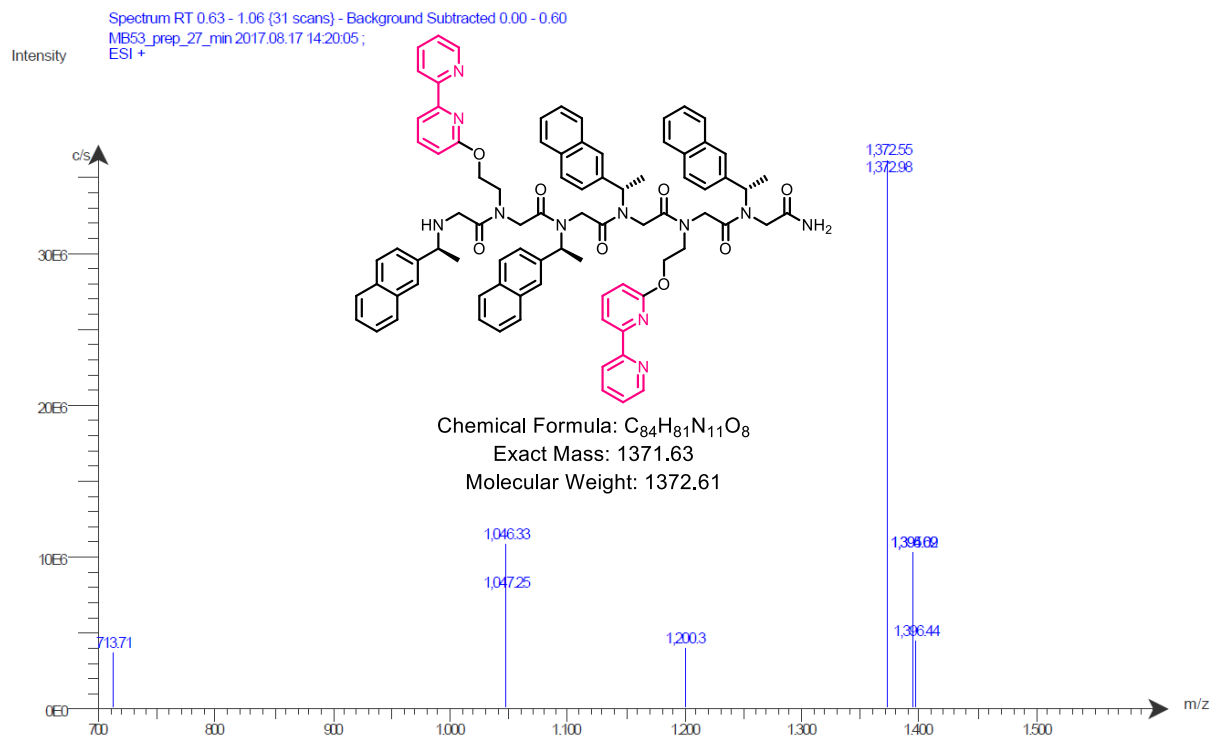


**Figure S50.** ESI-MS traces of peptoid oligomer **6P2**

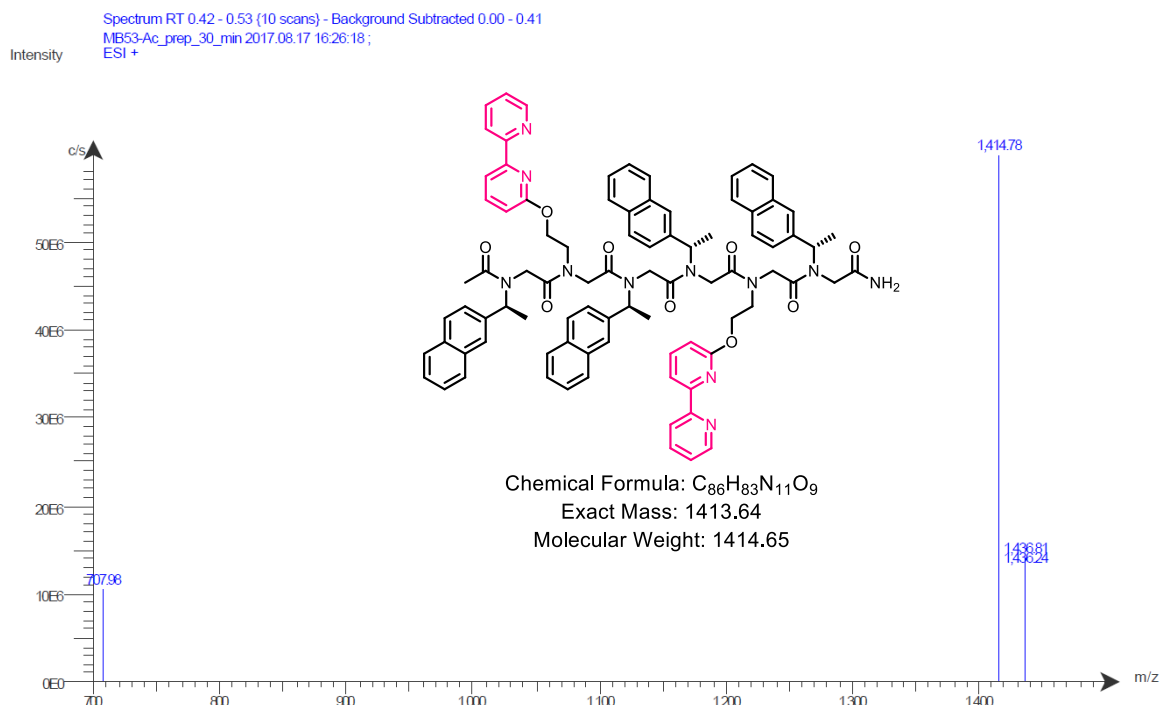


**Figure S51.** ESI-MS traces of peptoid oligomer **6P2Ac**

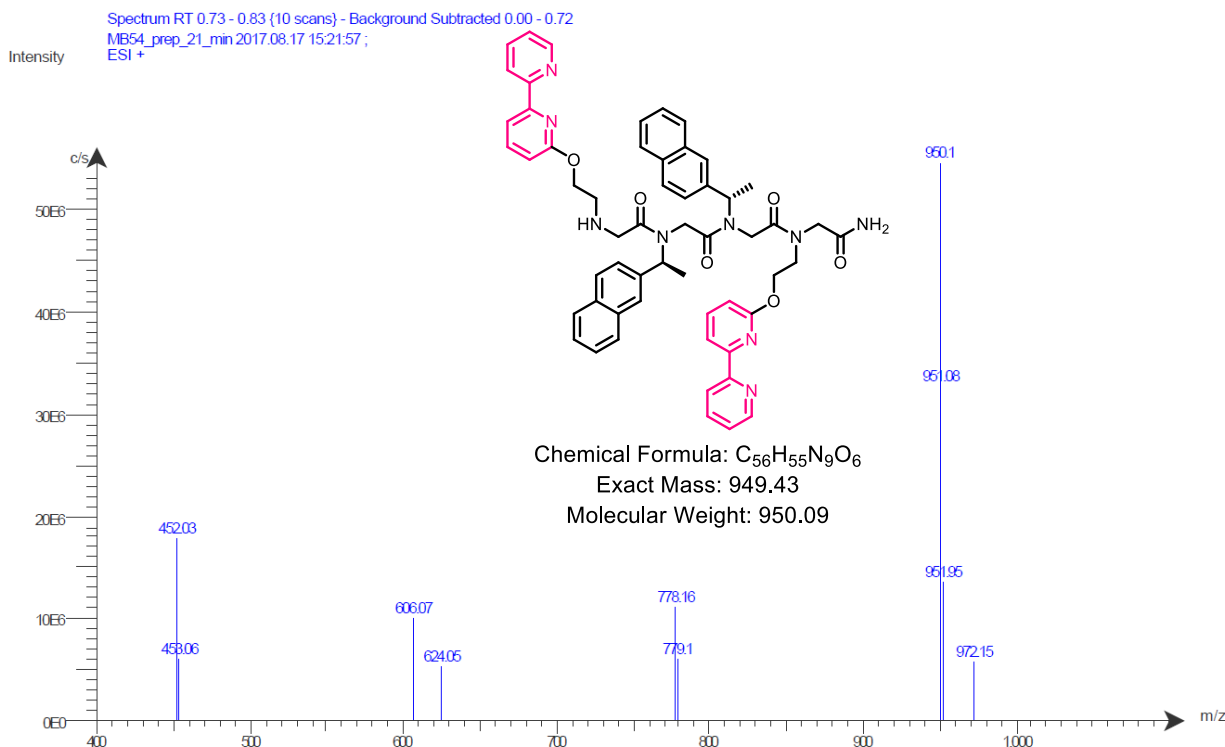


**Figure S52.** ESI-MS traces of peptoid oligomer **4P2**

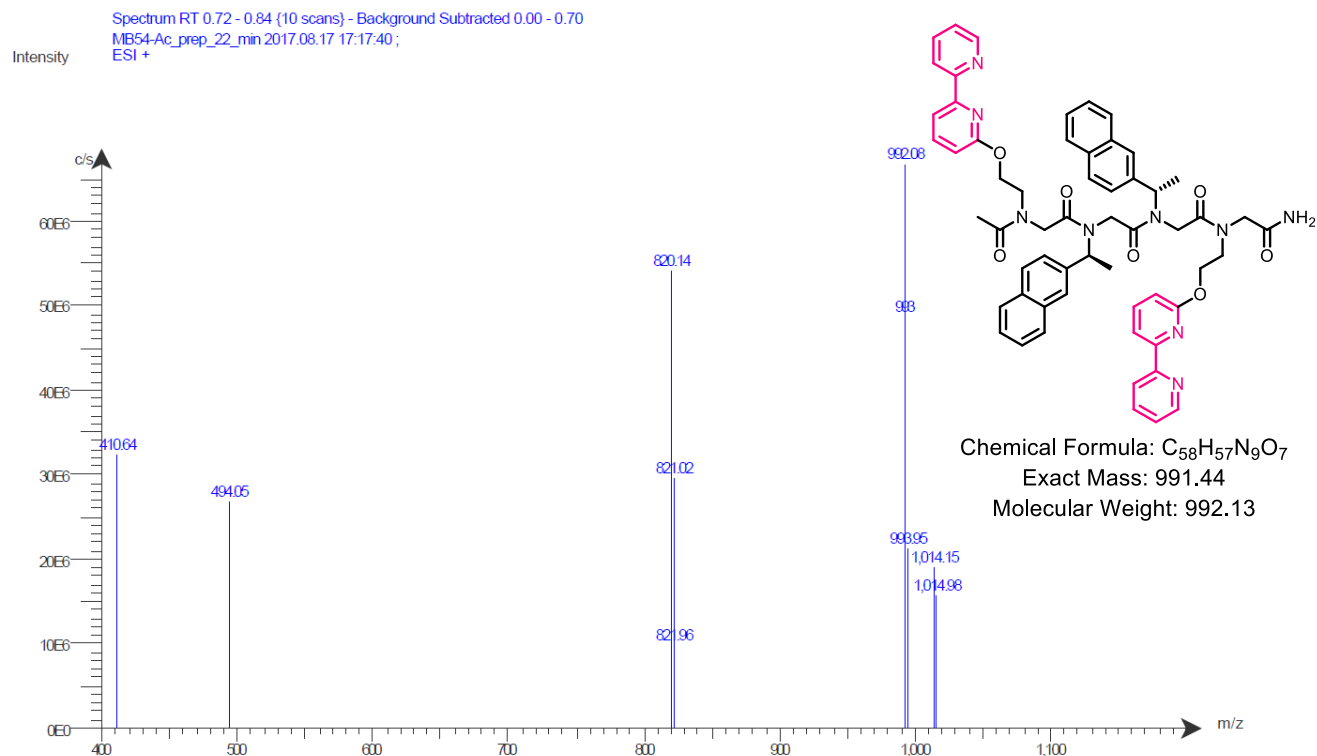


**Figure S53.** ESI-MS traces of peptoid oligomer **4P2Ac**

## ESI-MS of the metallopeptoids:

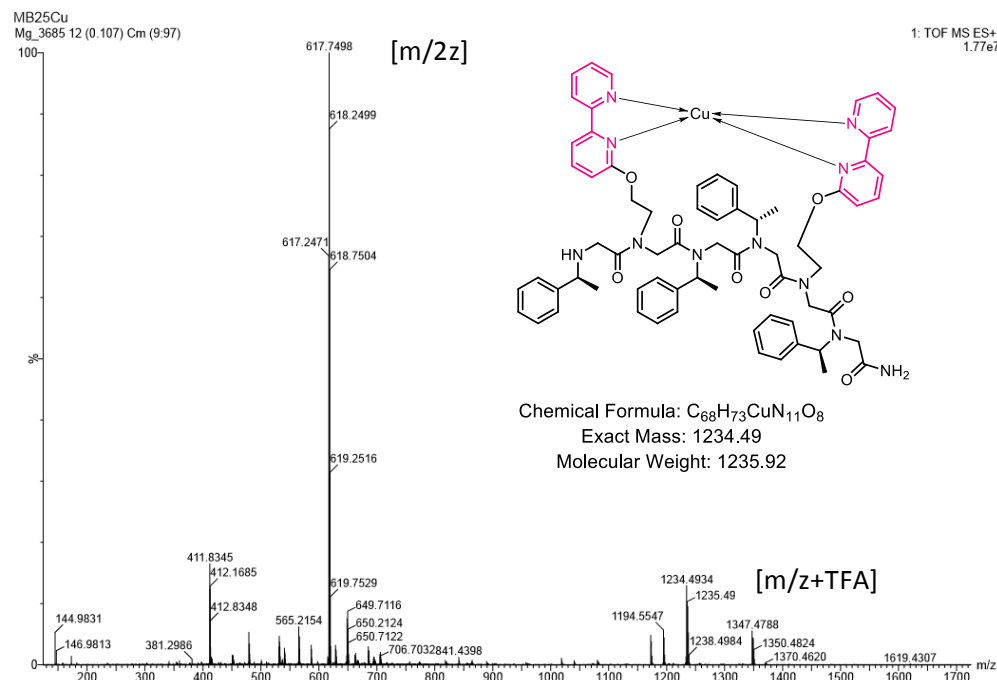


Figure S54. ESI-MS traces of L2BCu complex.

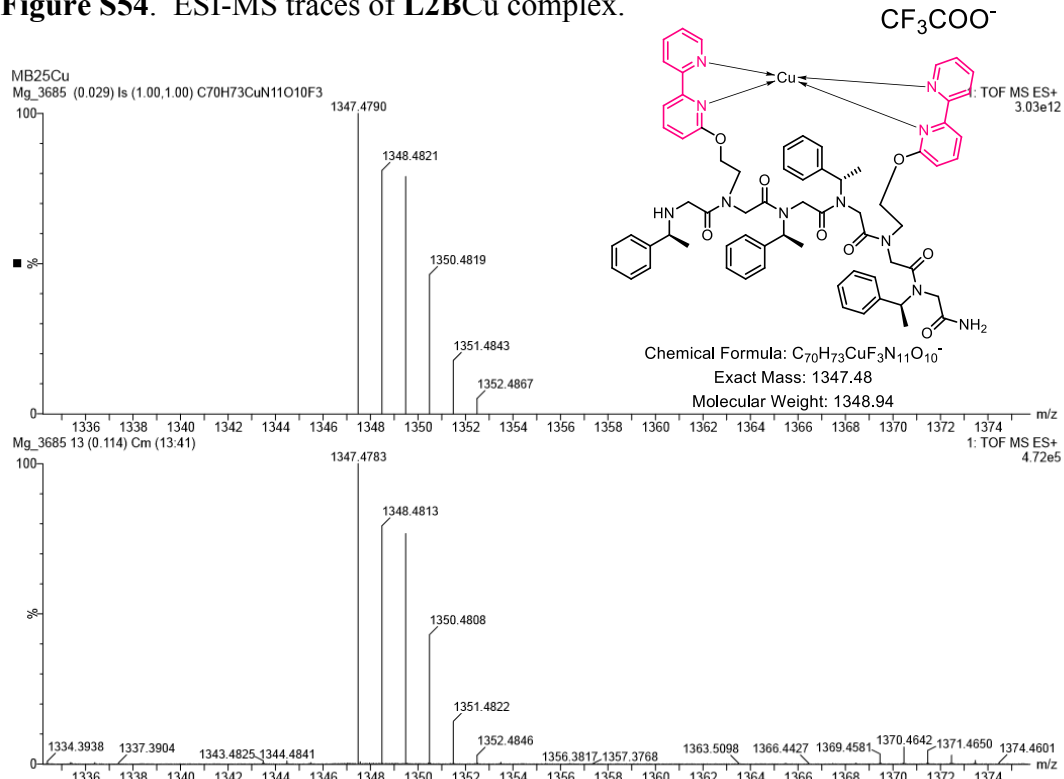
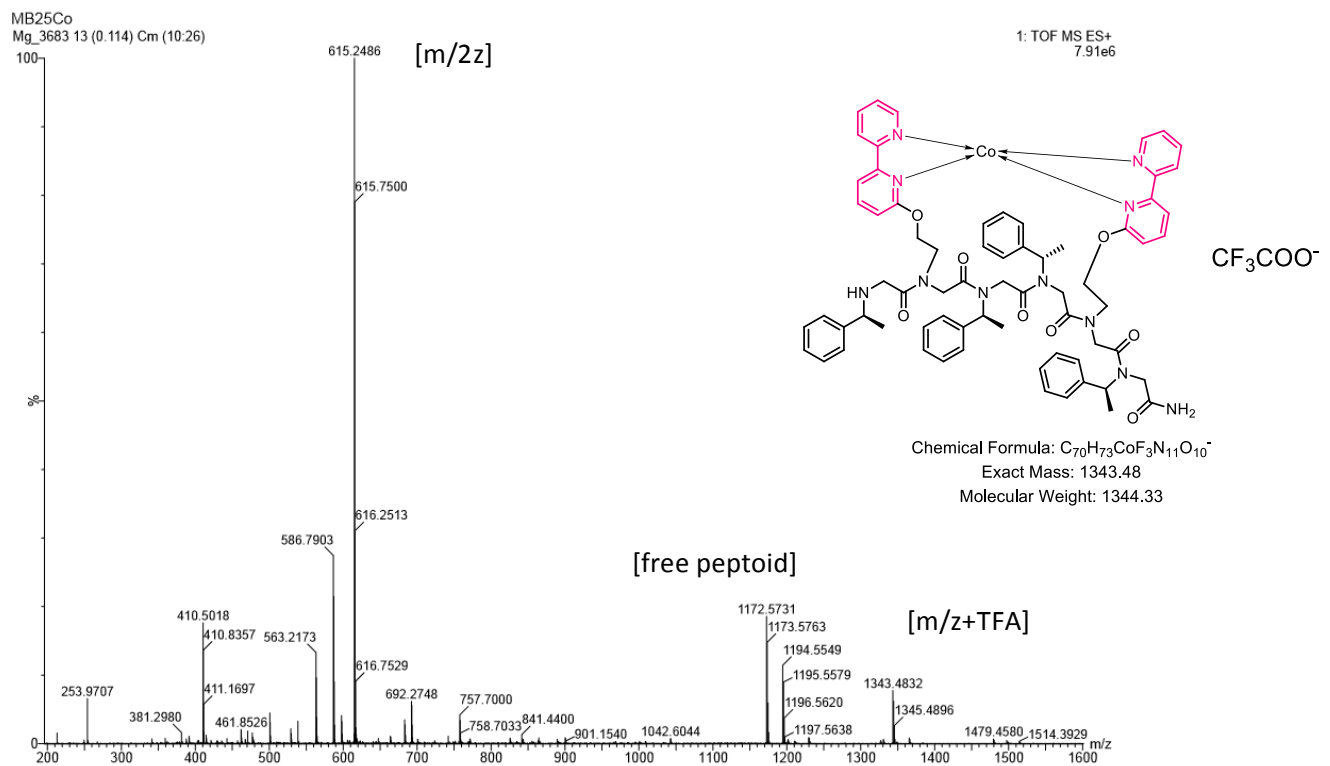
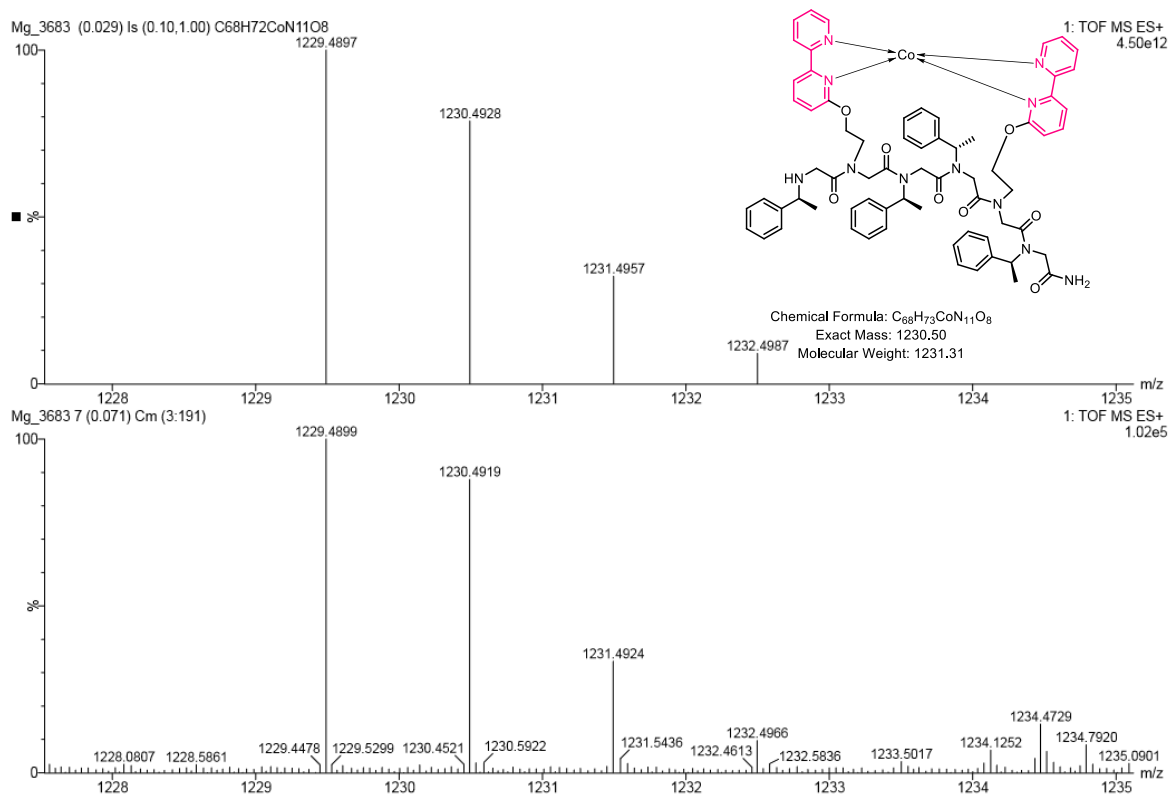


Figure S55. ESI-MS m/z traces of  $[L2BCu+TFA]^+$  (bottom) and calculated ESI-MS spectrum (top).



**Figure S56.** ESI-MS traces of L2BCo complex



**Figure S57.** ESI-MS m/z traces of L2BCo (bottom) and calculated ESI-MS spectrum (top).

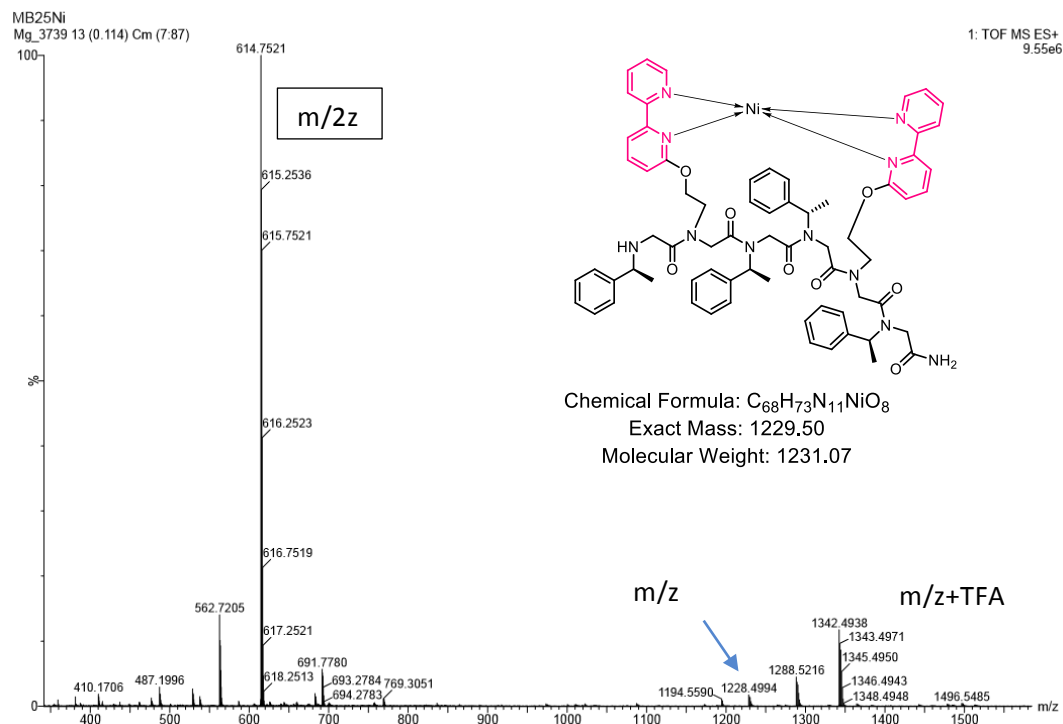


**Figure S58.** ESI-MS traces of L2BNi complex.

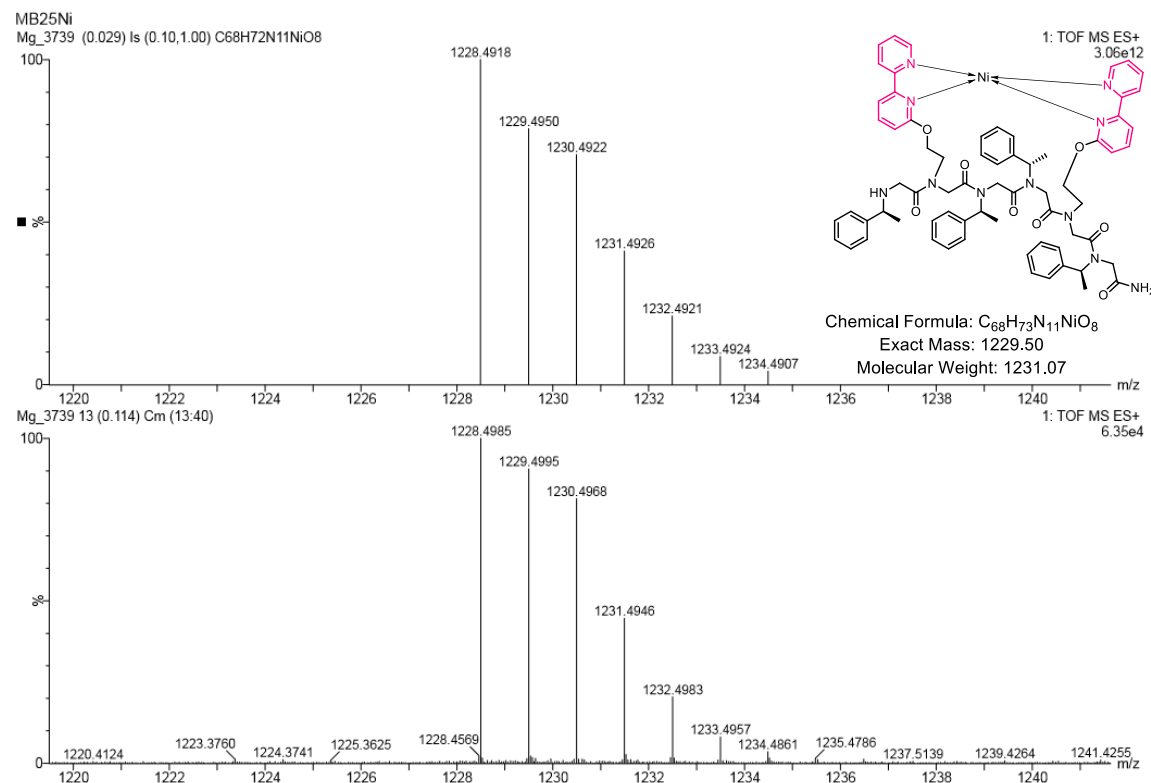


**Figure S59.** ESI-MS m/z traces of L2BNi (bottom) and calculated ESI-MS spectrum (top).

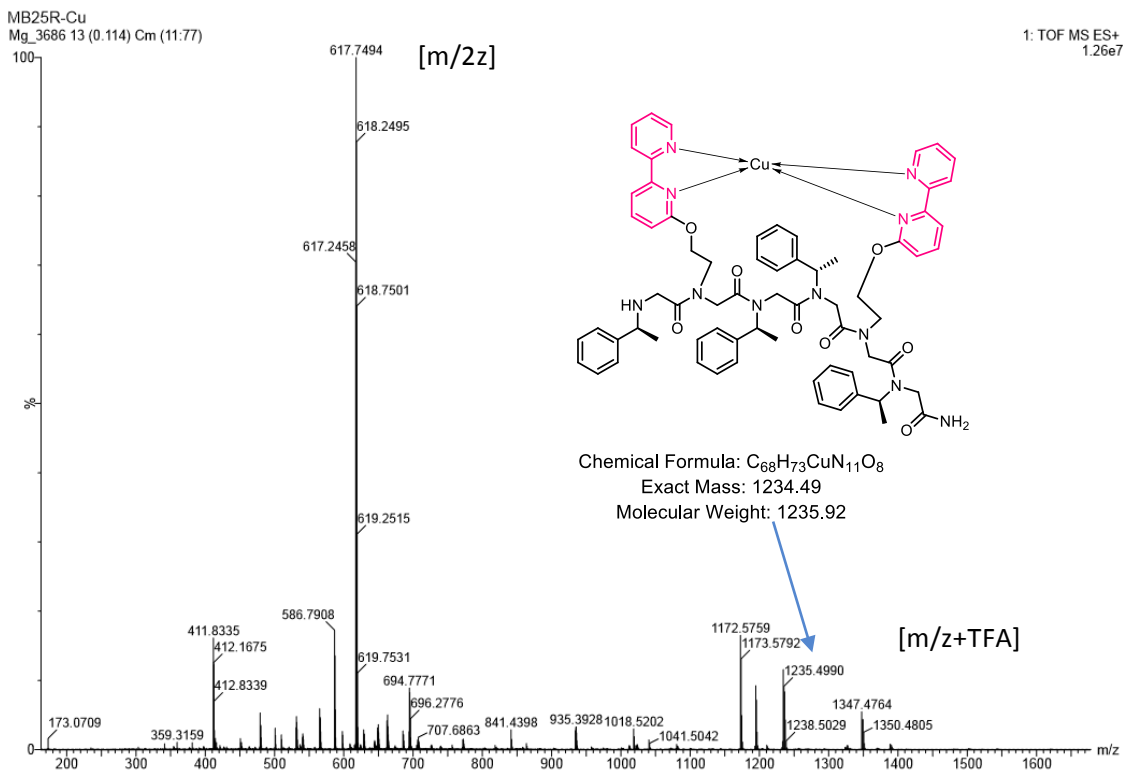


**Figure S60.** ESI-MS traces of R-L2BCu complex.

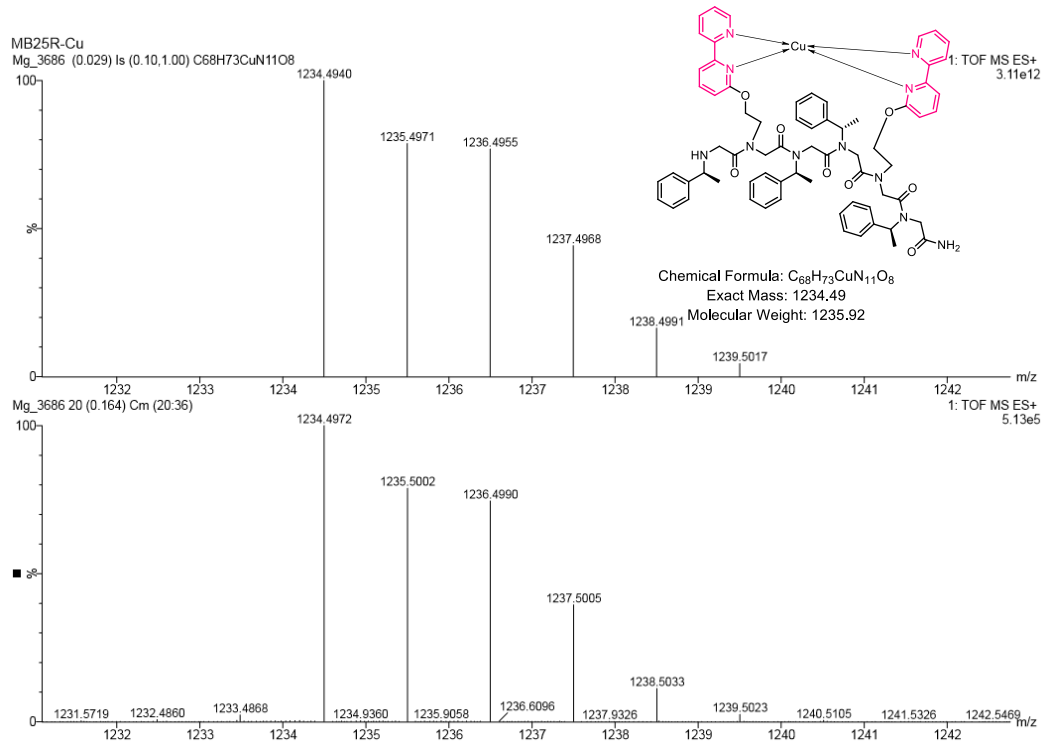


**Figure S61.** ESI-MS m/z traces of R-L2BCu (bottom) and calculated ESI-MS spectrum (top).

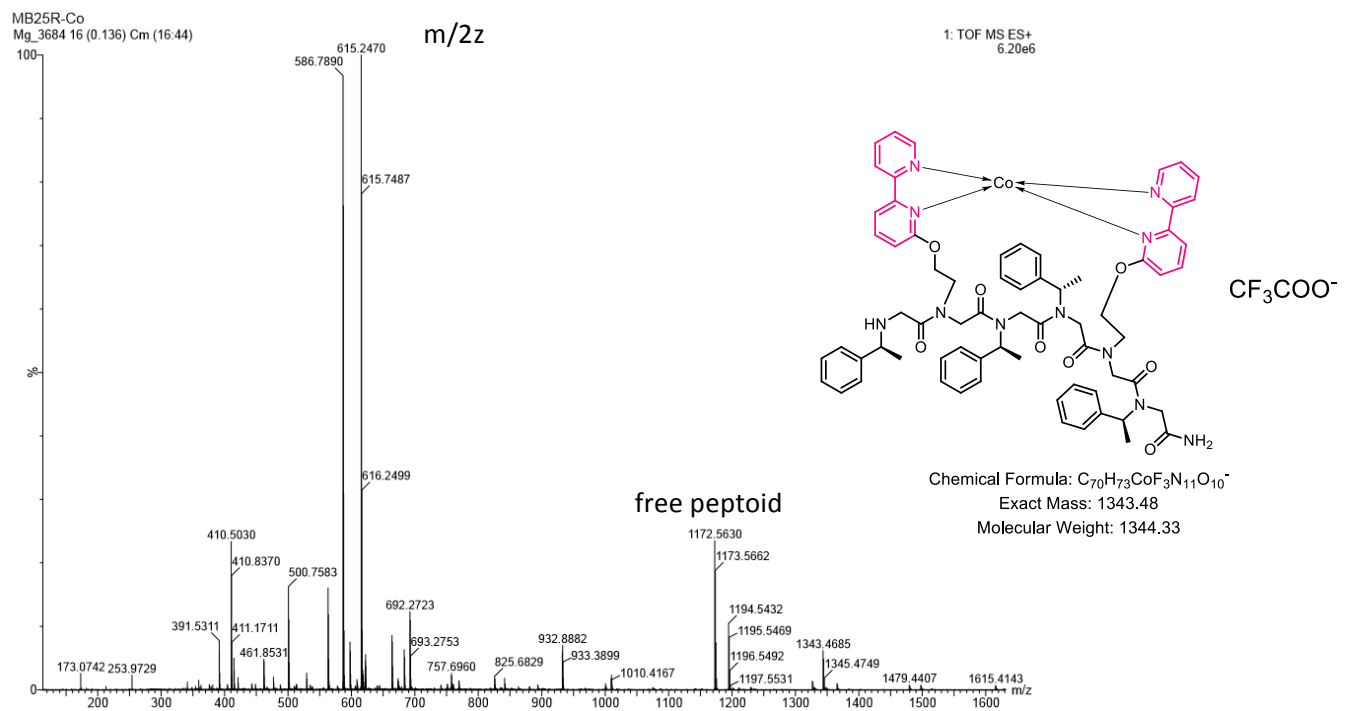


**Figure S62.** ESI-MS traces of R-L2BCo complex.

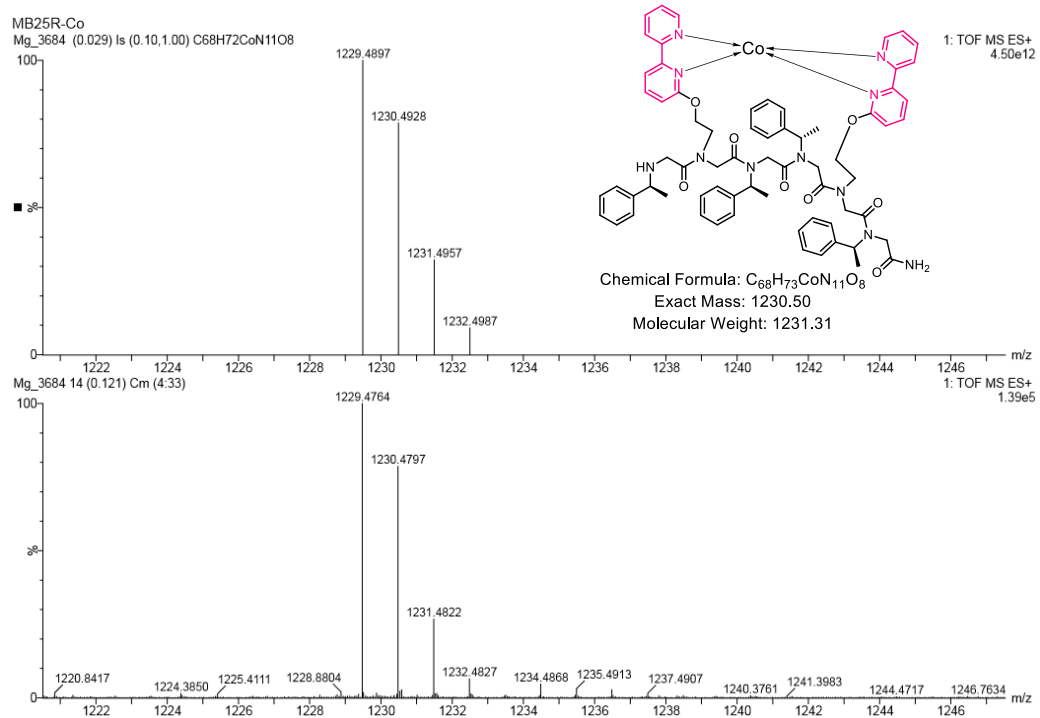


**Figure S63.** ESI-MS m/z traces of R-L2BCo (bottom) and calculated ESI-MS spectrum (top).

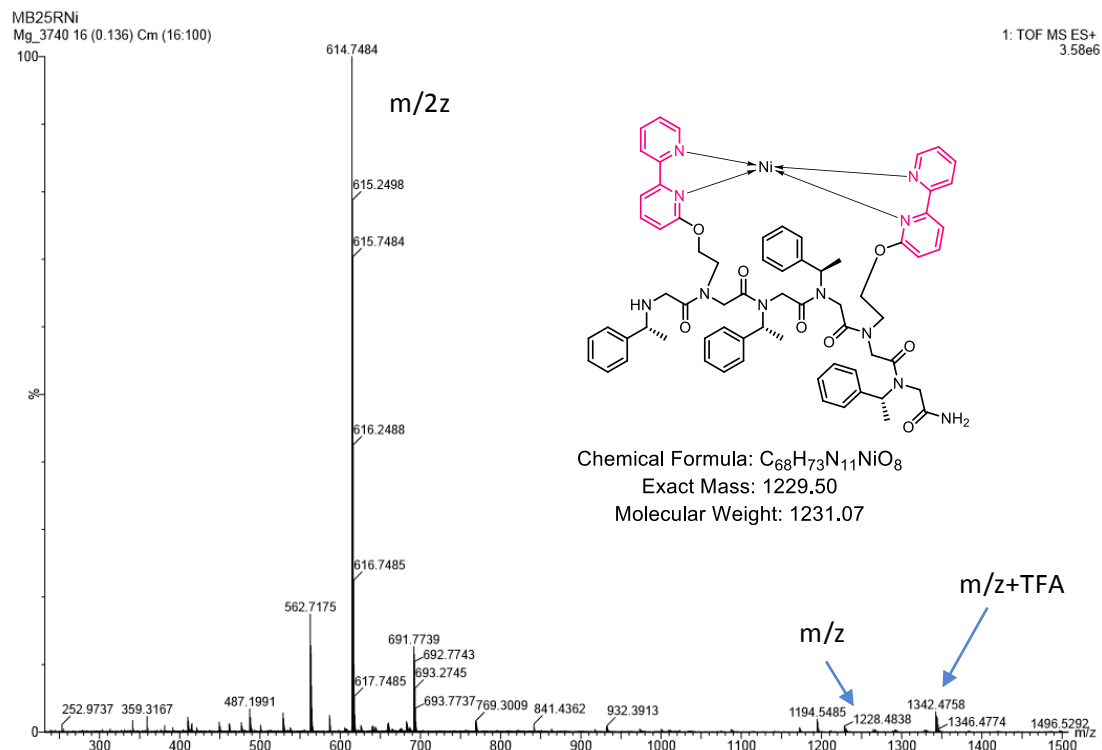


**Figure S64.** ESI-MS traces of R-L2BNi complex.

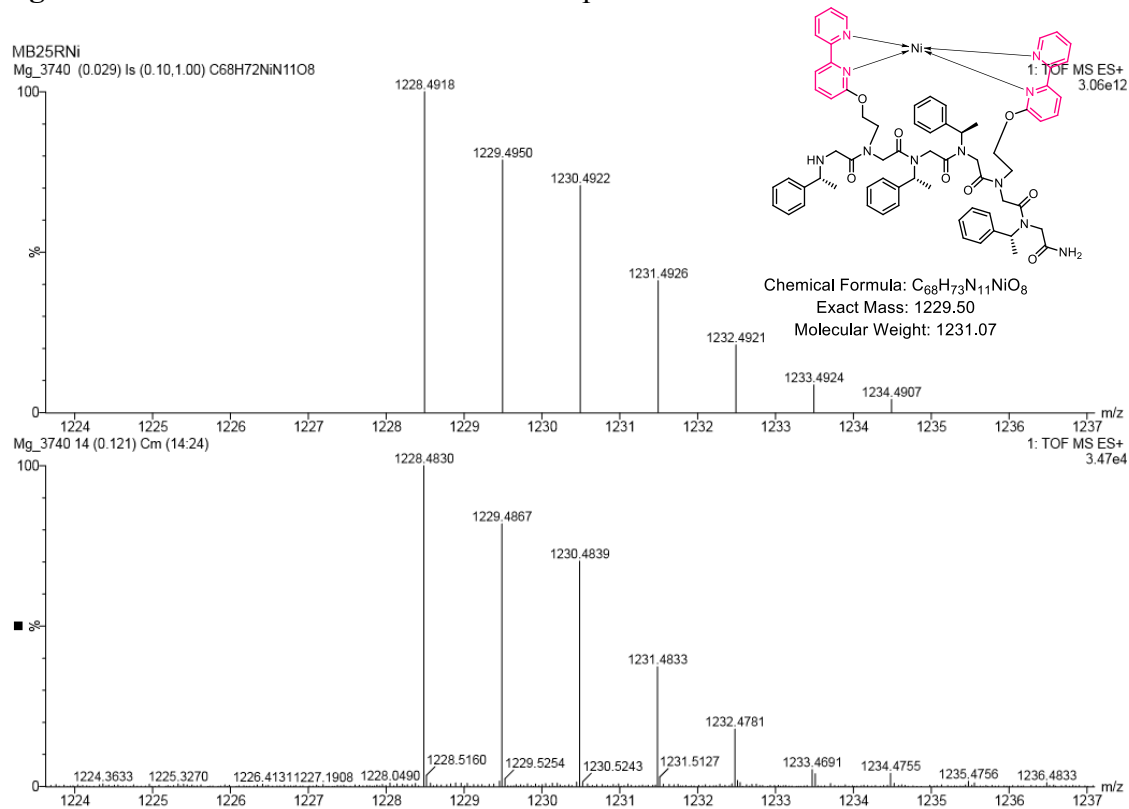


**Figure S65.** ESI-MS *m/z* traces of R-L2BNi (bottom) and calculated ESI-MS spectrum (top).

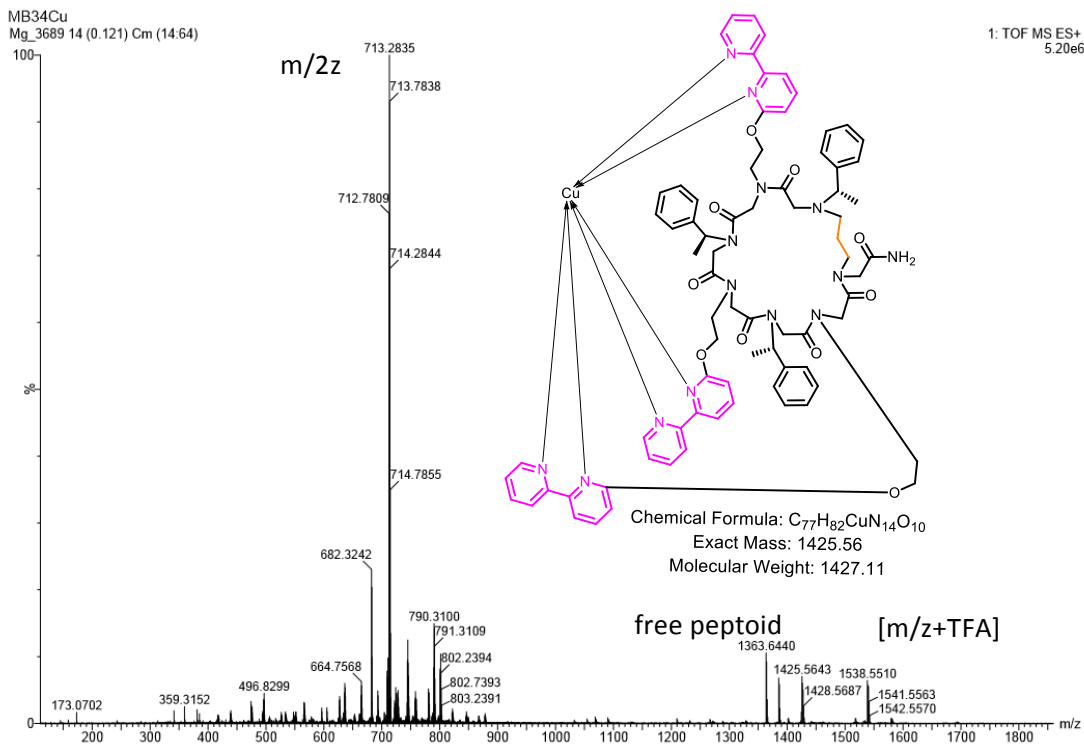


**Figure S66.** ESI-MS traces of C3BCu complex.

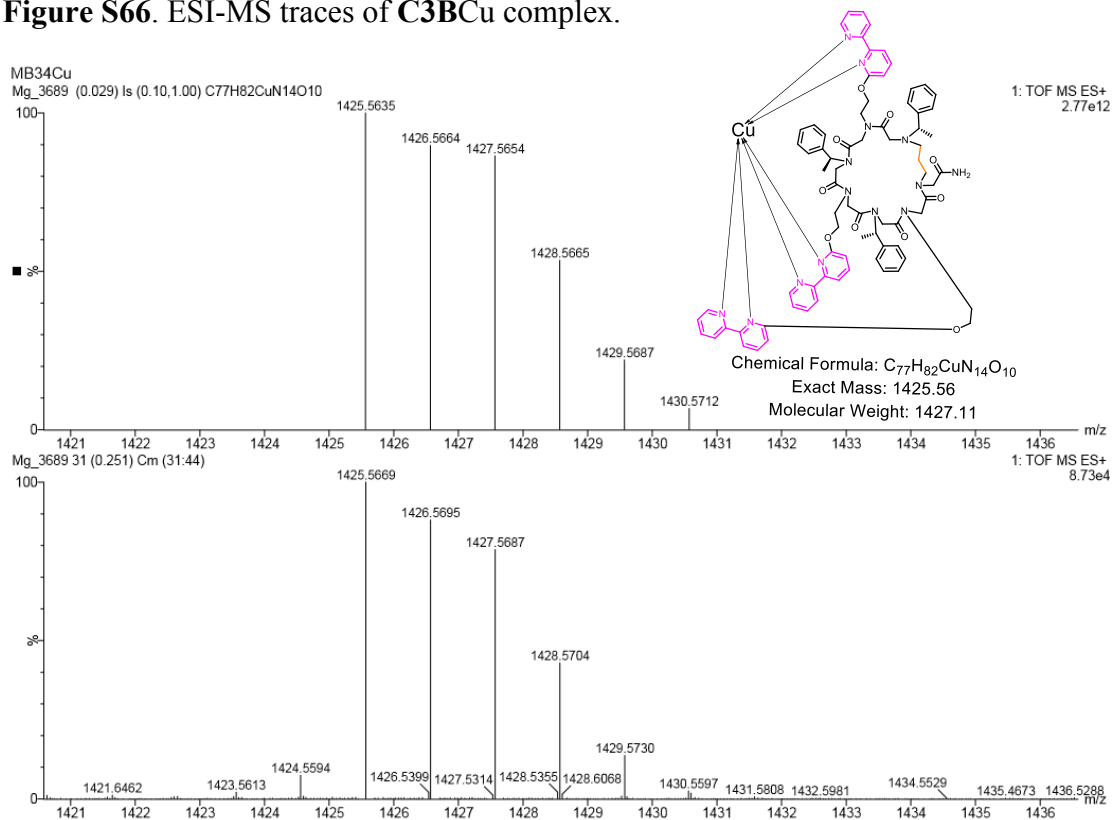


**Figure S67.** ESI-MS  $m/z$  traces of C3BCu (bottom) and calculated ESI-MS spectrum (top).

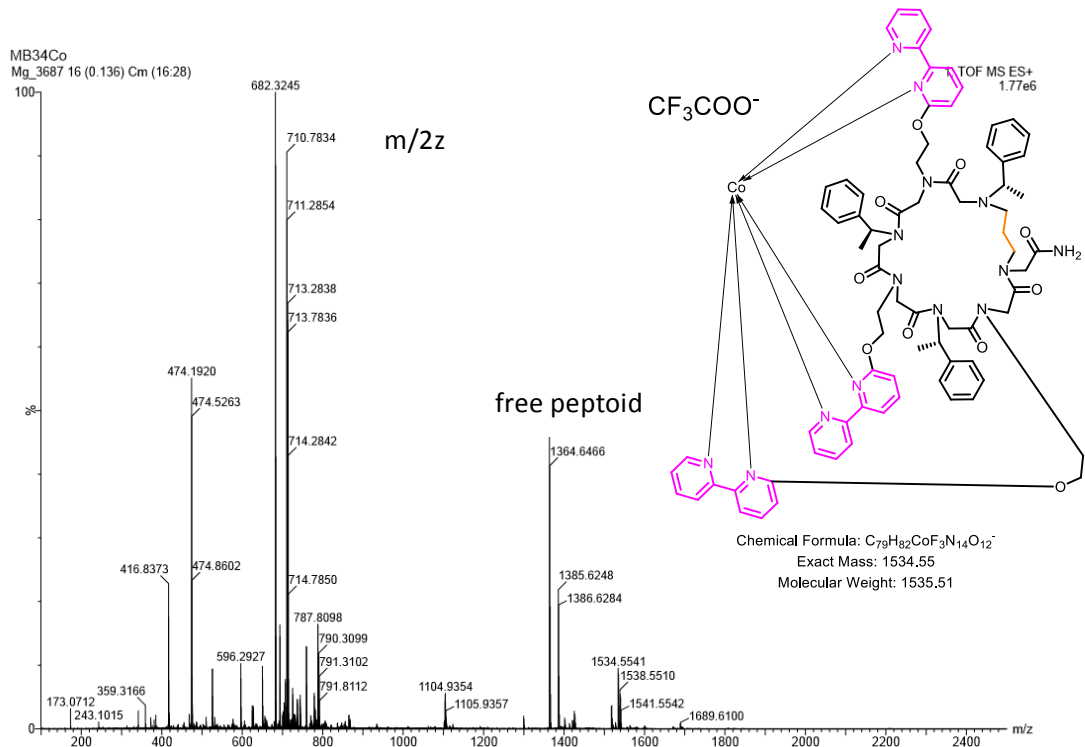


**Figure S68.** ESI-MS traces of C3BCo complex.

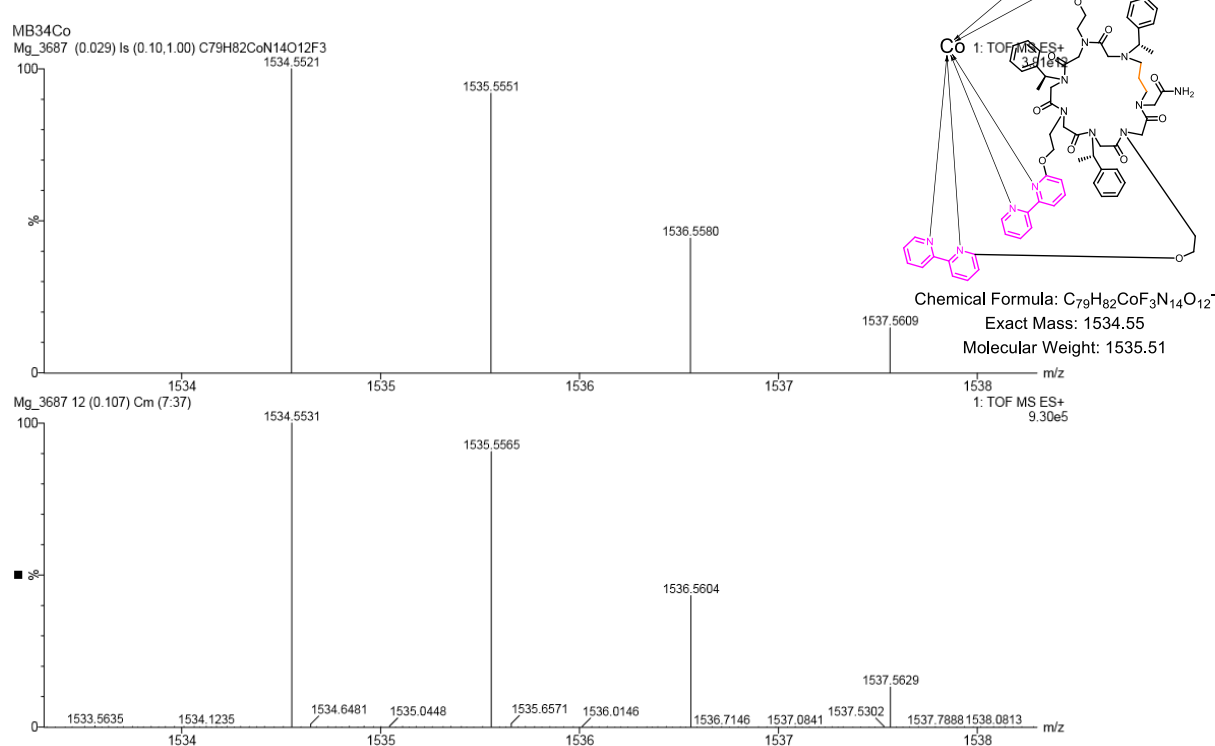


**Figure S69.** ESI-MS m/z traces of [C3BCo-TFA]<sup>+</sup> (bottom) and calculated ESI-MS spectrum (top).

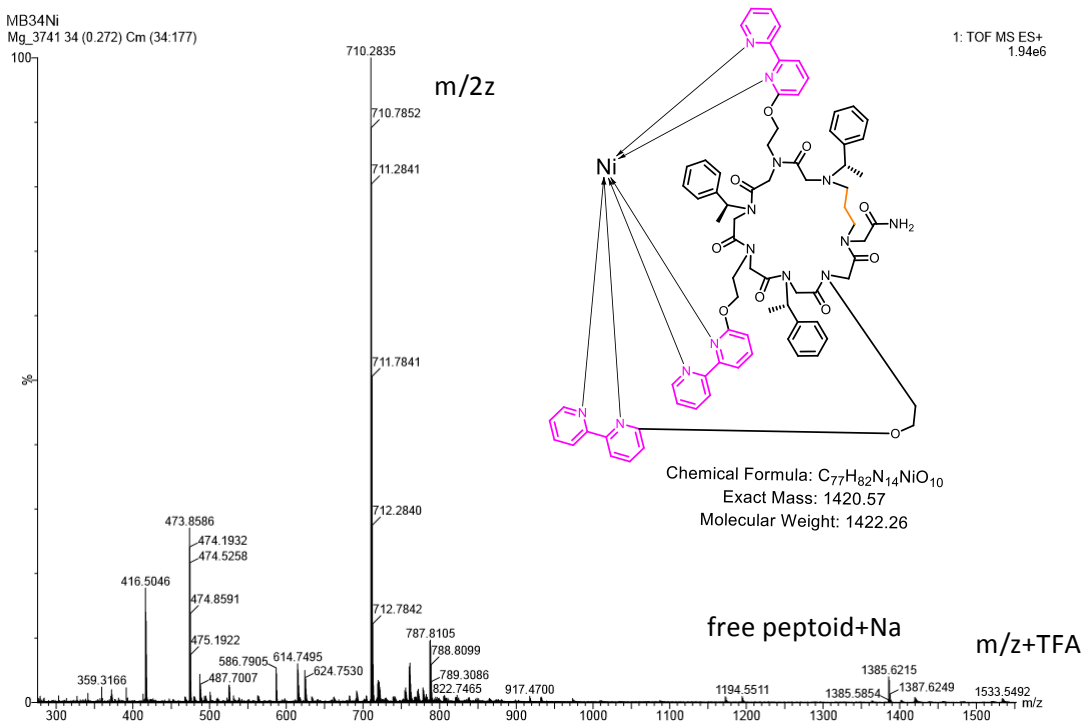


**Figure S70.** ESI-MS traces of C3BNi complex.

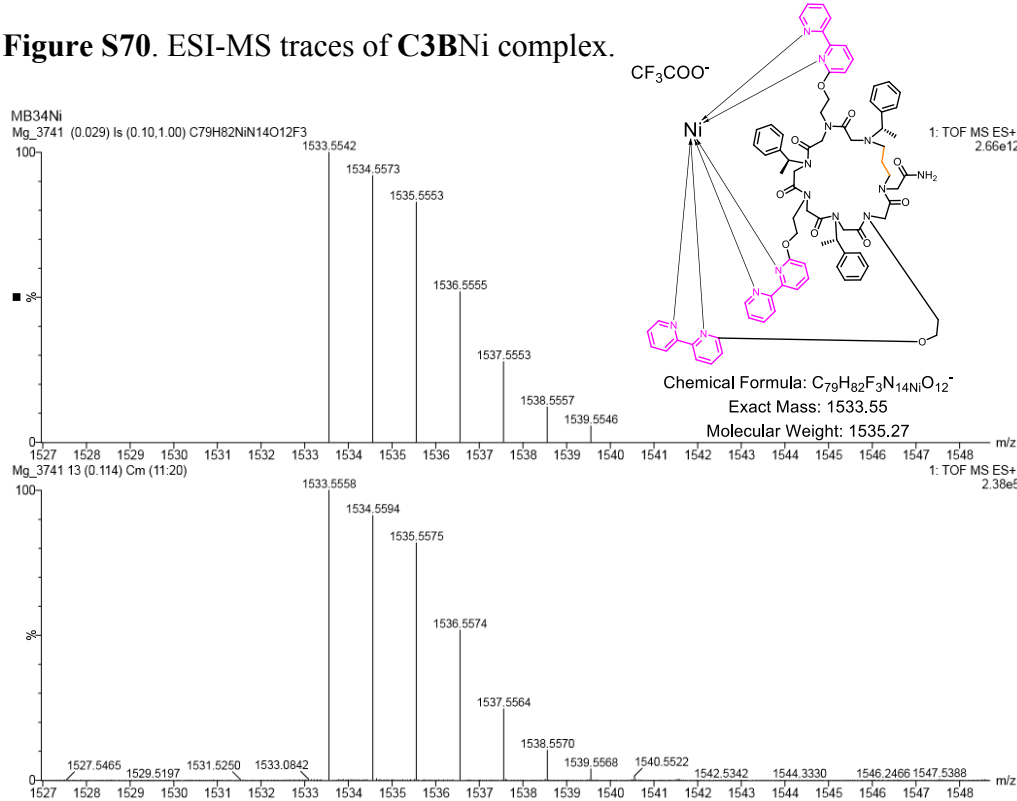


**Figure S71.** ESI-MS  $m/z$  traces of  $[C3BNi\text{-}TFA]^+$  (bottom) and calculated ESI-MS spectrum (top).

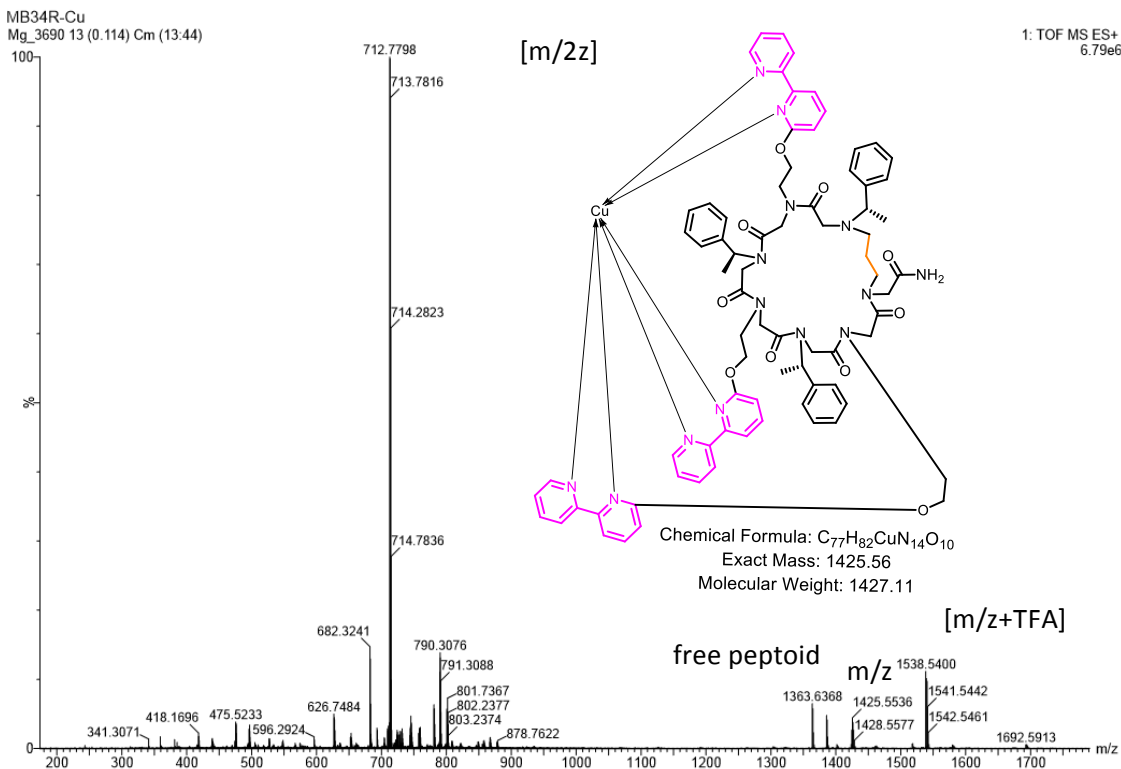


**Figure S72.** ESI-MS traces of R-C3BCu complex.

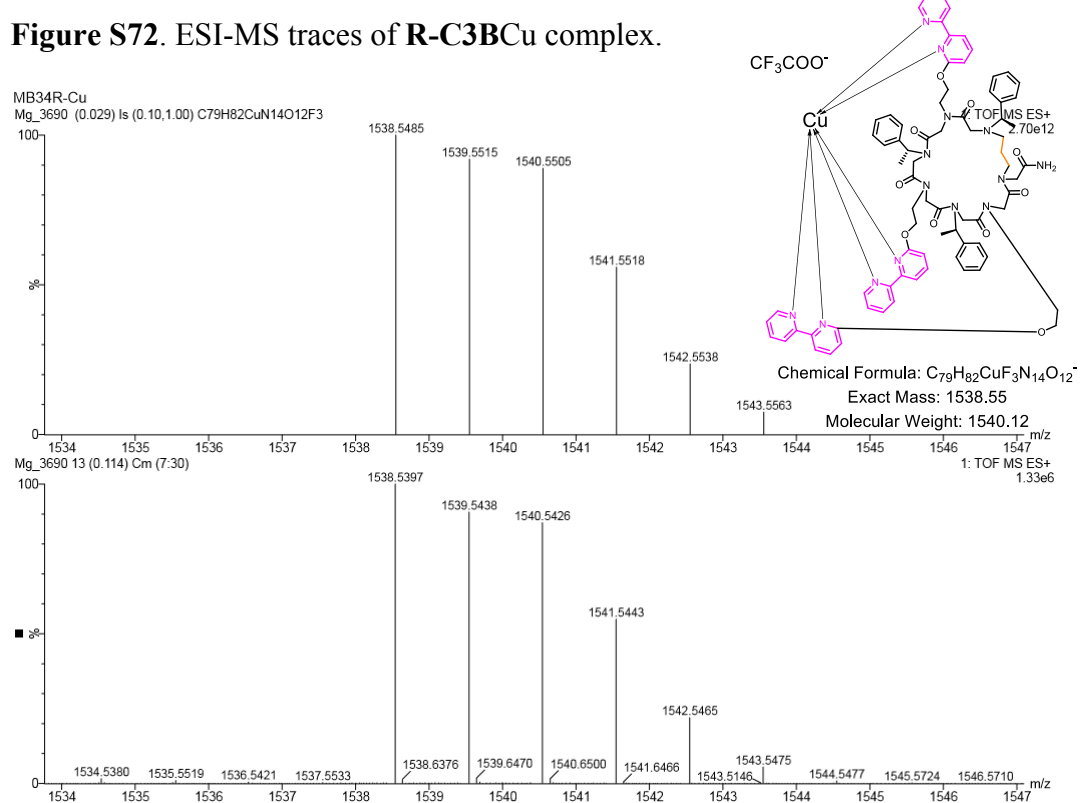


**Figure S73.** ESI-MS m/z traces of  $[\text{R-C3BCu-TFA}]^+$  (bottom) and calculated ESI-MS spectrum (top).

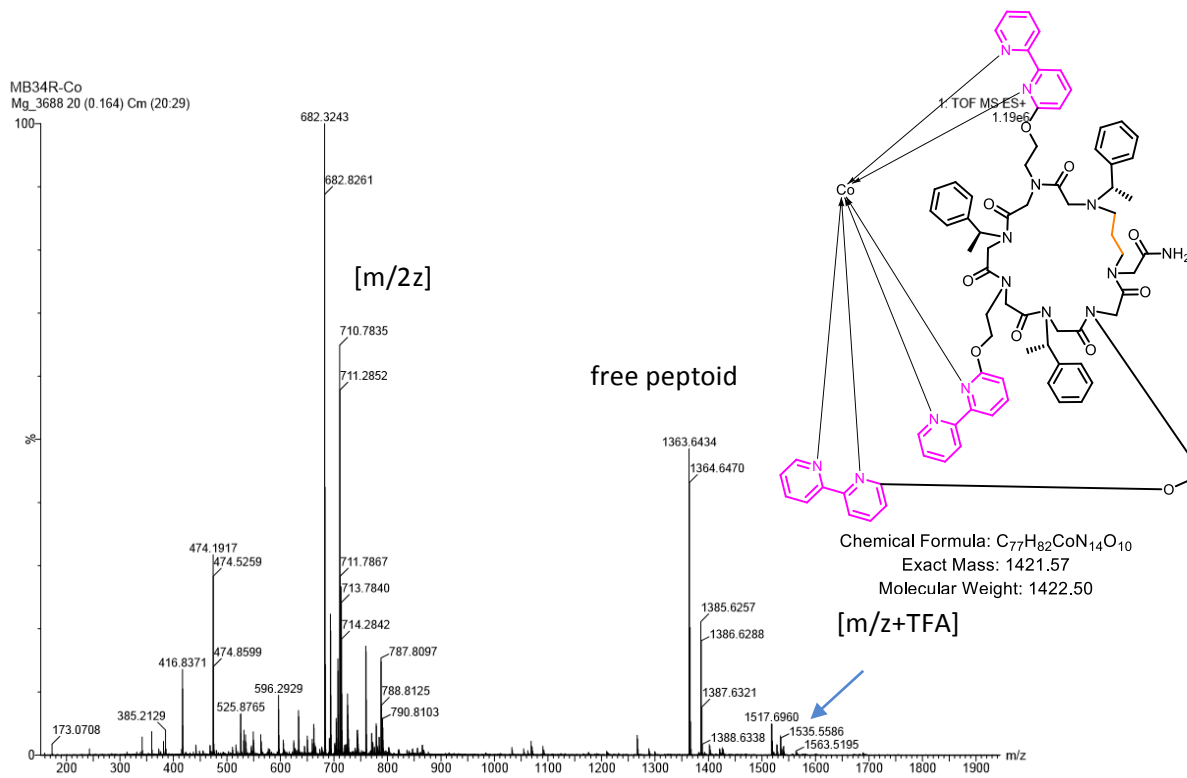


**Figure S74.** ESI-MS traces of R-C3BCo complex.

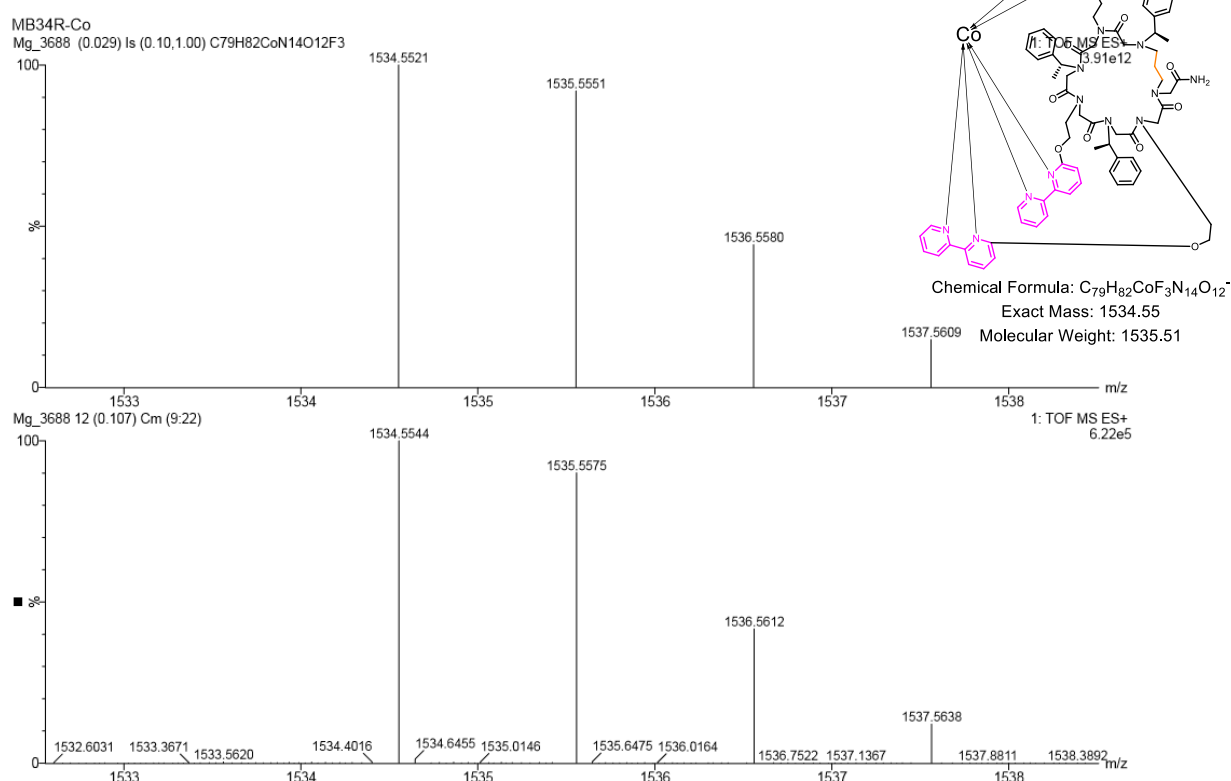


**Figure S75.** ESI-MS m/z traces of  $[\text{R-C3BCo-TFA}]^+$  (bottom) and calculated ESI-MS spectrum (top).

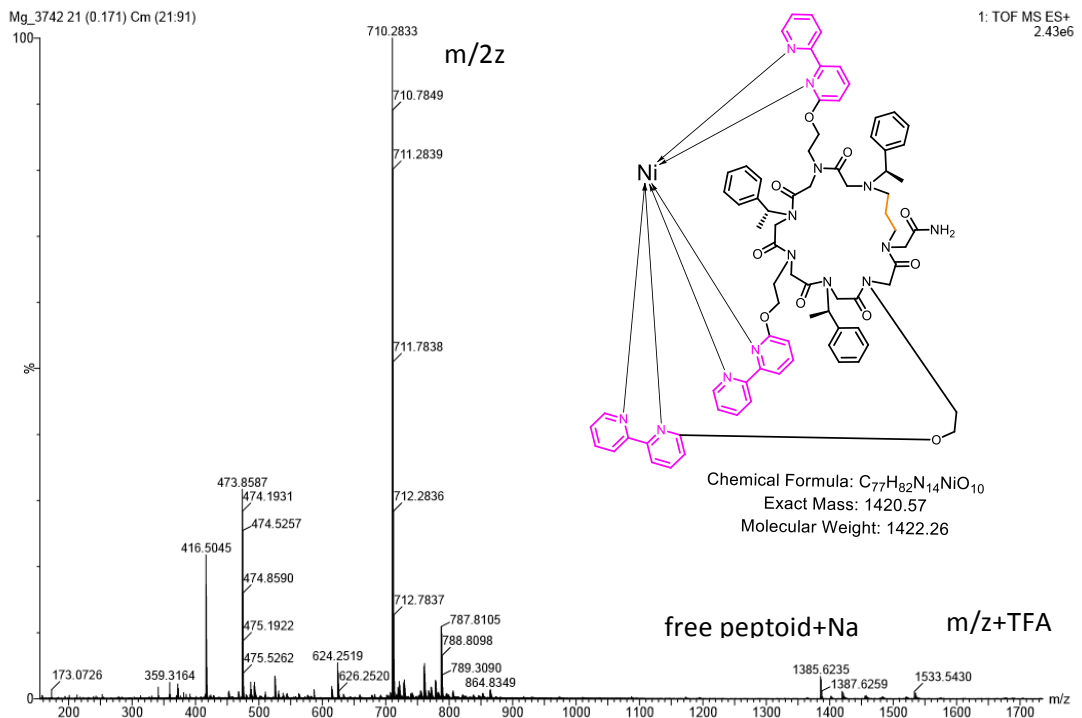


**Figure S76.** ESI-MS traces of R-C3BNi complex.

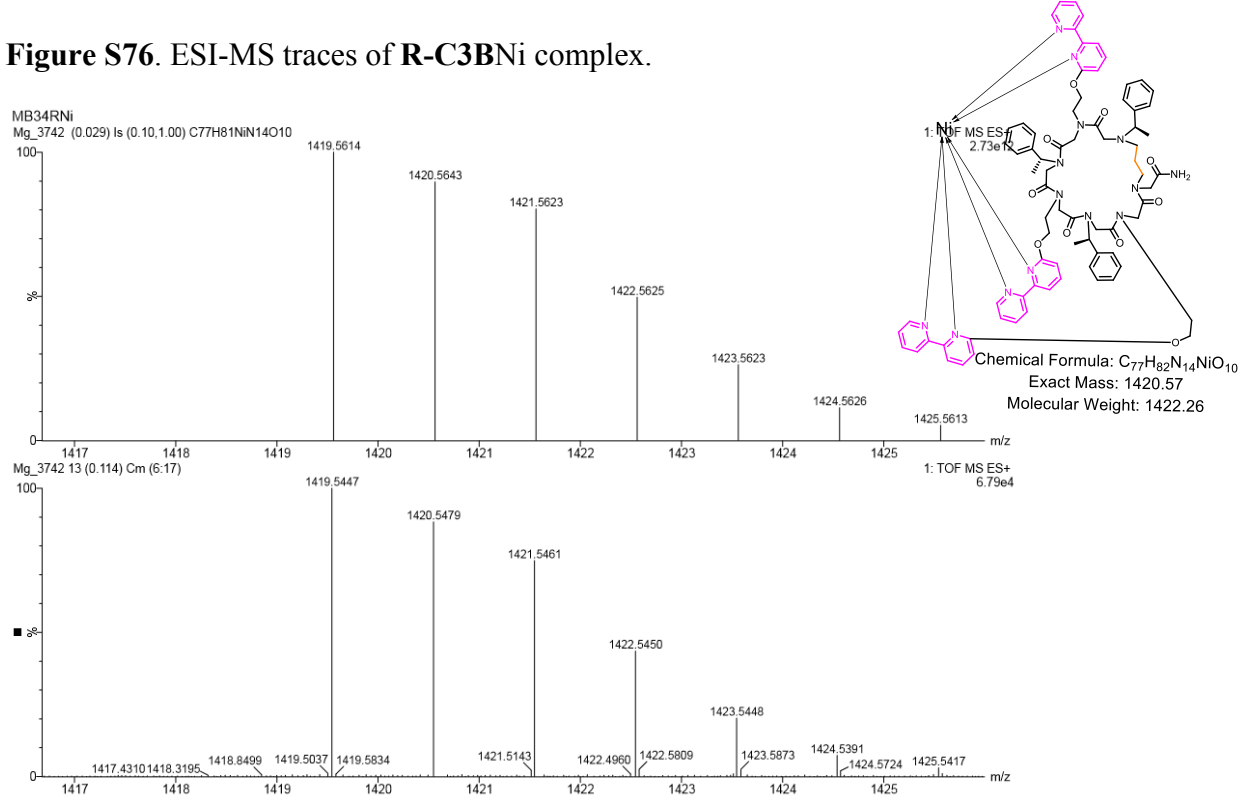


**Figure S77.** ESI-MS  $m/z$  traces of R-C3BNi (bottom) and calculated ESI-MS spectrum (top).

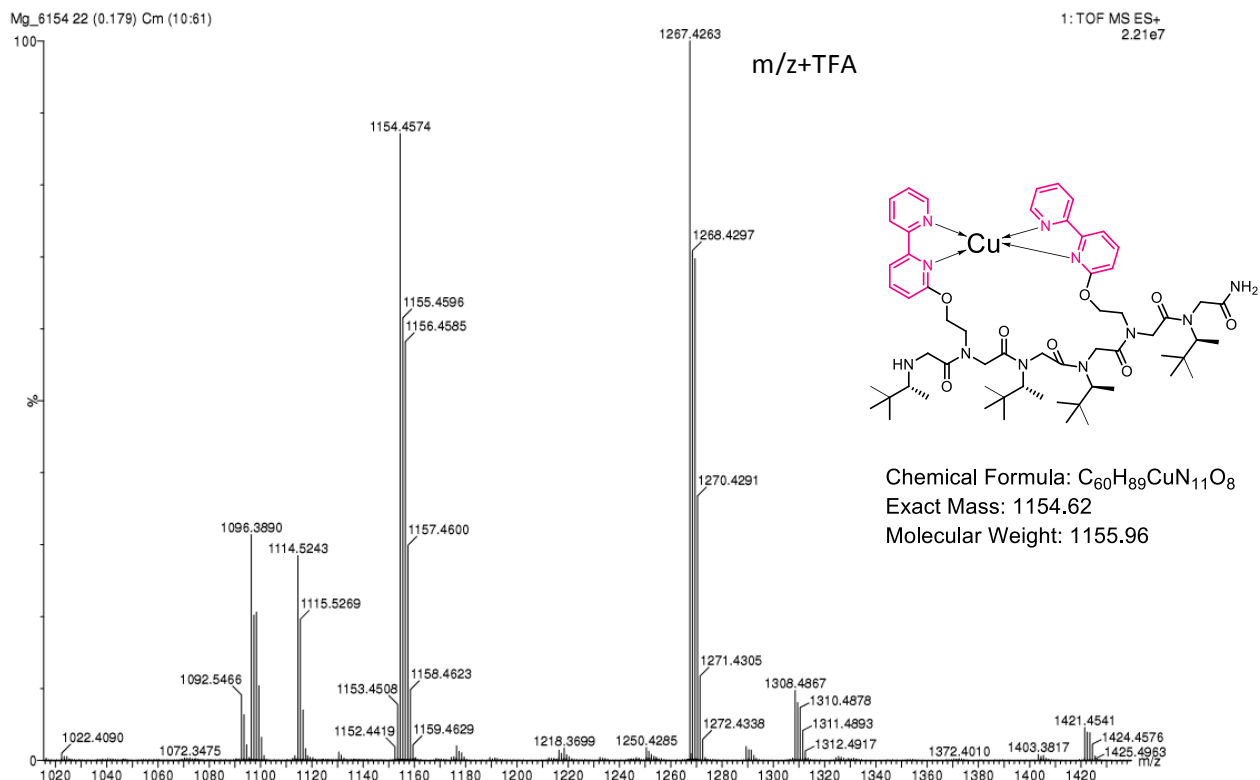


**Figure S78.** ESI-MS traces of 6P1Cu complex.

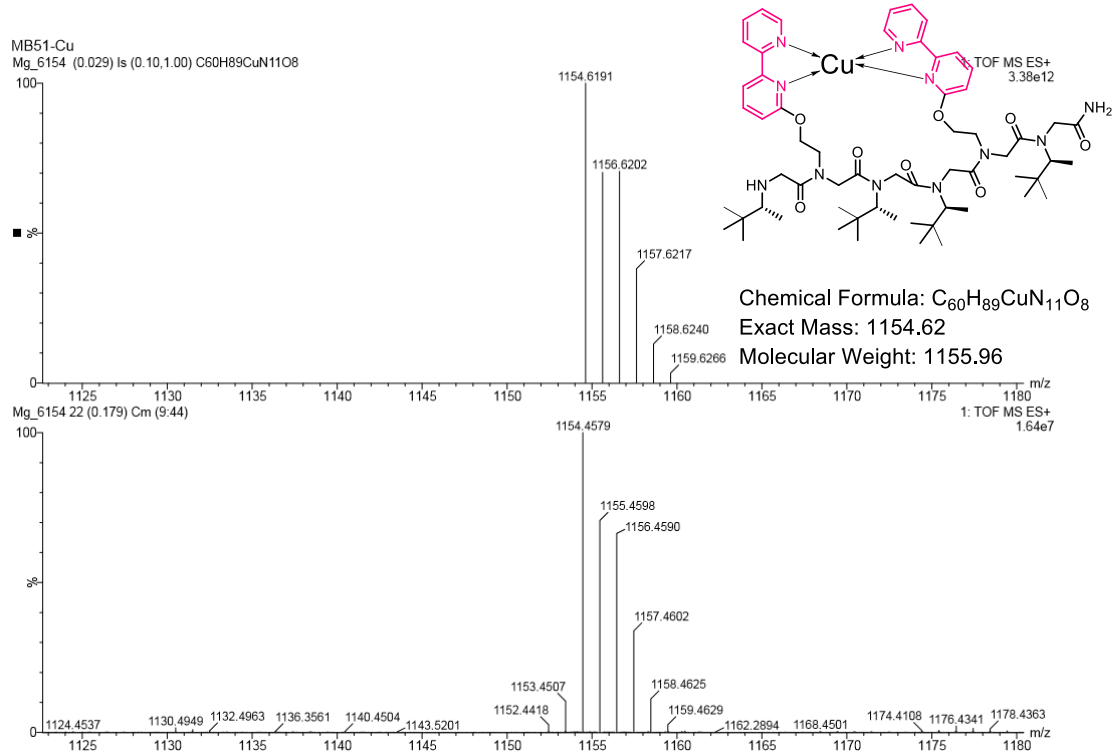


**Figure S79.** ESI-MS m/z traces of 6P1Cu (bottom) and calculated ESI-MS spectrum (top).

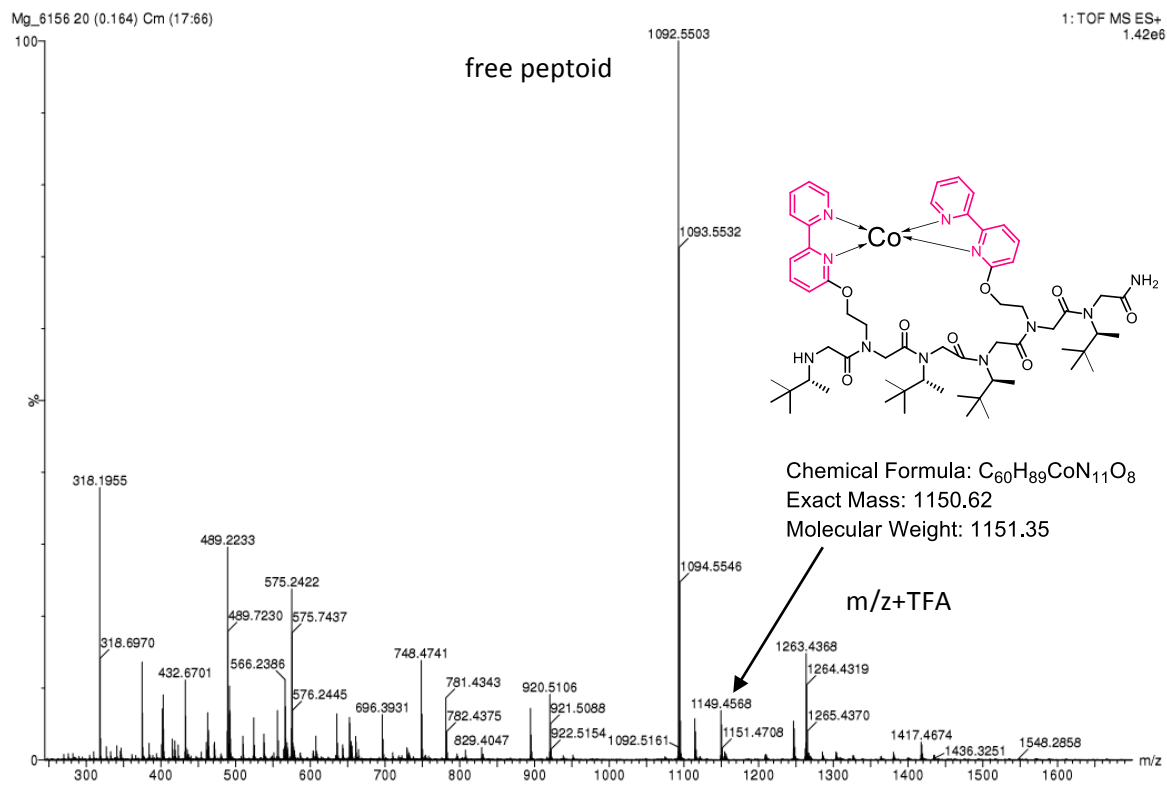


**Figure S80.** ESI-MS traces of **6P1Co** complex.

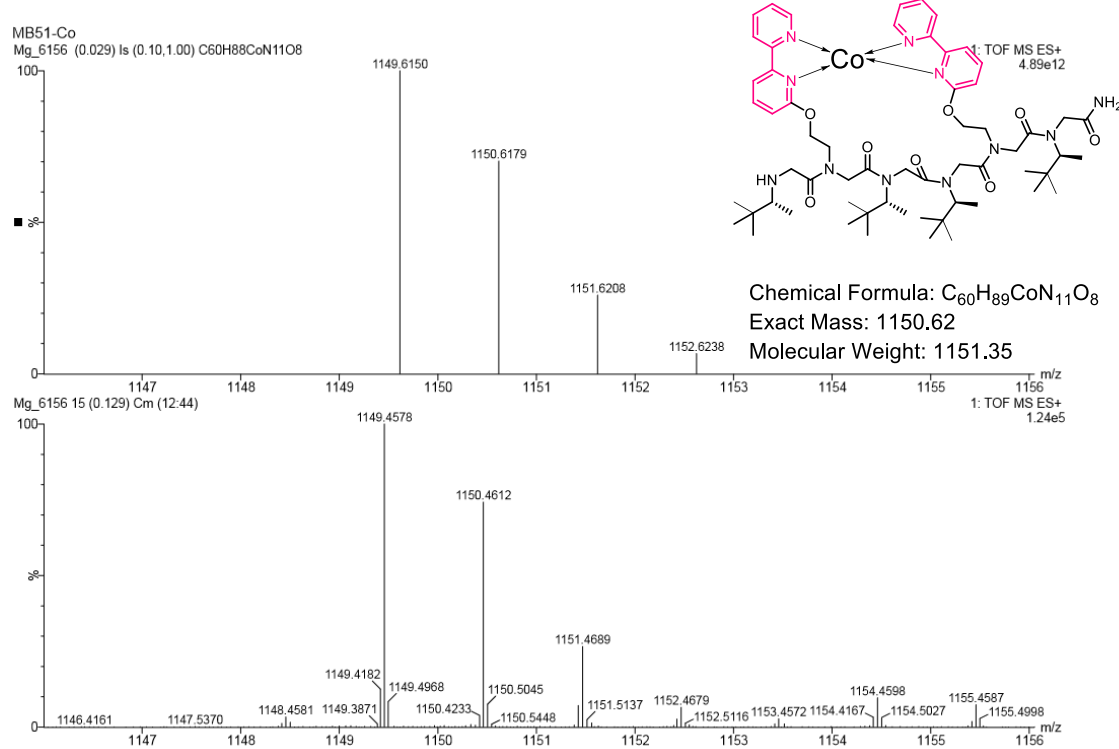


**Figure S81.** ESI-MS m/z traces of **6P1Co** (bottom) and calculated ESI-MS spectrum (top).

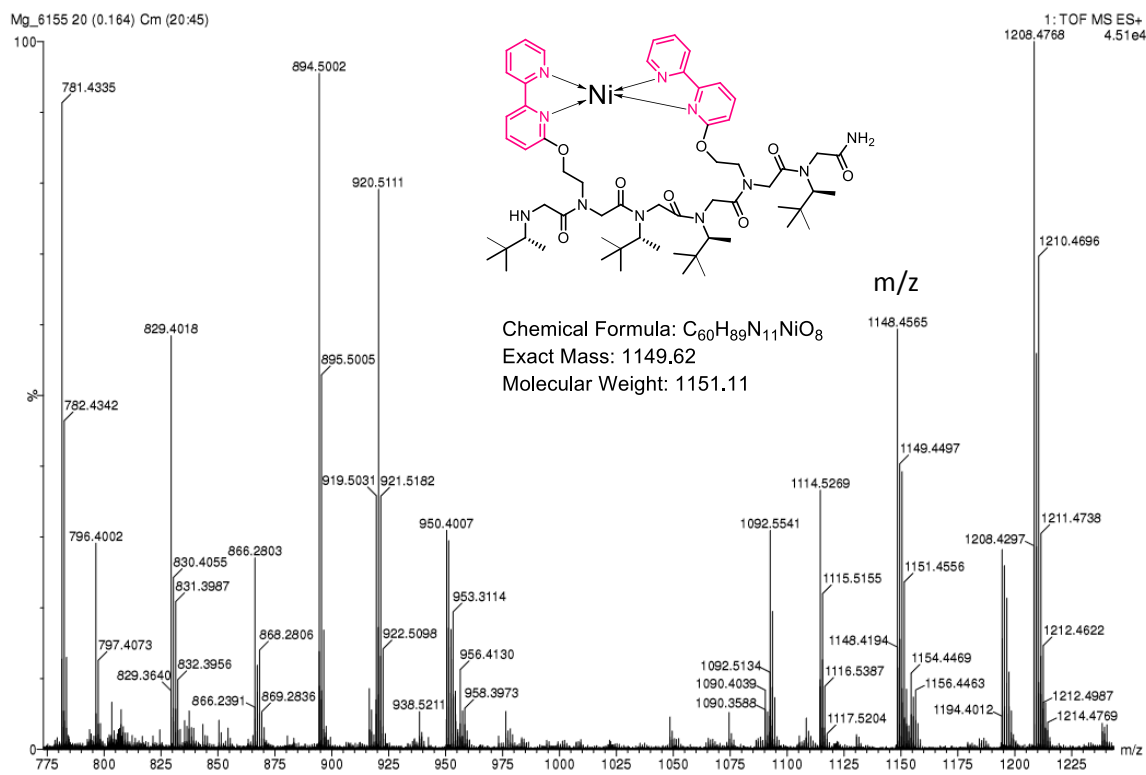


Figure S82. ESI-MS traces of **6P1Ni** complex.

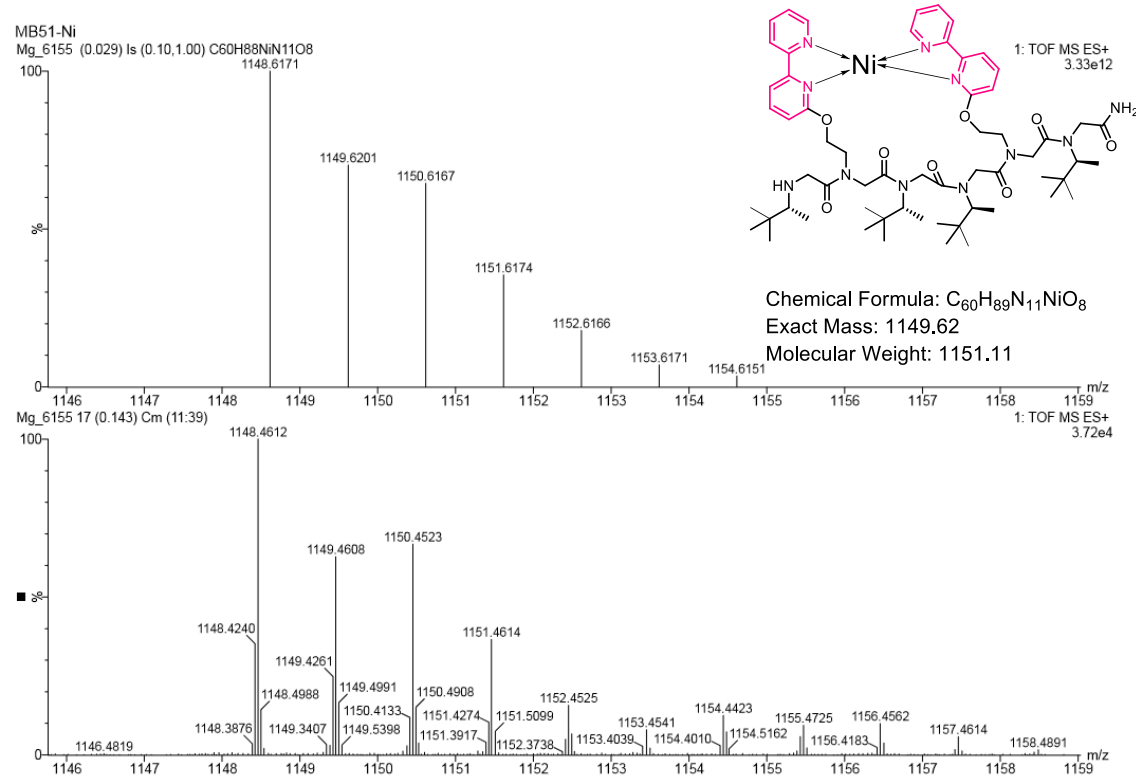
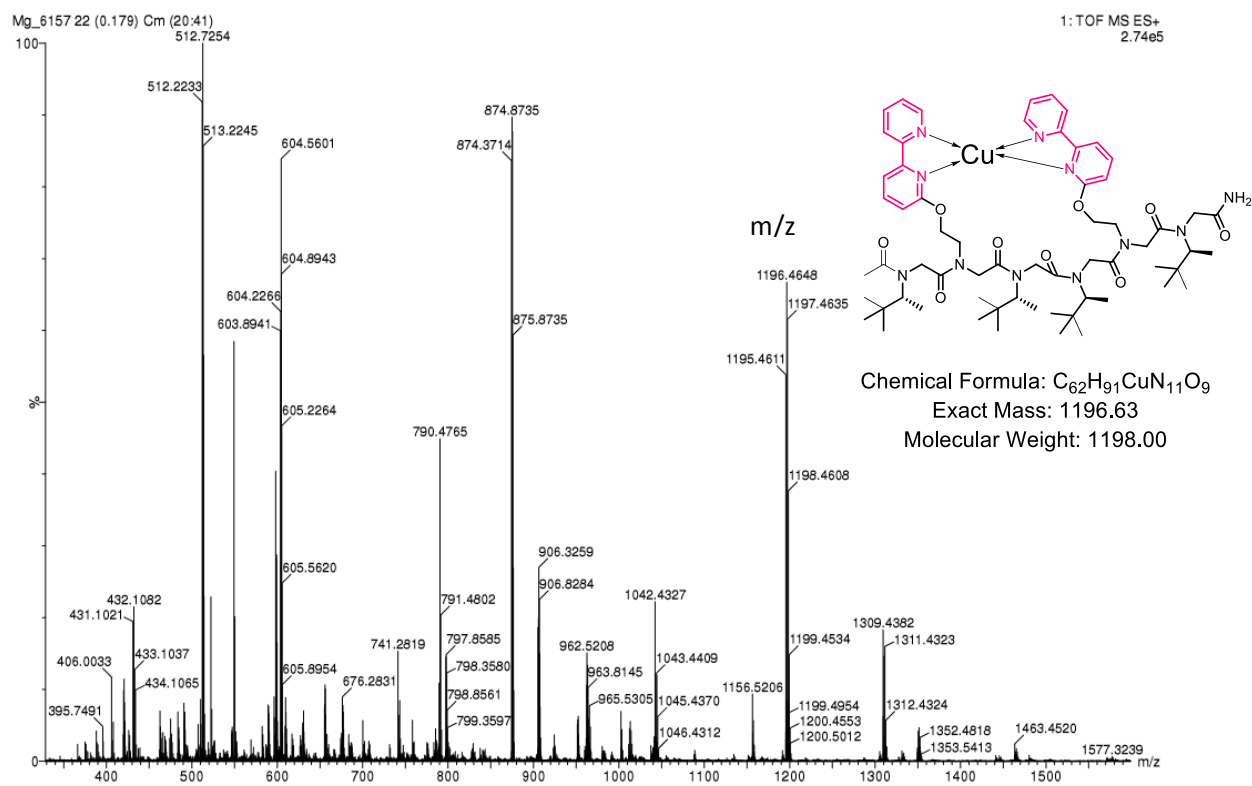
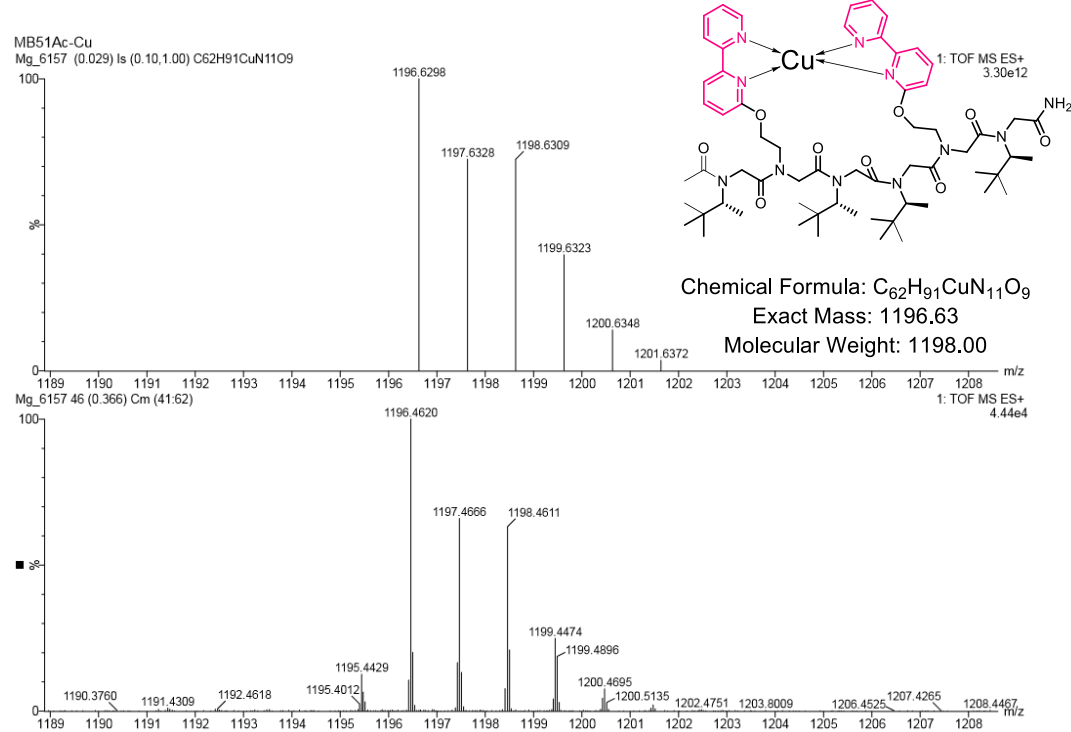


Figure S83. ESI-MS m/z traces of **6P1Ni** (bottom) and calculated ESI-MS spectrum (top).



**Figure S84.** ESI-MS traces of **6P1AcCu** complex.



**Figure S85.** ESI-MS m/z traces of **6P1AcCu** (bottom) and calculated ESI-MS spectrum (top).

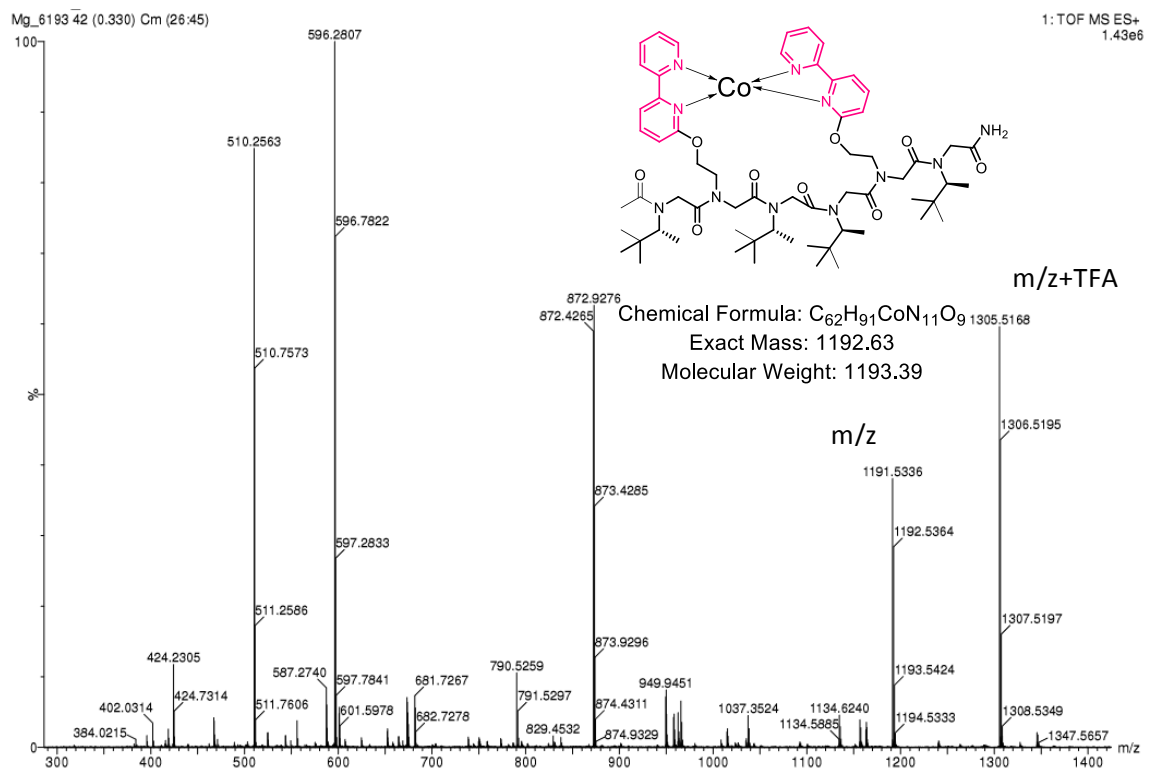


**Figure S86.** ESI-MS traces of **6P1AcCo** complex.

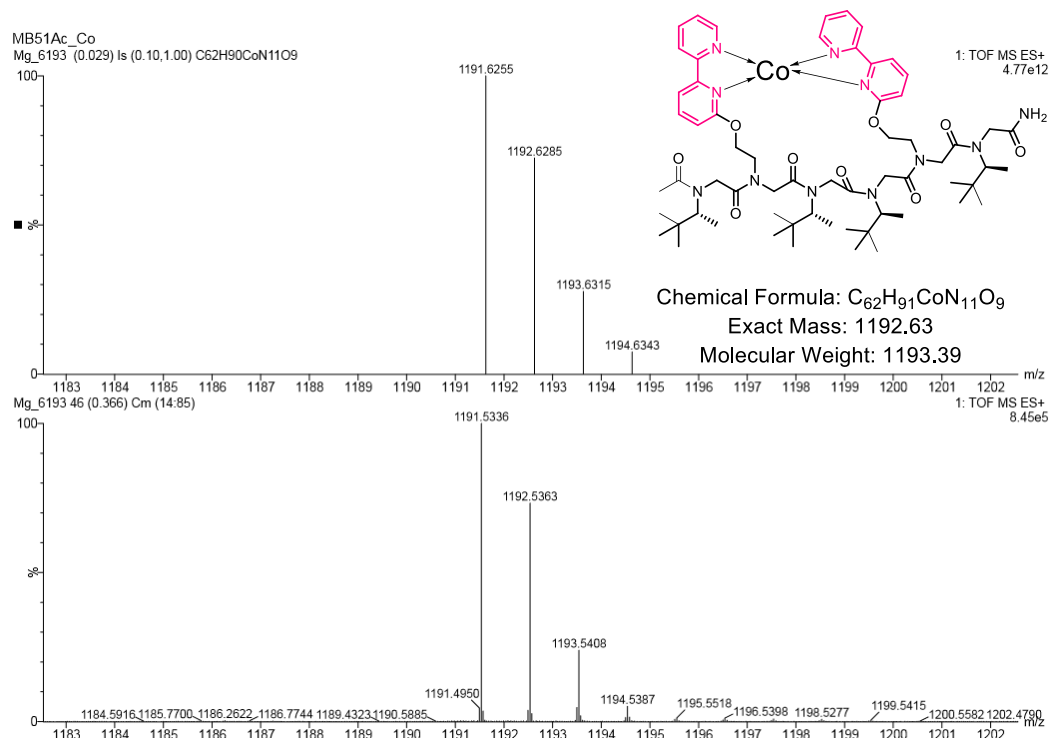


**Figure S87.** ESI-MS m/z traces of **6P1AcCo** (bottom) and calculated ESI-MS spectrum (top).

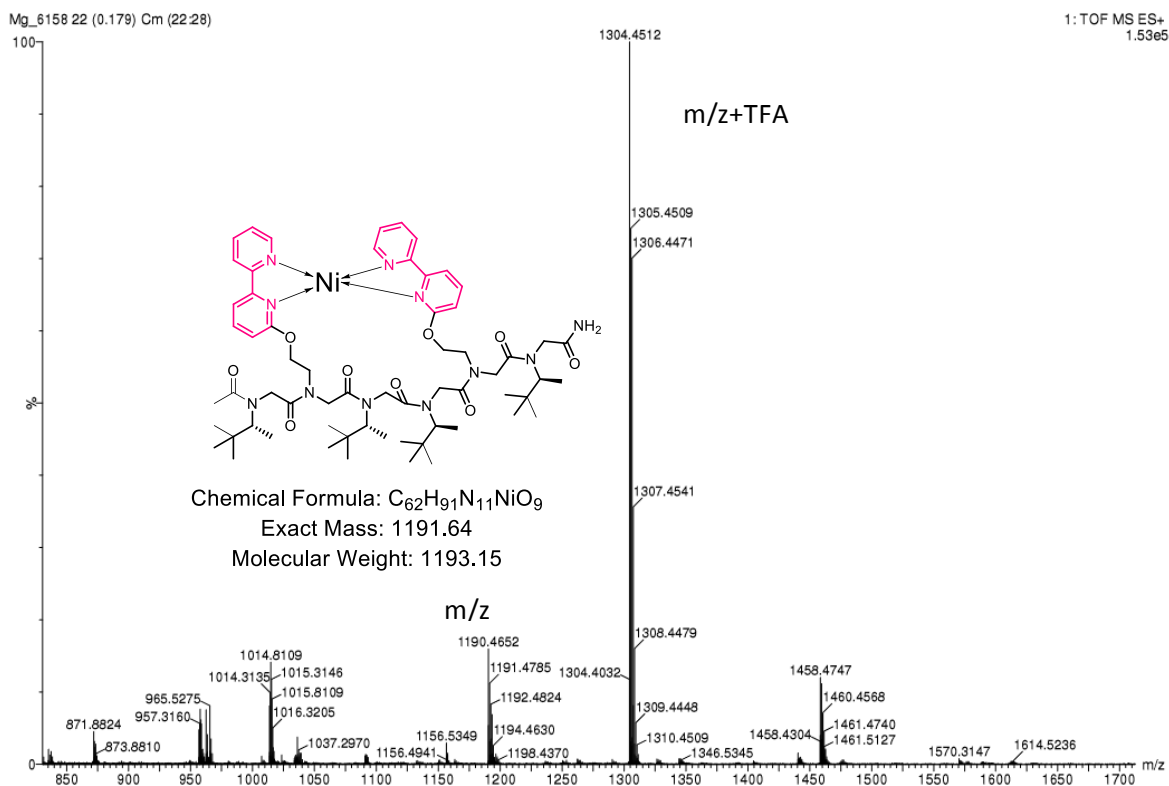


**Figure S88.** ESI-MS traces of 6P1AcNi complex.

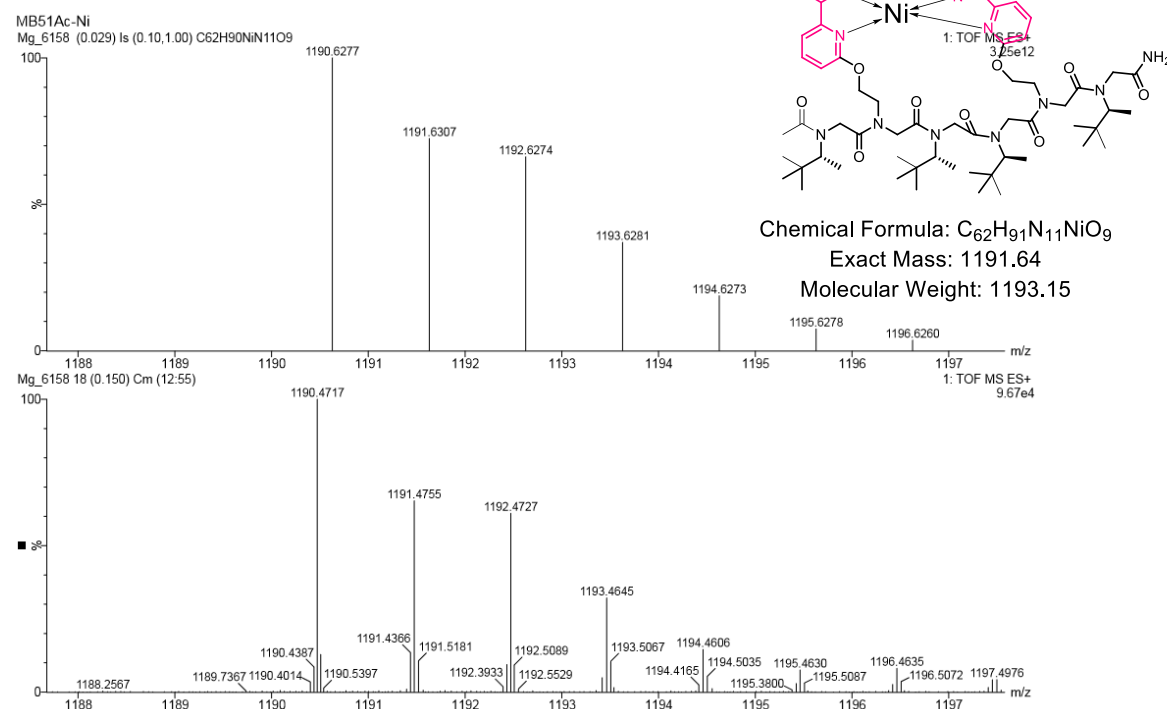


**Figure S89.** ESI-MS m/z traces of 6P1AcNi (bottom) and calculated ESI-MS spectrum (top).

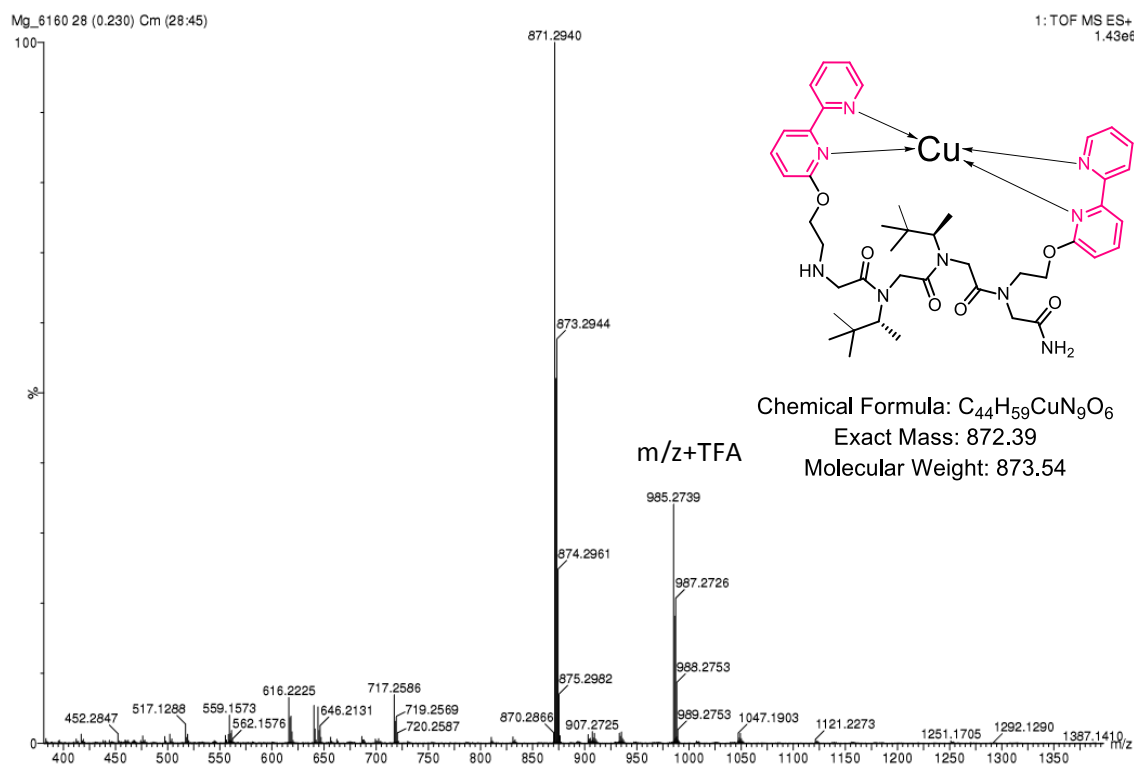


**Figure S90.** ESI-MS traces of **4P1Cu** complex.

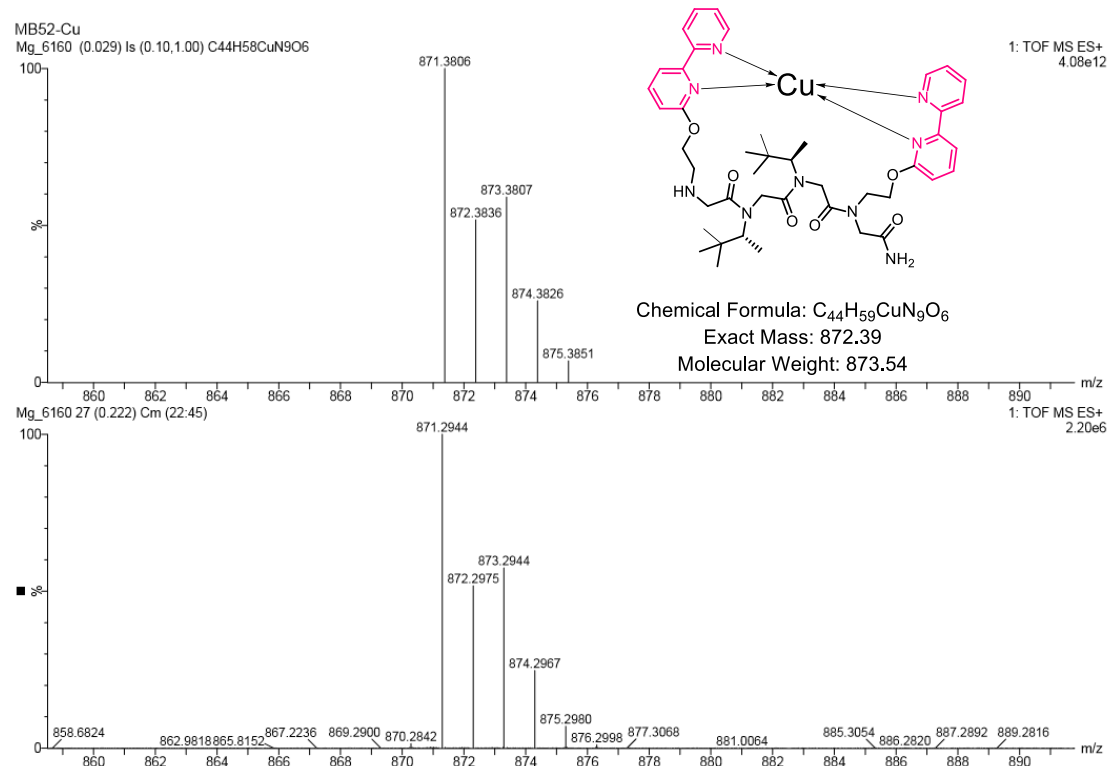


**Figure S91.** ESI-MS m/z traces of **4P1Cu** (bottom) and calculated ESI-MS spectrum (top).

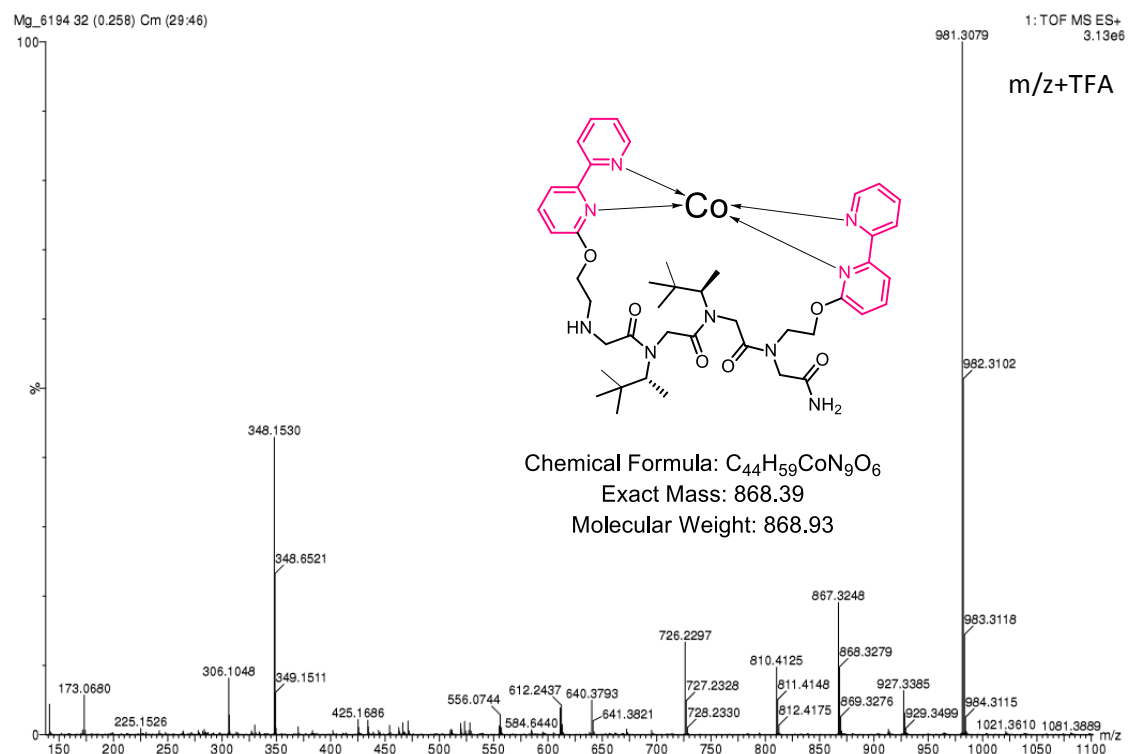


Figure S92. ESI-MS traces of 4P1Co complex.

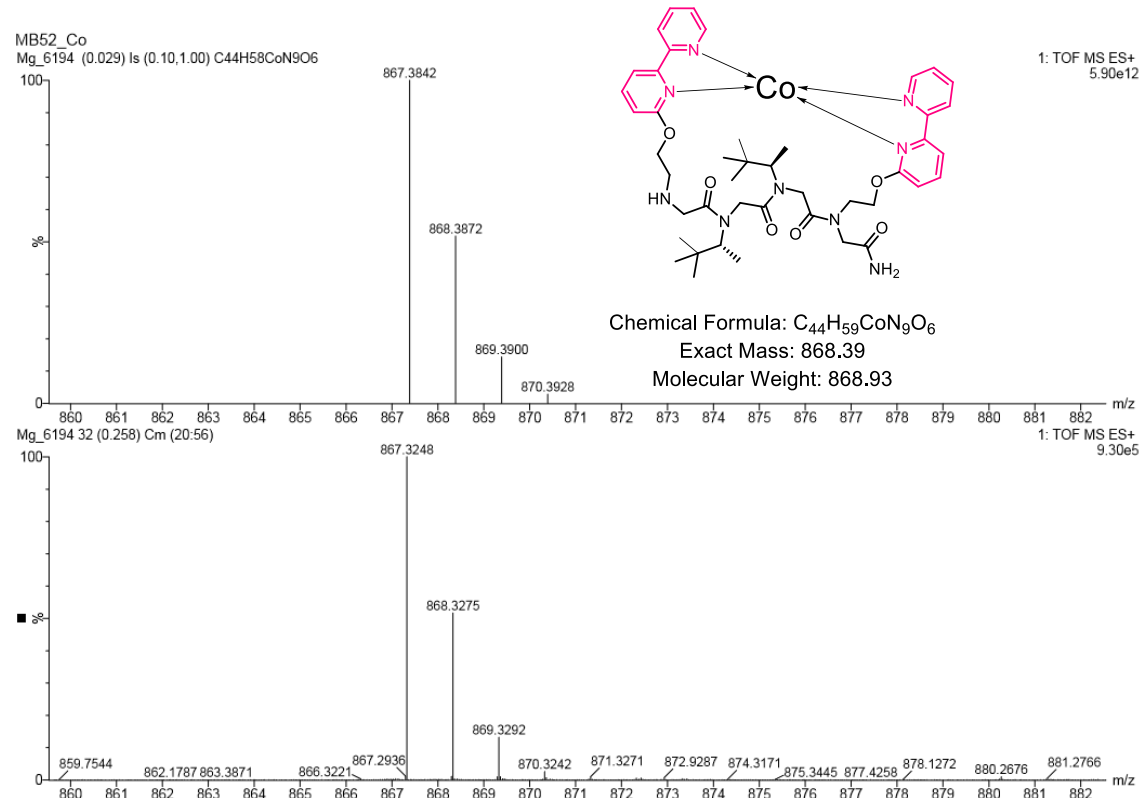


Figure S93. ESI-MS m/z traces of 4P1Co (bottom) and calculated ESI-MS spectrum (top).

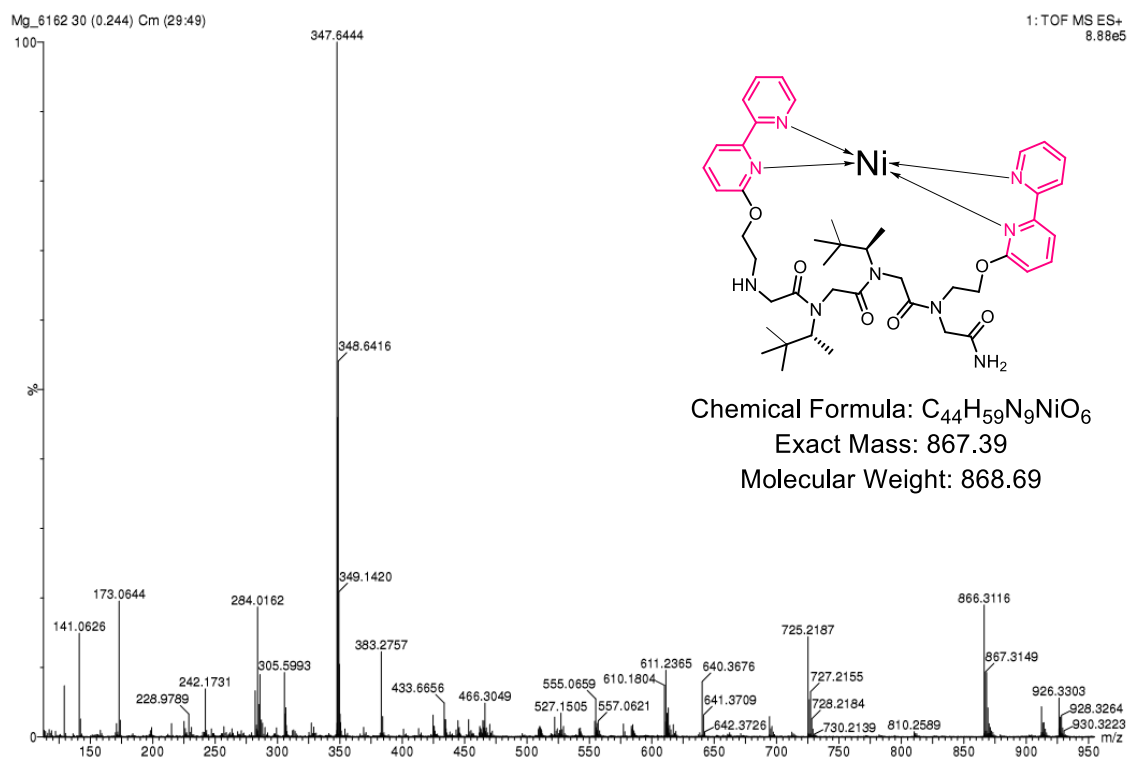


Figure S94. ESI-MS traces of  $4P1Ni$  complex.

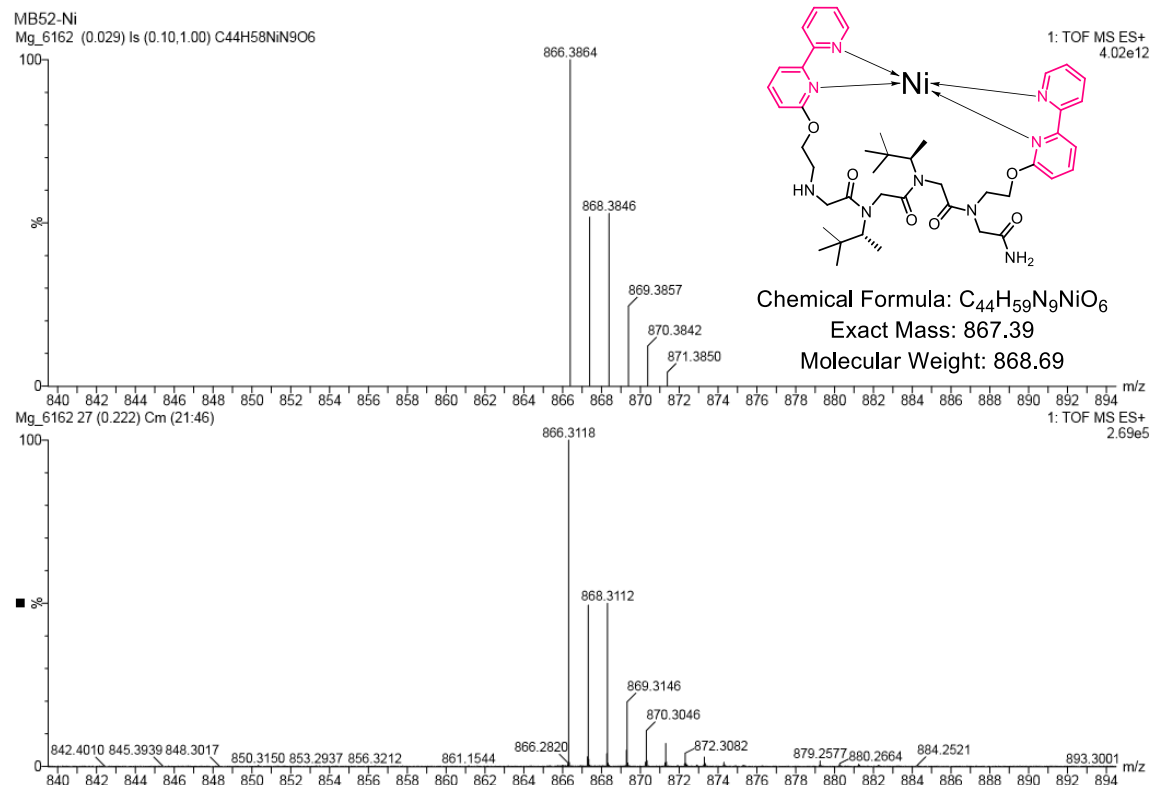
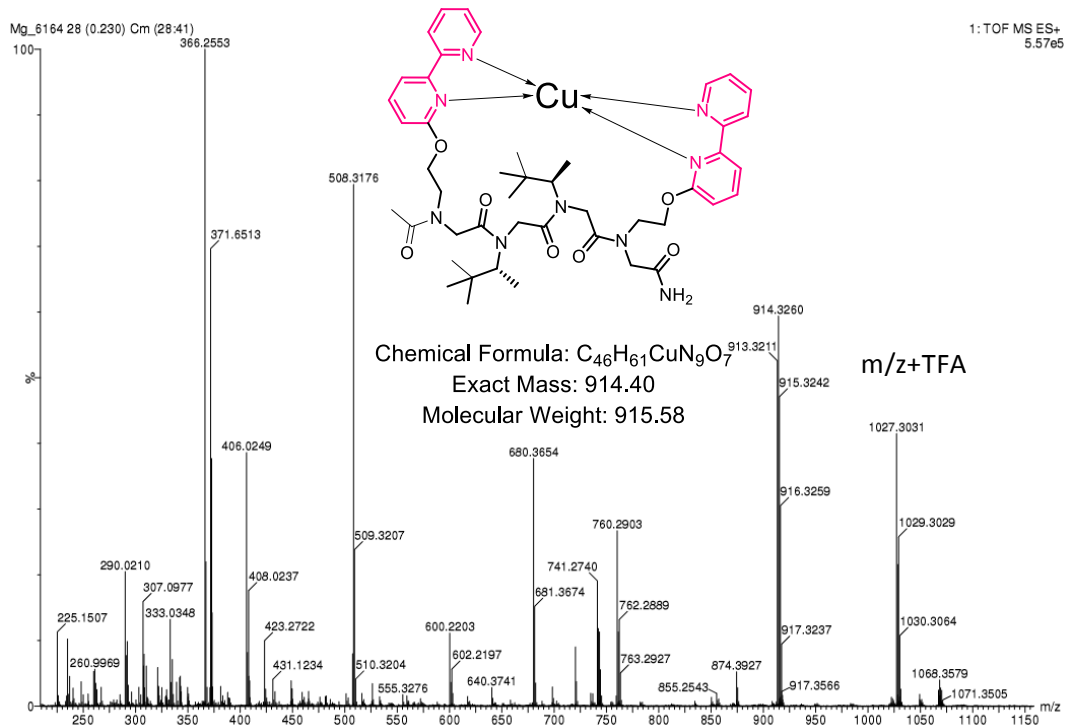
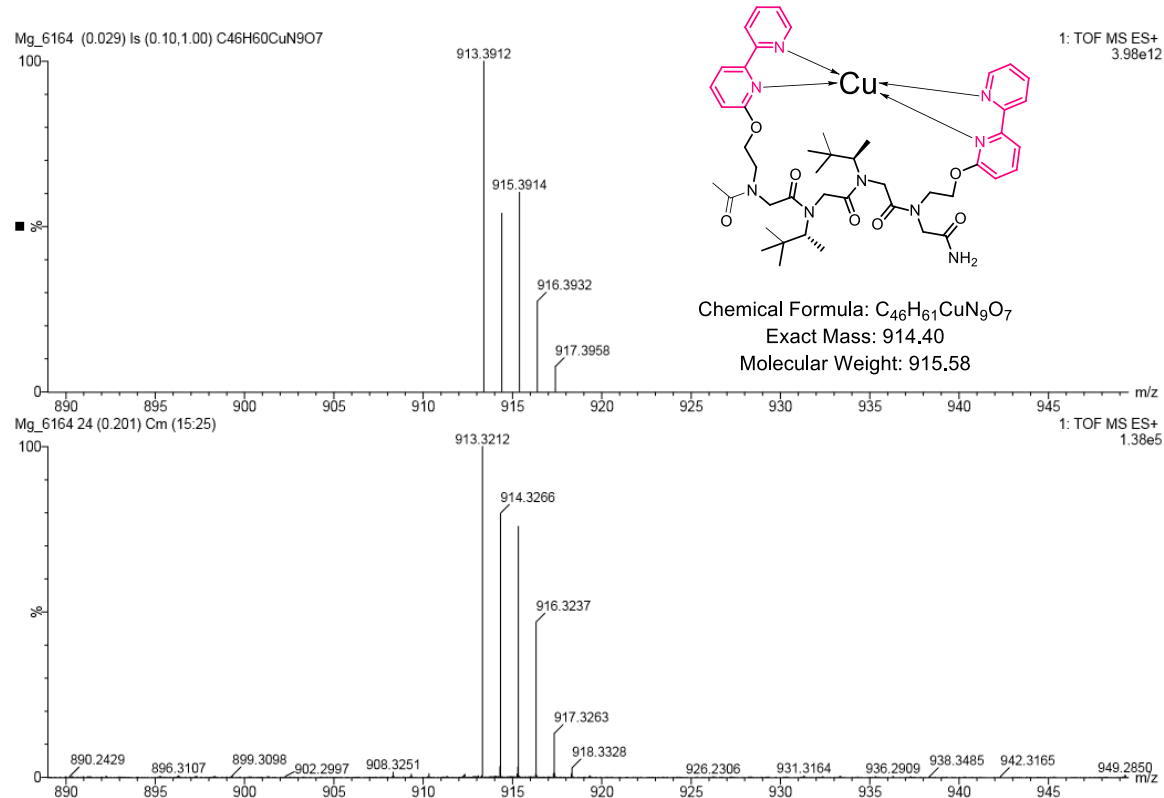


Figure S95. ESI-MS m/z traces of  $4P1Ni$  (bottom) and calculated ESI-MS spectrum (top).



**Figure S96.** ESI-MS traces of **4P1AcCu** complex.



**Figure S97.** ESI-MS m/z traces of **4P1AcCu** (bottom) and calculated ESI-MS spectrum (top).

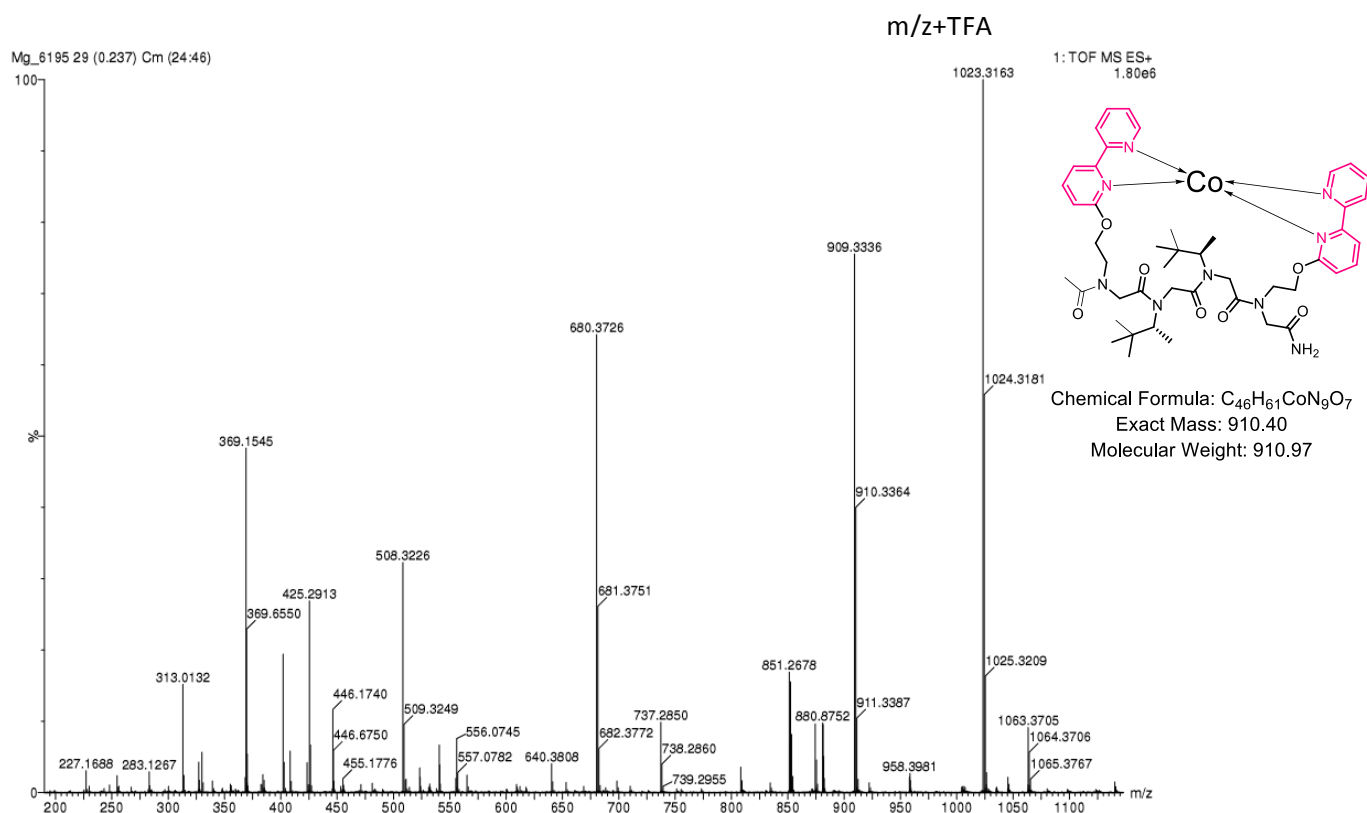


**Figure S98.** ESI-MS traces of 4P1AcCo complex.

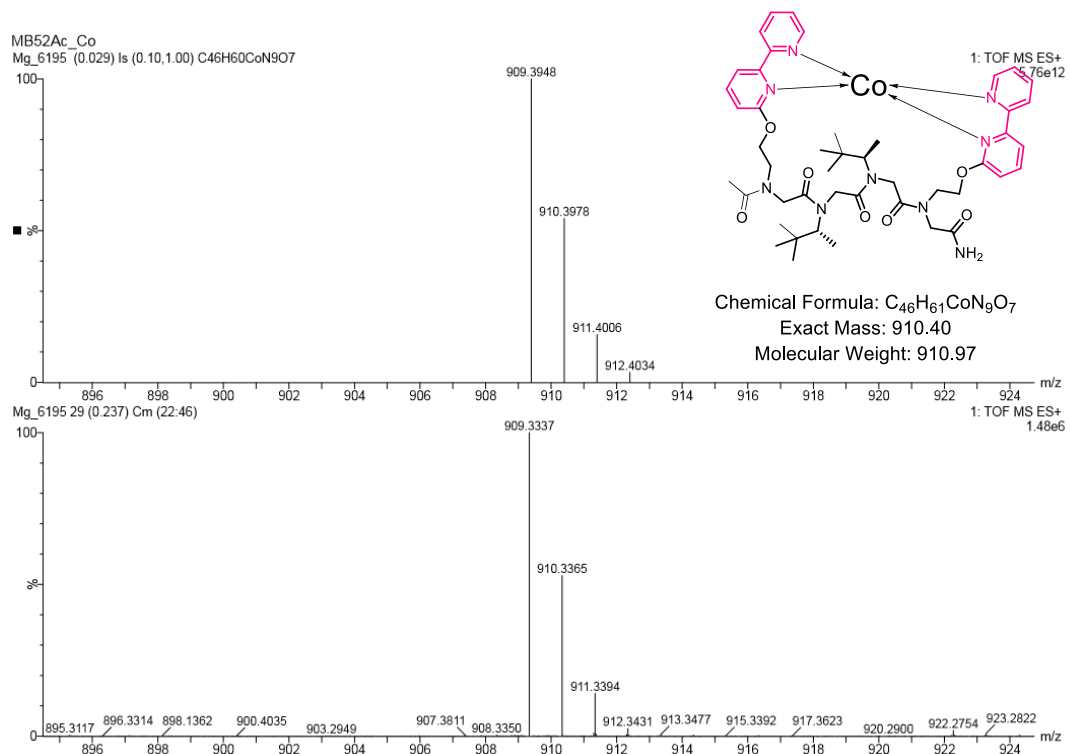


**Figure S99.** ESI-MS m/z traces of 4P1AcCo (bottom) and calculated ESI-MS spectrum (top).

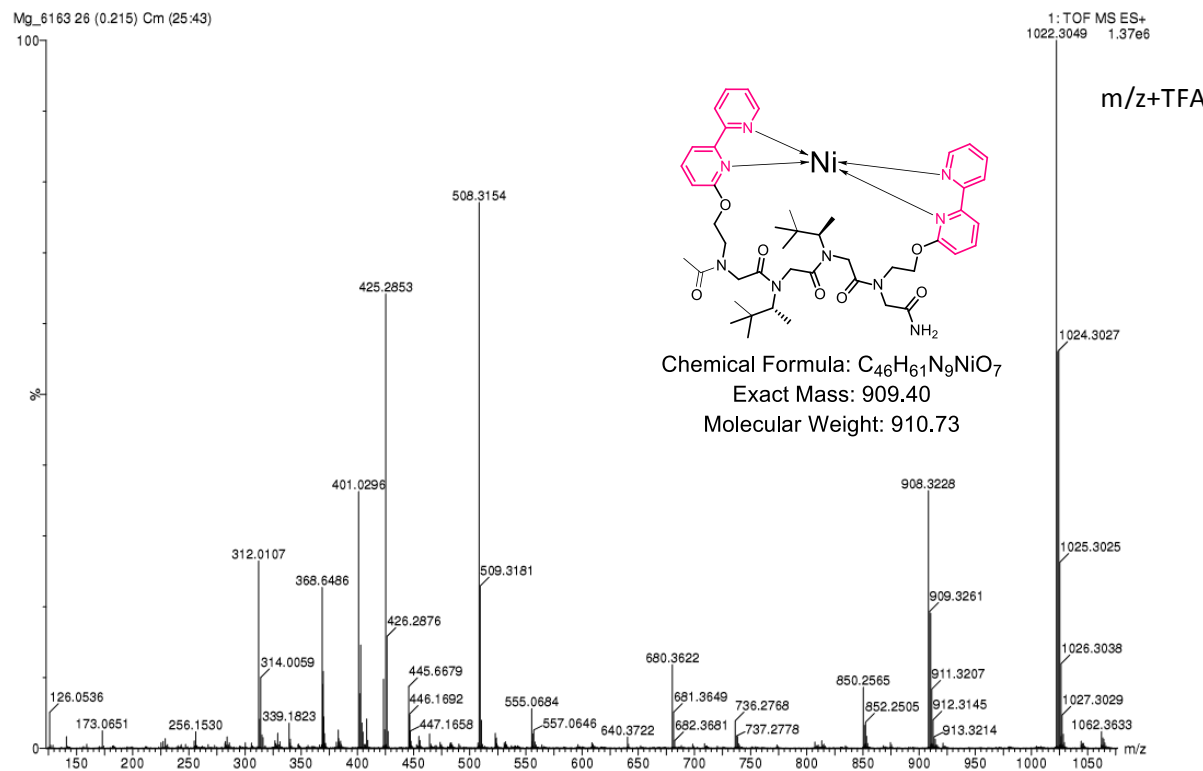


**Figure S100.** ESI-MS traces of 4P1AcNi complex.

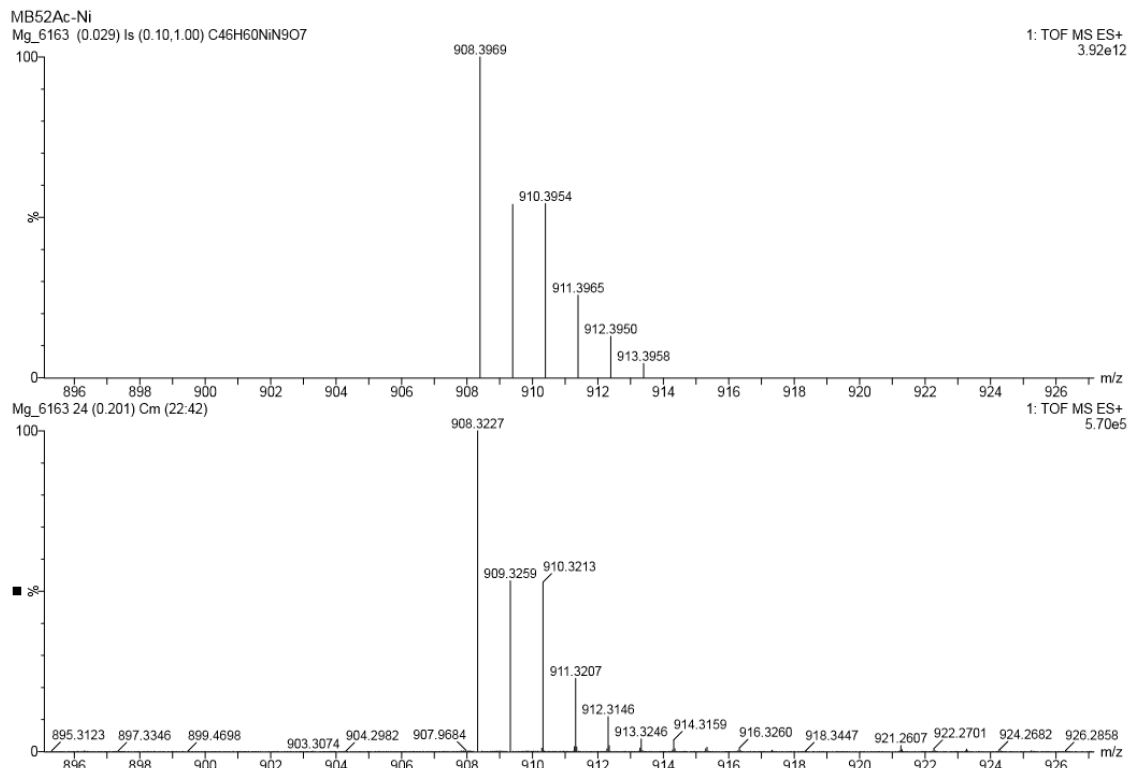


**Figure S101.** ESI-MS m/z traces of 4P1AcNi (bottom) and calculated ESI-MS spectrum (top).

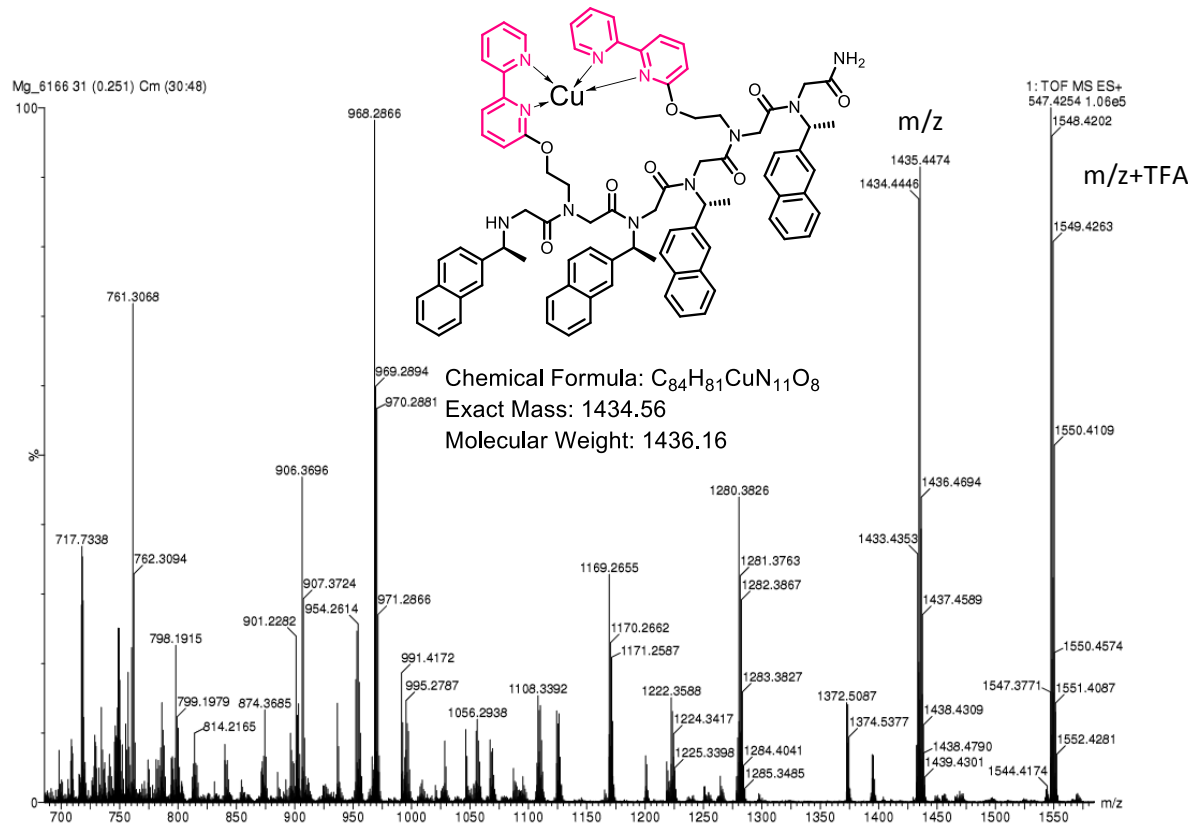


**Figure S102.** ESI-MS traces of 6P2Cu complex.

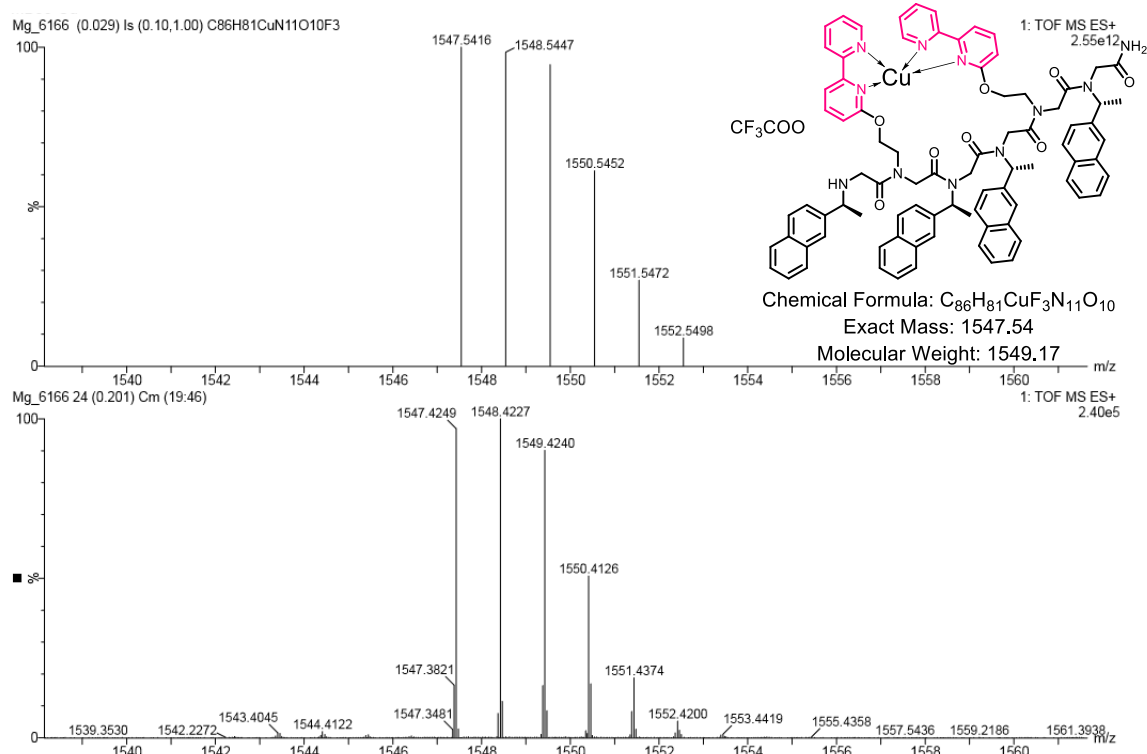


**Figure S103.** ESI-MS m/z traces of  $[6\text{P}2\text{Cu-TFA}]^+$  (bottom) and calculated ESI-MS spectrum (top).

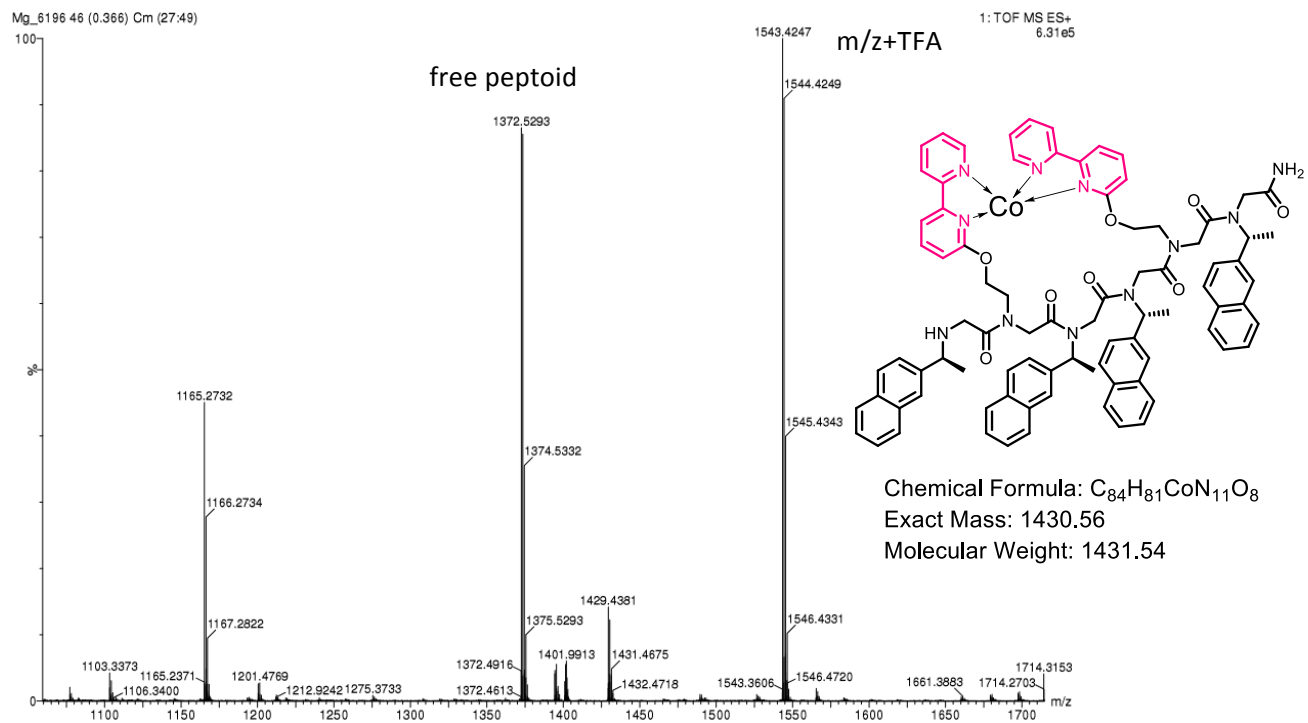


**Figure S104.** ESI-MS traces of **6P2Co** complex.

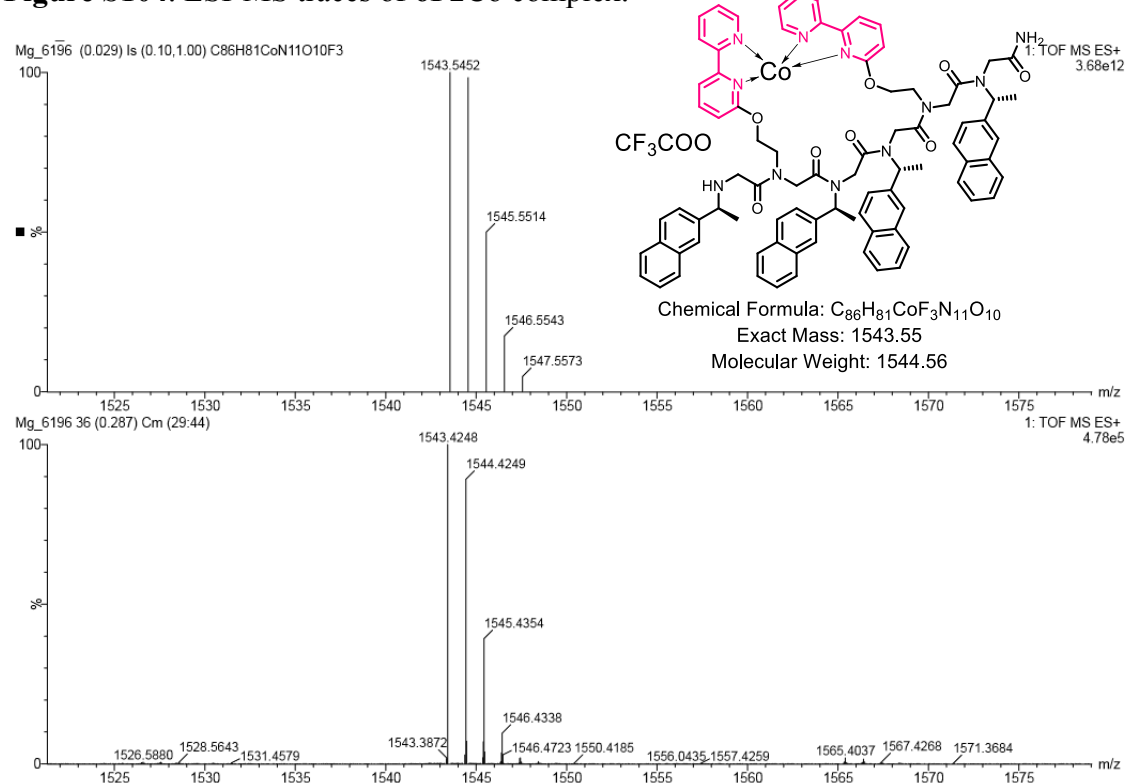


**Figure S105.** ESI-MS  $m/z$  traces of  $[\mathbf{6P2Co}\text{-TFA}]^+$  (bottom) and calculated ESI-MS spectrum (top).

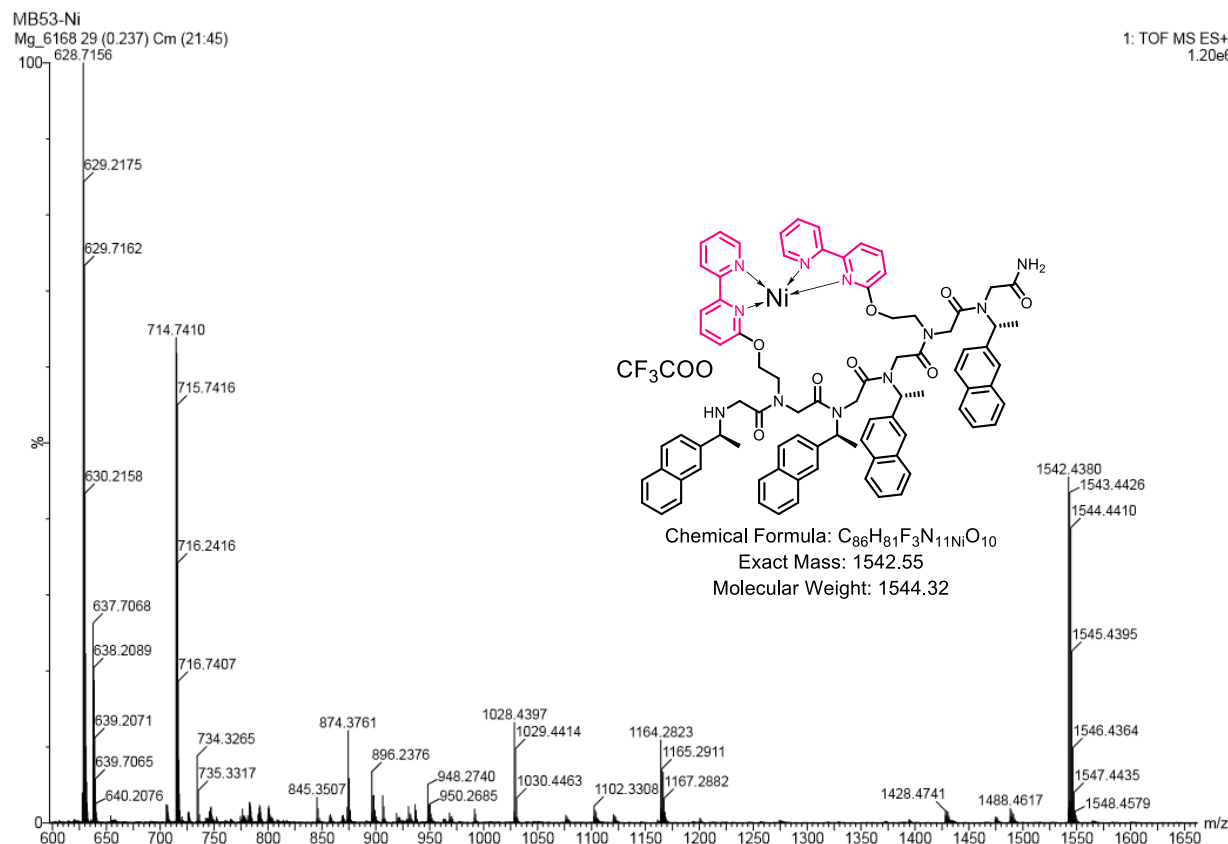


**Figure S106.** ESI-MS traces of **6P2Ni** complex.

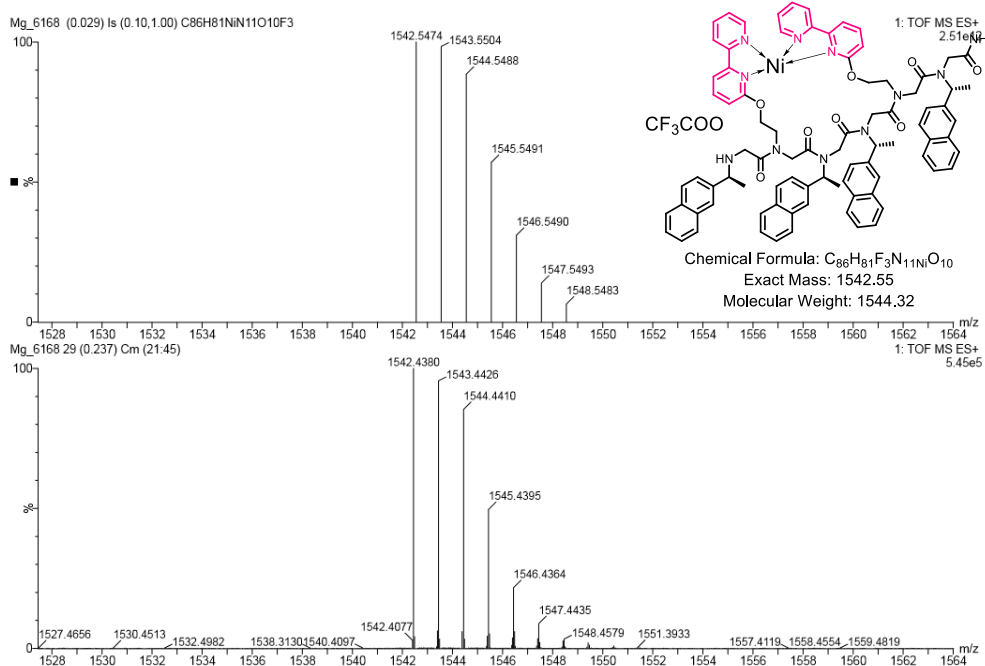


**Figure S107.** ESI-MS m/z traces of  $[6P2Ni\text{-TFA}]^+$  (bottom) and calculated ESI-MS spectrum (top).

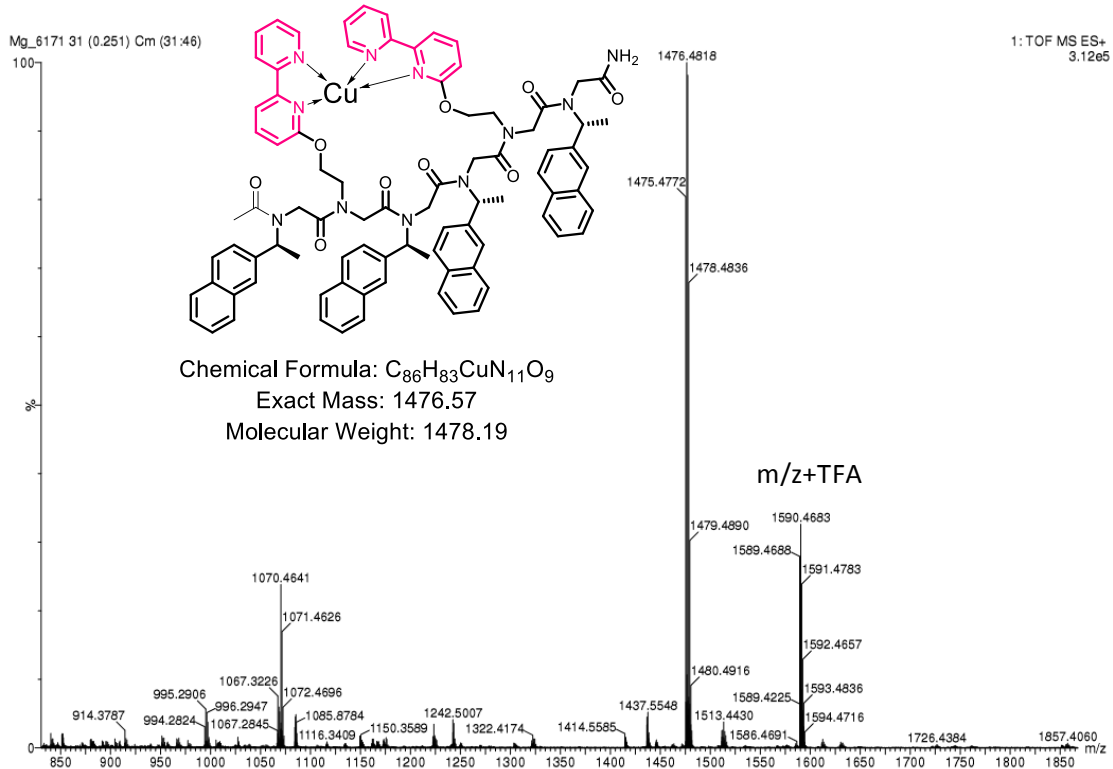


**Figure S108.** ESI-MS traces of **6P2AcCu** complex.

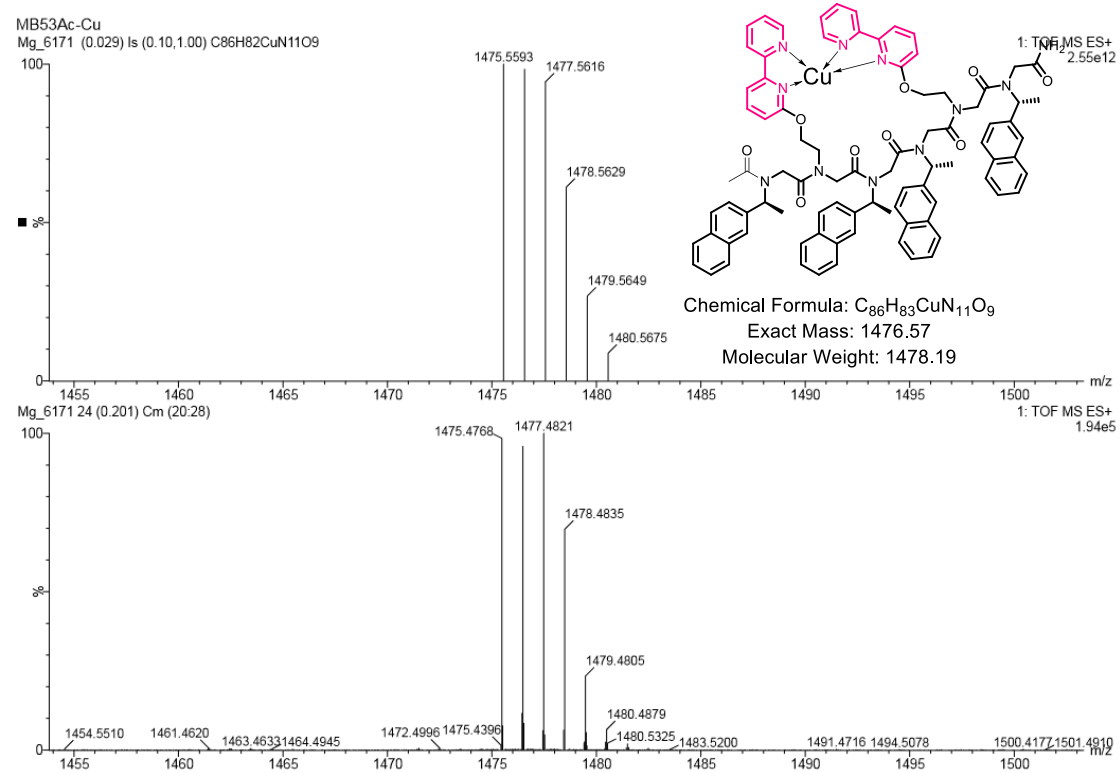


**Figure S109.** ESI-MS m/z traces of **6P2AcCu** (bottom) and calculated ESI-MS spectrum (top).

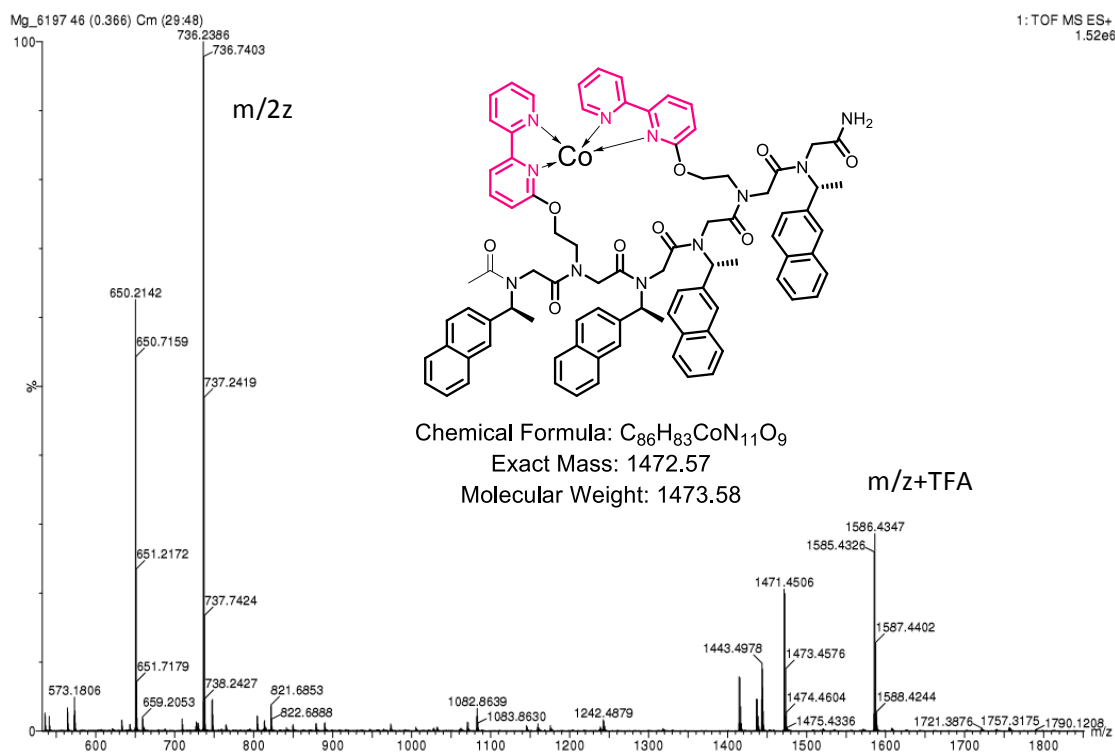


**Figure S110.** ESI-MS traces of **6P2AcCo** complex.

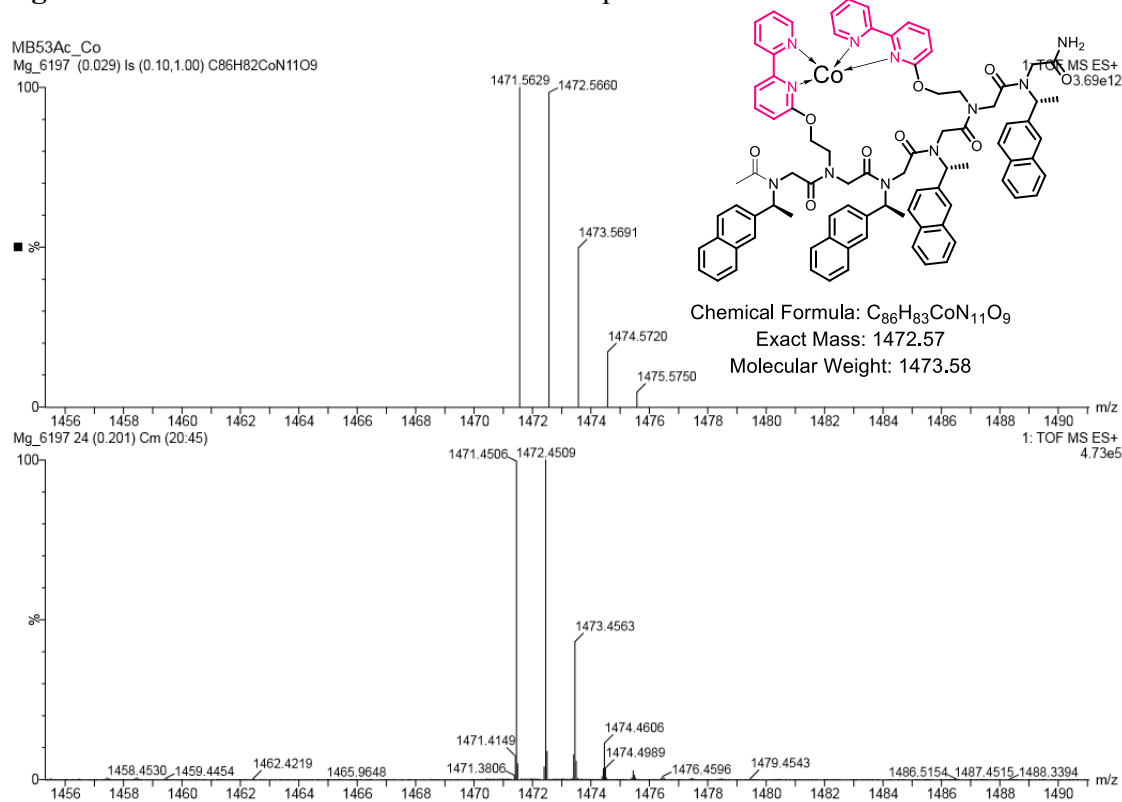


**Figure S111.** ESI-MS  $m/z$  traces of **6P2AcCo** (bottom) and calculated ESI-MS spectrum (top).

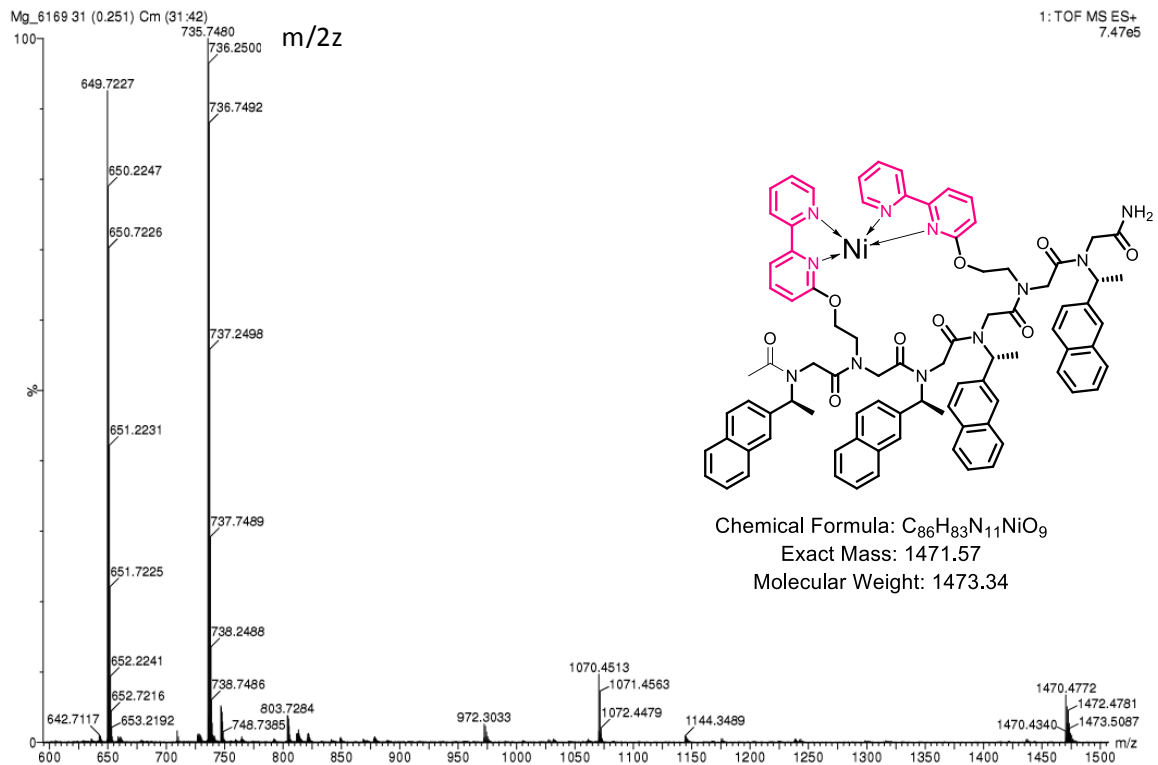


**Figure S112.** ESI-MS traces of **6P2AcNi** complex.

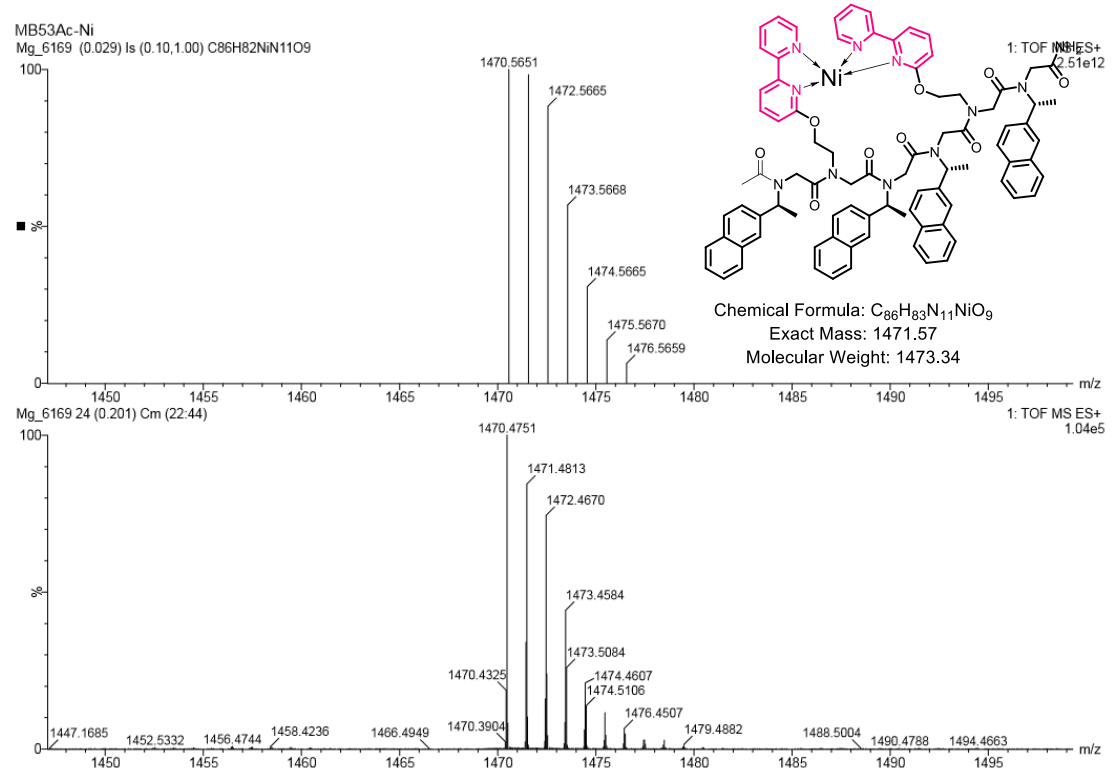


**Figure S113.** ESI-MS m/z traces of **6P2AcNi** (bottom) and calculated ESI-MS spectrum (top).

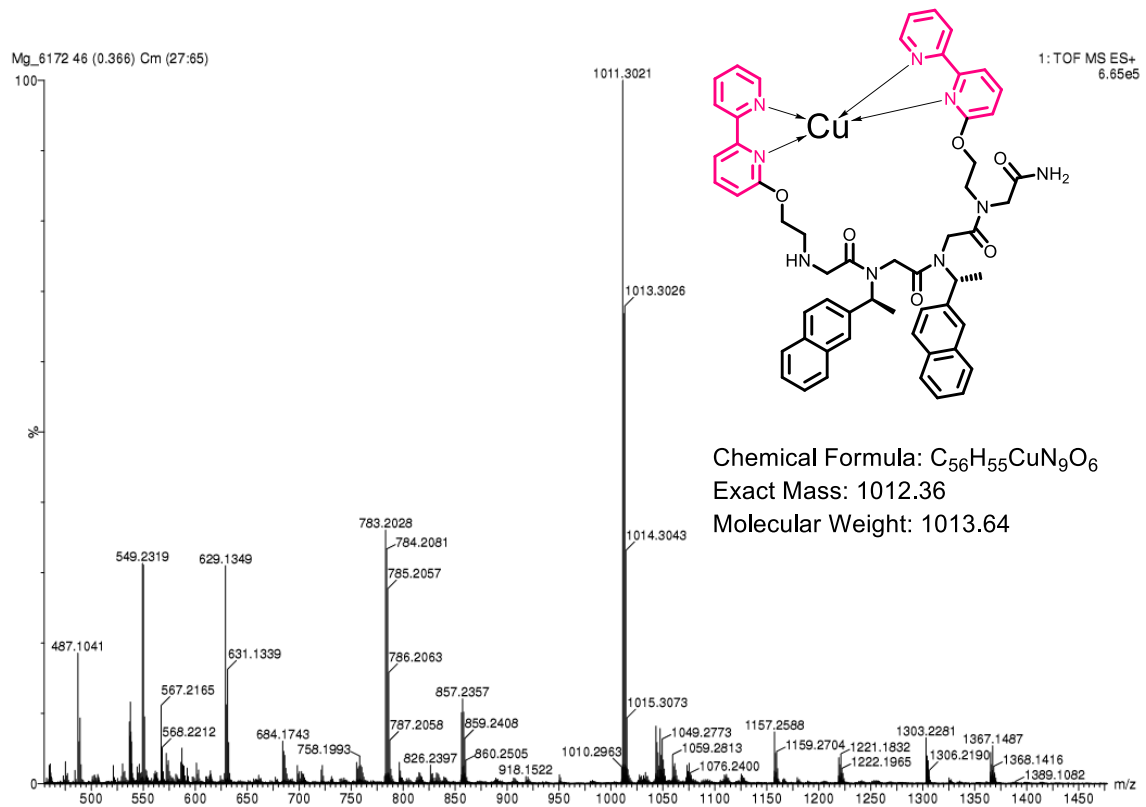


**Figure S114.** ESI-MS traces of **4P2Cu** complex.

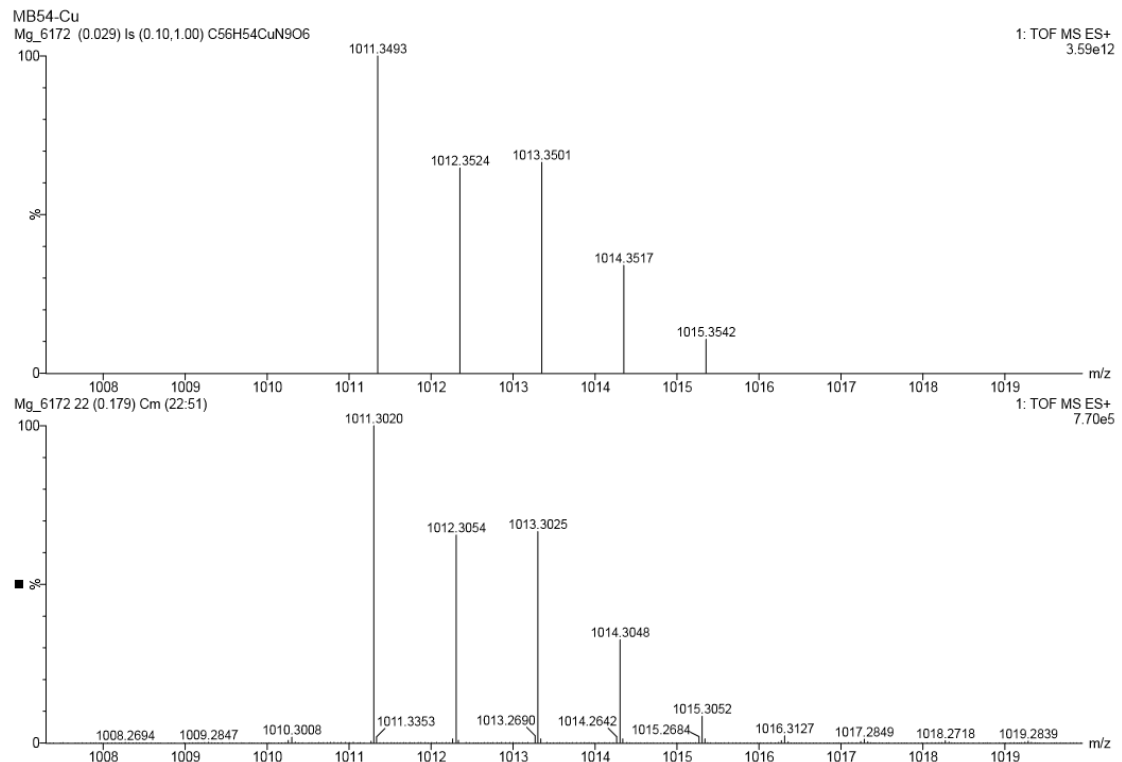


**Figure S115.** ESI-MS m/z traces of **4P2Cu** (bottom) and calculated ESI-MS spectrum (top).

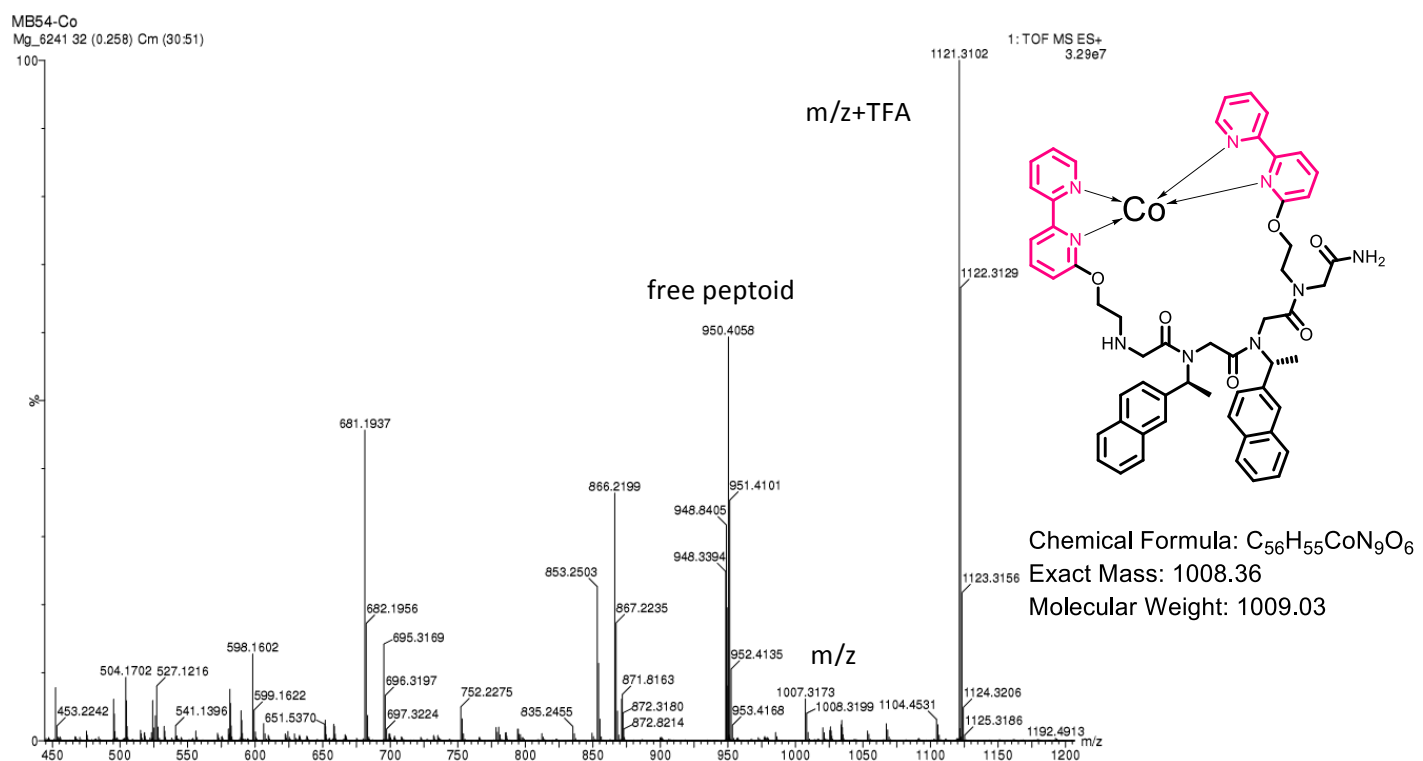


**Figure S116.** ESI-MS traces of **4P2Co** complex.

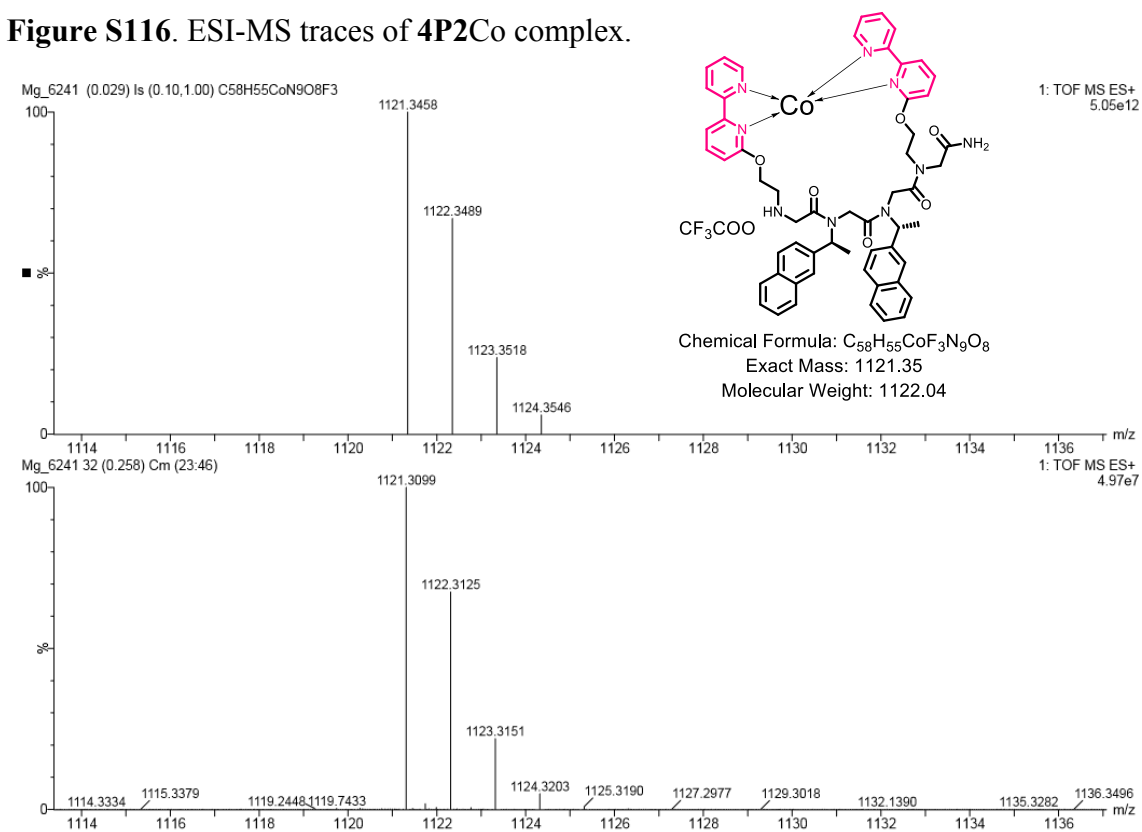


**Figure S117.** ESI-MS m/z traces of  $[4P2Co\text{-TFA}]^+$  (bottom) and calculated ESI-MS spectrum (top).

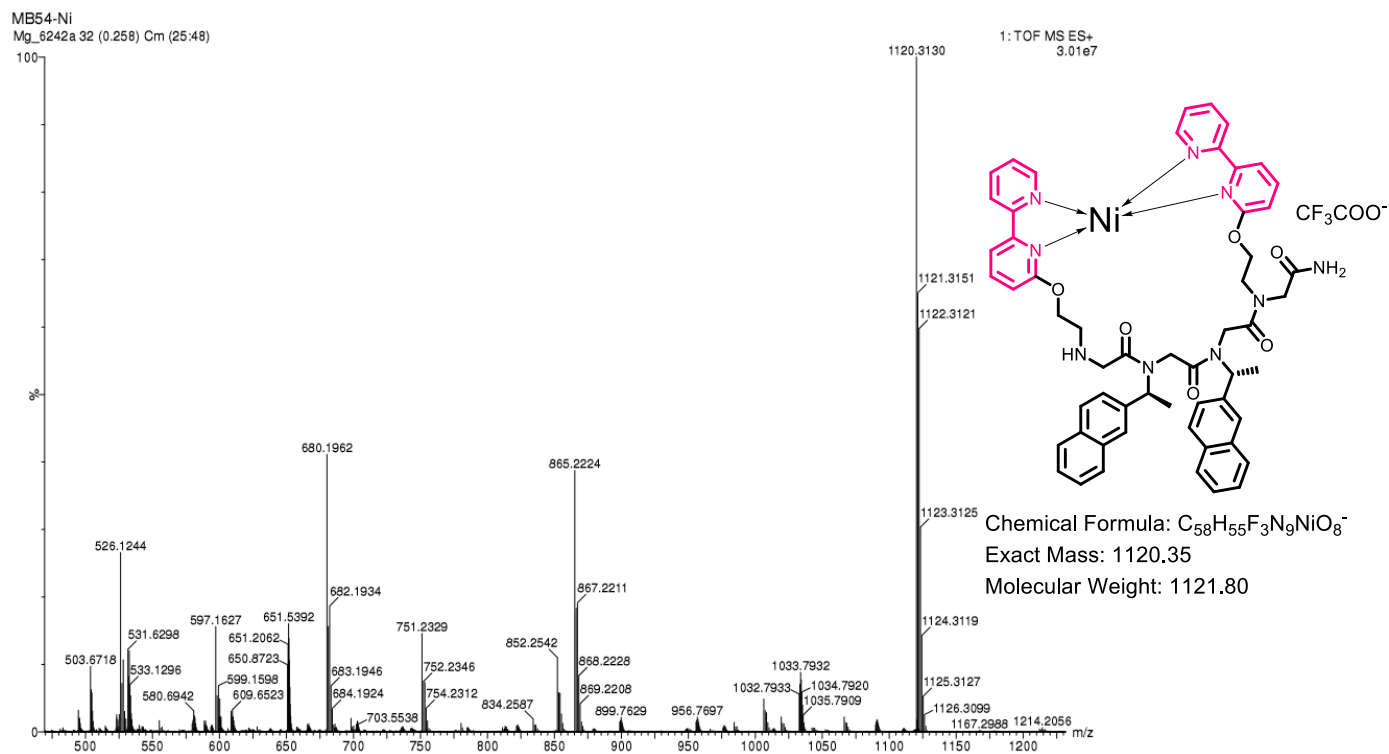


**Figure S118.** ESI-MS traces of **4P2Ni** complex.

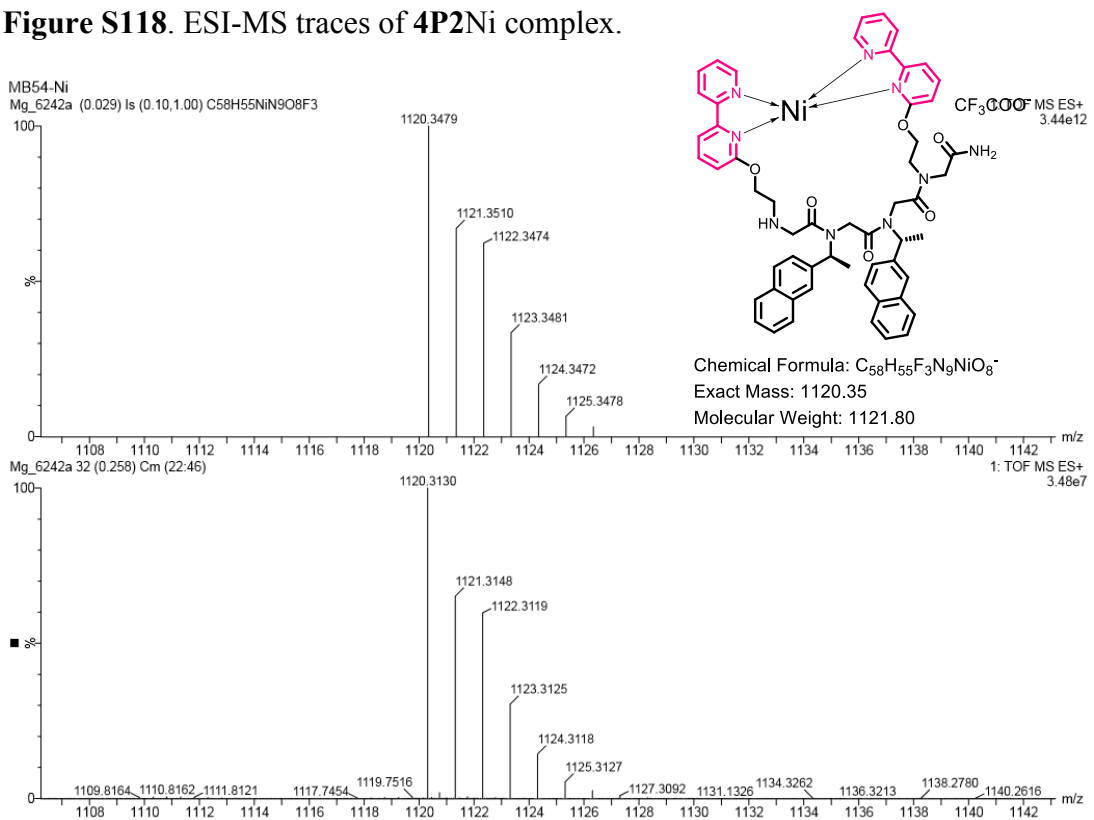


**Figure S119.** ESI-MS m/z traces of  $[4P2Ni\text{-TFA}]^+$  (bottom) and calculated ESI-MS spectrum (top).

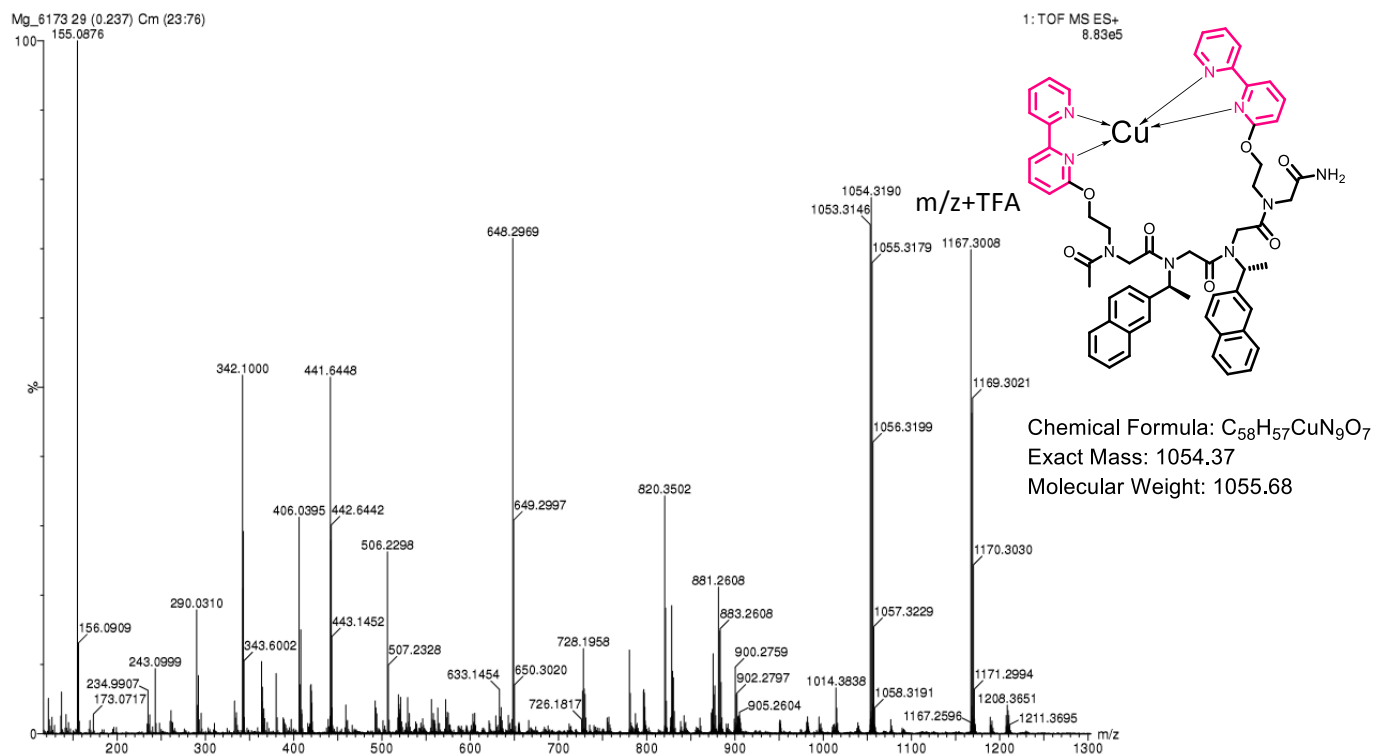


**Figure S120.** ESI-MS traces of **4P2AcCu** complex.

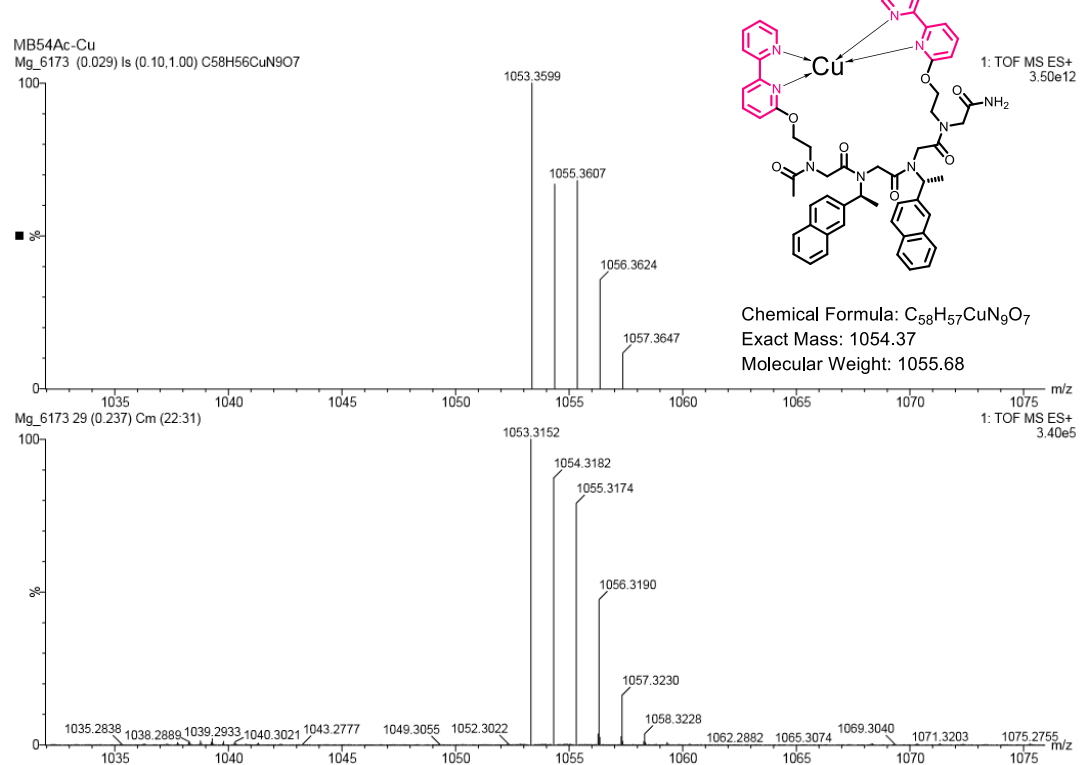


**Figure S121.** ESI-MS  $m/z$  traces of **4P2AcCu** (bottom) and calculated ESI-MS spectrum (top).

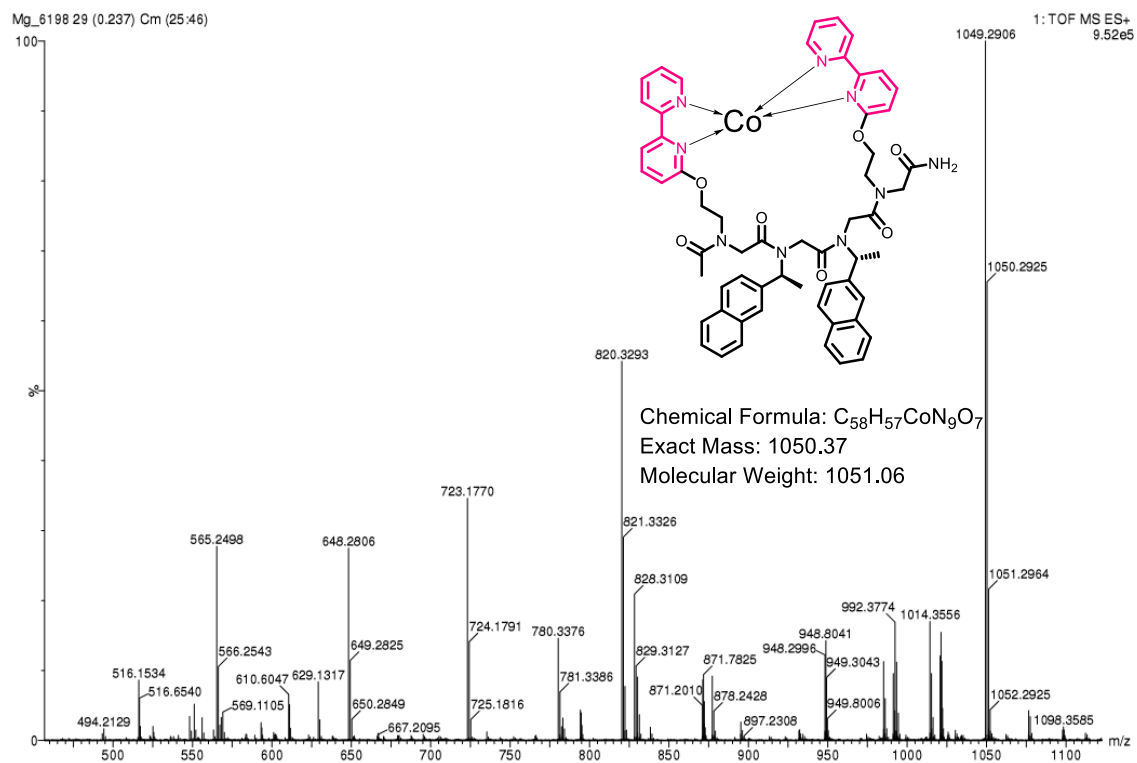


**Figure S122.** ESI-MS traces of **4P2AcCo** complex.

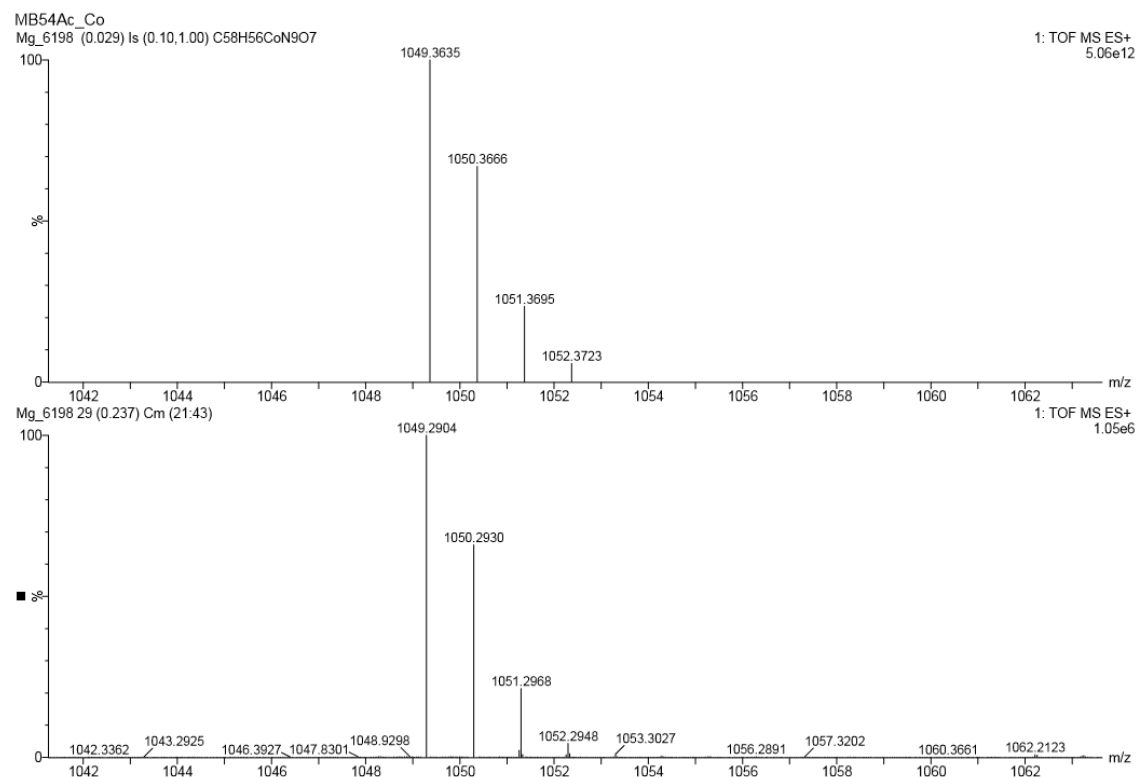


**Figure S123.** ESI-MS m/z traces of **4P2AcCo** (bottom) and calculated ESI-MS spectrum (top).

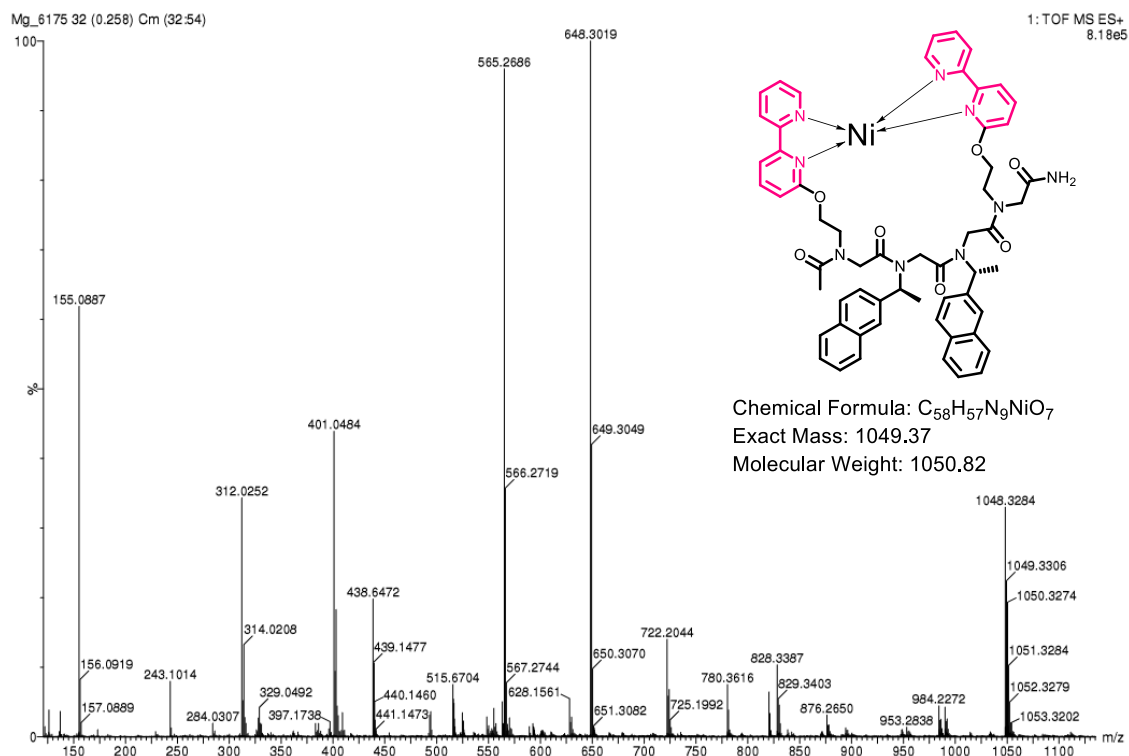


**Figure S124.** ESI-MS traces of 4P2AcNi complex.

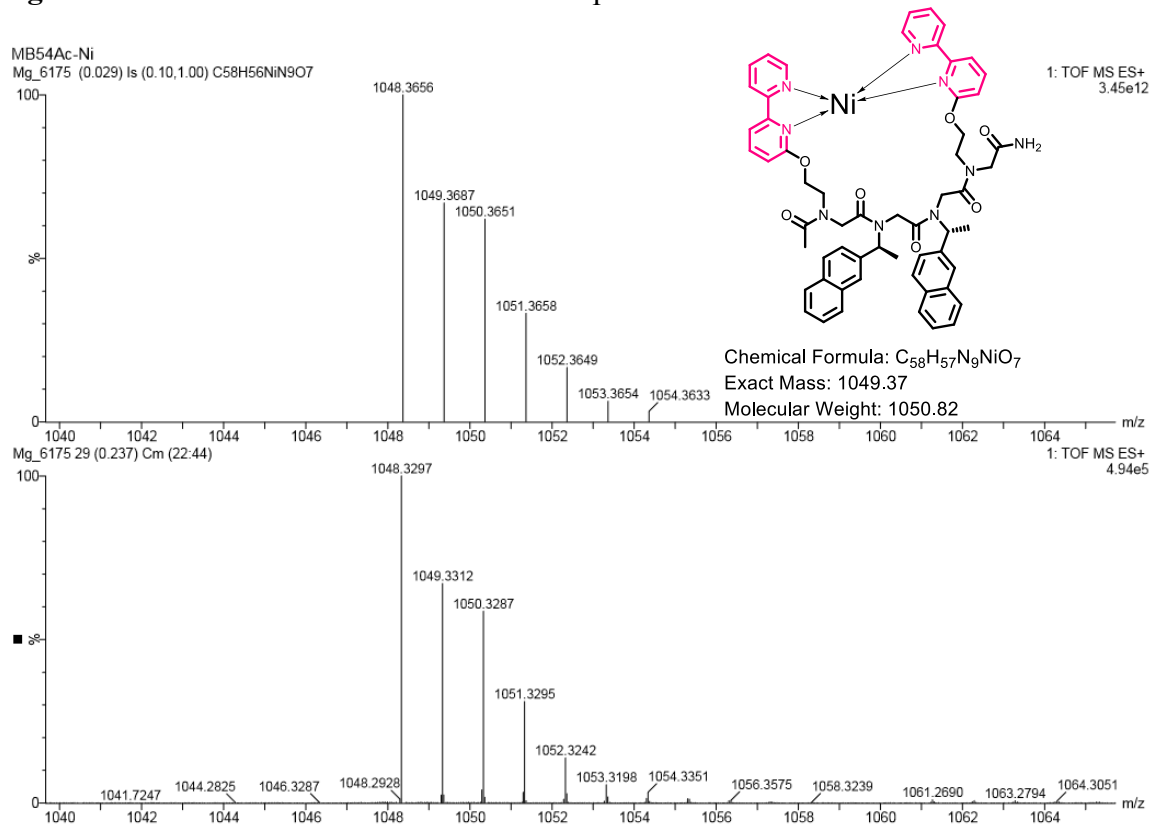


**Figure S125.** ESI-MS m/z traces of 4P2AcNi (bottom) and calculated ESI-MS spectrum (top).